ACTA GEOGRAPHICA SLOVENICA

GEOGRAFSKI ZBORNIK

2025
65
2

ACTA GEOGRAPHICA SLOVENICA

GEOGRAFSKI ZBORNIK

65-2

2025

ZNANSTVENORAZISKOVALNI CENTER
SLOVENSKE AKADEMIJE ZNANOSTI IN UMETNOSTI
GEOGRAFSKI INŠTITUT ANTONA MELIKA
•
RESEARCH CENTRE OF
THE SLOVENIAN ACADEMY OF SCIENCES AND ARTS
ANTON MELIK GEOGRAPHICAL INSTITUTE

ACTA GEOGRAPHICA SLOVENICA

GEOGRAFSKI ZBORNIK

65-2

2025

Založba ZRC

LJUBLJANA
2025

ACTA GEOGRAPHICA SLOVENICA

65-2
2025

ISSN: 1581-6613
UDC: 91
2025, ZRC SAZU, Geografski inštitut Antona Melika

Issued by/izdajatelj: Geografski inštitut Antona Melika ZRC SAZU
Published by/založnik: Založba ZRC
Co-published by/sozaložnik: Slovenska akademija znanosti in umetnosti

Address/naslov: Geografski inštitut Antona Melika ZRC SAZU, Gosposka ulica 13, p. p. 306, SI – 1000 Ljubljana, Slovenija; ags@zrc-sazu.si

The articles are available on-line/prispevki so dostopni na medmrežju: http://ags.zrc-sazu.si (ISSN: 1581–8314)

Ordering/naročanje: Založba ZRC, Novi trg 2, p. p. 306, SI – 1001 Ljubljana, Slovenija; zalozba@zrc-sazu.si

Annual subscription/letna naročnina: 20 €
Single issue/cena posamezne številke: 12 €

Cartography/kartografija: Geografski inštitut Antona Melika ZRC SAZU
Translations/prevodi: DEKS, d. o. o., Živa Malovrh
DTP/prelom: SYNCOMP, d. o. o.
Printed by/tiskarna: Birografika Bori
Print run/naklada: 250 copies/izvodov

The journal is subsidized by the Slovenian Research and Innovation Agency (B6-7614) and is issued in the framework of the Geography of Slovenia core research programme (P6-0101)/Revija izhaja s podporo Javne agencije za znanstvenoraziskovalno in inovacijsko dejavnost Republike Slovenije (B6-7614) in nastaja v okviru raziskovalnega programa Geografija Slovenije (P6-0101).

The journal is indexed also in/revija je vključena tudi v: Clarivate Web of Science (SCIE – Science Citation Index Expanded; JCR – Journal Citation Report/Science Edition), Scopus, ERIH PLUS, GEOBASE Journals, Current geographical publications, EBSCOhost, Georef, FRANCIS, SJR (SCImago Journal & Country Rank), OCLC WorldCat, Google Scholar, CrossRef, and DOAJ.

Design by/Oblikovanje: Matjaž Vipotnik

Front cover photography: The lights of settlements illuminate the landscape near Kranj, NW Slovenia (photograph: Xseon, Shutterstock.com).
Fotografija na naslovnici: Luči naselij osvetljujejo pokrajino v okolici Kranja na severozahodu Slovenije (fotografija: Xseon, Shutterstock.com).

ACTA GEOGRAPHICA SLOVENICA

ISSN: 1581-6613
UDC: 91
Number: 65-2
Year: 2025

Contents

Acta geographica Slovenica, 65-2, 2025, 7–27

MORPHOMETRIC CLASSIFICATION AND SPATIAL DISTRIBUTION OF DOLINES IN SOUTHERN SLOVENIA

Sašo Stefanovski, Mateja Ferk, Timotej Verbovšek, Uroš Stepišnik

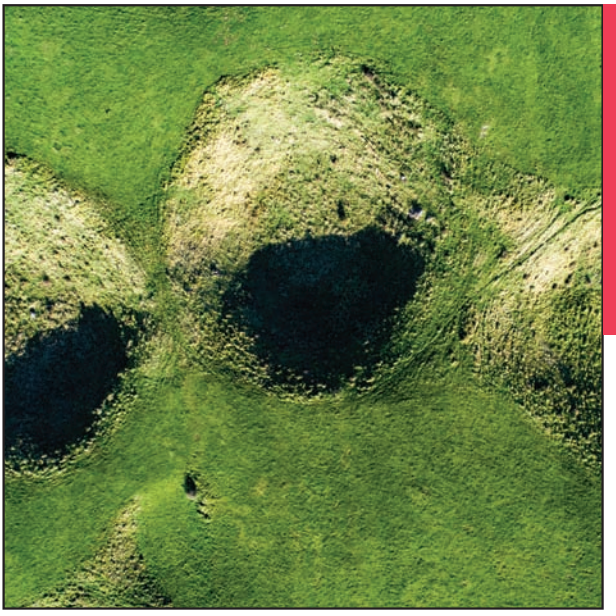

URO Š STEPIŠNIK

Dolines of the Rajndol corrosion plain.

DOI: https://doi.org/10.3986/AGS.13940
UDC: 551.435.82(497.4-13)

Sašo Stefanovski[1], Mateja Ferk[2], Timotej Verbovšek[3], Uroš Stepišnik[1]

Morphometric classification and spatial distribution of dolines in southern Slovenia

ABSTRACT: Dolines have traditionally been classified based on qualitative descriptions. This research presents the first attempt to connect a morphometric classification of dolines with existing morphological typologies in Slovenia. Using an automatic detection algorithm on a digital elevation model, we identified 179,288 standalone dolines and classified them into four classes based on morphometric characteristics. The classes were interpreted using statistical and spatial analyses. Dolines in Slovenia can be grouped into bowl-, funnel-, well-shaped, and elongated types. The type and distribution of dolines reflect the properties of karst, particularly sediment coverage and cone karst features. This research marks an initial step toward the systematic study of dolines, laying a foundation for further research.

KEYWORDS: karst, typology, data clustering, digital terrain model, Slovenia

Morfometrična klasifikacija in prostorska razporeditev vrtač v južni Sloveniji

POVZETEK: Vrtače so bile tradicionalno razvrščene na podlagi kvalitativnih opisov. Ta raziskava je prvi poskus povezave morfometrične klasifikacije vrtač z obstoječimi morfološkimi tipizacijami v Sloveniji. Z uporabo algoritma za samodejno zaznavanje vrtač na podlagi digitalnega modela višin smo identificirali 179.288 samostojnih vrtač in jih razvrstili v štiri razrede glede na njihove morfometrične značilnosti. Razrede smo interpretirali s statističnimi in prostorskimi analizami. Vrtače v Sloveniji lahko po obliki razvrstimo v skledaste, lijakaste, vodnjakaste in koritaste tipe. Tip in razporeditev vrtač odražata lastnosti krasa, zlasti prekritost s sedimentom in prisotnost kopastega krasa. Ta raziskava pomeni začetni korak k sistematičnemu preučevanju vrtač in postavlja temelje za nadaljnje raziskave.

KLJUČNE BESEDE: kras, tipizacija, podatkovno razvrščanje, digitalni model višin, Slovenija

The article was submitted for publication on September 21st, 2024.
Uredništvo je prejelo prispevek 21. septembra 2024.

[1] University of Ljubljana, Faculty of Arts, Ljubljana, Slovenia
saso.stefanovski@ff.uni-lj.si (https://orcid.org/0000-0002-7822-451X), uros.stepisnik@ff.uni-lj.si (https://orcid.org/0000-0002-8475-8630)

[2] Research Centre of the Slovenian Academy of Sciences and Arts, Ljubljana, Slovenia
mateja.ferk@zrc-sazu.si (https://orcid.org/0000-0003-0145-7590)

[3] University of Ljubljana, Faculty of Natural Sciences and Engineering, Ljubljana, Slovenia
timotej.verbovsek@ntf.uni-lj.si (https://orcid.org/0000-0002-1908-5759)

1 Introduction

Karst is a distinctive geomorphic system characterised by the predominance of subterranean water flow. The primary geomorphic process governing karst development is chemical denudation of bedrock, primarily via dissolution. Dissolution also extends deep within the subsurface, resulting in the formation of cavities with high effective permeability (White 1988). The heterogeneous nature of surface denudation, which is predominantly influenced by dissolution and supplemented by other mechanical processes that facilitate the transfer of material across the surface and into the subsurface, leads to the development of a complex karst landscape. This landscape is marked by a diversity of geomorphological features, including both positive and negative topographical forms (Jennings 1985; Habič 1986; Ford and Williams 2007). A very common surface landform in karst areas within the temperate climate zone is a doline or a sinkhole (Sauro 2003). This term refers to circular depressions, typically up to 100 m diameter and around 10 m deep (Gams et al. 1973; Jennings 1985; White 1988; Gams 2003; Ford and Williams 2007; Mihevc and Mihevc 2021; Stefanovski et al. 2024). Due to their prevalence, dolines are often considered the most typical or even diagnostic landform of karst landscapes (Sweeting 1973; Ford and Williams 2007; Sauro 2019). These landforms exhibit a wide variety of shapes and sizes, making their classification both challenging and crucial for understanding karst dynamics. Despite this, classification and typification of dolines are mostly based on their formation processes (e.g., Cramer 1941; Waltham and Fookes 2003; De Waele and Gutiérrez 2022) rather than on morphometric or morphographic characteristics (e.g., Cviji 1893; Gams et al. 1962; Jeanpert et al. 2016). The morphogenesis of certain dolines has been well-documented in previous studies, leading to the widespread adoption of classification systems centred on their morphogenetic mechanisms. Cvijić (1893) was among the first to categorise dolines by their formation processes. Cramer (1941) upgraded the findings of Cvijić (1893) and introduced a systematic morphogenetic typology that remains largely relevant today, distinguishing dolines into types such as collapse, subsidence, solution, suffosion, and alluvial dolines.

Geomorphological investigations involve various methods and steps. Morphological analysis describes dolines qualitatively, focusing on their shape, while morphometric analysis measures their numerical properties. The two are closely linked, as morphometric data provide exact values about the same features that morphological analysis describes (Pavlopoulos et al. 2009). Modern morphometric and morphographic typologies of dolines are relatively uncommon. Morphometric approaches mostly focus on the calculation and interpretation of general morphometric properties (e.g., Bondesan et al. 1992; Telbisz et al. 2009; Šegina et al. 2018; Verbovšek and Gabor 2019). Cvijić (1893) proposed the earliest typology, classifying dolines into bowl-shaped, funnel-shaped, and well-shaped types based on the depth-to-diameter ratio and slope inclination. Subsequent typologies have largely built upon Cvijić's findings (e.g., Gams et al. 1962; Gams et al. 1973; Gams 1974; Gams 2003; Sauro 2003; Ford and Williams 2007; Jeanpert et al. 2016; De Waele and Gutiérrez 2022). In the past, morphometric and morphographic classifications were less practical due to the time-consuming nature of field data collection through geomorphological mapping and measurements. Consequently, classifications of dolines were predominantly qualitative, with limited quantitative classifications (Péntek et al. 2007; Jeanpert et al. 2016). With the availability of high-resolution digital terrain models (DTMs) and advances in computer technology, manual geomorphological mapping is increasingly being complemented or replaced by advanced GIS-based delineation methods. Since dolines are one of the main features of karst surfaces, various methods for their delineation have been developed (e.g., Obu and Podobnikar 2013; Grlj and Grigillo 2014; Telbisz 2021; Ciglič et al. 2022). For instance, Mihevc and Mihevc (2021) created a comprehensive doline database for the karst areas of Slovenia using machine learning-supported U-Net segmentation. Their work also provides a valuable description of doline distribution, representing a significant contribution to karst research in Slovenia.

However, some limitations of the approach of Mihevc and Mihevc (2021) merit consideration. First, the delineation of dolines was not entirely precise, as the study did not define dolines as closed depressions, leading to the inclusion of false positives cases (gullies and other concave features) in the database. Second, the classification of dolines was based on genesis – categorised into collapse dolines, solution dolines, and suffosion dolines – primarily relying on the authors' terrain knowledge. While this approach offers valuable insights, it is inherently subjective, as it lacks explicitly defined quantitative or qualitative criteria for classification. The absence of such criteria or parameters makes it challenging to replicate or validate their classifications fully.

A recent study by Stefanovski et al. (2024) explored new approaches to doline delineation, comparing existing methods with a newly developed approach. Their findings suggest that the new method achieves higher accuracy in delineating dolines than previously employed methods (Obu and Podobnikar 2013; Zumpano et al. 2019; Mihevc and Mihevc 2021).

This study focuses on three main objectives. First, it aims to use the detailed spatial database based on the method provided by Stefanovski et al. (2024) to classify dolines in Slovenia based on their morphometric characteristics. Second, it seeks to connect the existing morphographic classifications and terminology to a new updated typology of dolines using this data, with the aim of bridging existing knowledge with current methods to ensure consistency and avoid unnecessary introduction of new terms or definitions. Instead, the study refines and enhances what has already been described, ensuring continuity and consistency in doline research. Third, it aims to analyse the relation between doline types, sediment presence, corrosion plains and cone karst areas. This analysis will help us better understand how dolines are distributed across various karst landscapes; however, it does not address their formation processes, as doing so would be overly speculative and require a dedicated, in-depth study focused specifically on these aspects.

2 Review of doline typologies: a theoretical overview

Dolines are typical geomorphological features of temperate karst landscapes. Some authors regard them as among the most characteristic karst landforms (Ford and Williams 2007) or even as diagnostic forms of karst surfaces (Sweeting 1973). However, it is important to note that dolines do not occur in all karst environments, but rather in areas where the vadose zone is developed. This type of karst is defined as deep karst (Šerko 1947; Bögli 1980; Šušteršič 1994). In other karst settings, such as fluviokarst, glaciokarst, or shallow karst, they are either absent or the karst depressions are not classified genetically as dolines (Stepišnik 2024). Due to the large number of dolines in karst areas of temperate geographic latitudes, early studies aimed to classify these landforms. Since the first detailed descriptions and studies of dolines, numerous typologies have been proposed by various authors (e.g., Cvijić 1893; Cramer 1941; Gams et al. 1962). Although these typologies are diverse, they can generally be grouped into four main categories. The first category includes morphometric and morphographic typologies (e.g., Cvijić 1893; Gams 2003; Sauro 2019), which are the focus of this research and are therefore examined in greater detail in the first part of the subsequent literature review. Dolines can also be categorised based on geological settings, morphogenetic and morphodynamic processes (e.g., Cramer 1941; Gams 2000; Čar 2001; Péntek et al. 2007; Verbovšek and Gabor 2019; De Waele and Gutiérrez 2022).

Morphometric typologies of dolines are relatively uncommon, even though most studies have included general morphometric analyses, such as depth, area and elongation, within their research (e.g., Bondesan et al. 1992; Telbisz et al. 2009; Šegina et al. 2018; Verbovšek and Gabor 2019; Ciglič et al. 2022). The sheer number of dolines can make data collection extremely time-consuming (Šušteršič 1994; Šušteršič 2006; Šušteršič 2017). Before the availability of LiDAR data in Slovenia, these measurements had to be collected manually in the field, or by examining large scale topographic maps (e.g., Čar 1982; Čar 2001; Frelih 2014; Čar 2018) further adding to the difficulty and effort required.

Morphographic typologies are more common, but are rarely supported by morphometric descriptions, which would make them more reliable and objectively comparable. The earliest morphographic typology of dolines was developed by Cvijić (1893) who used morphometric properties to provide a more precise description. He described the depressions we now define as dolines as round or elliptical in plan, with depths ranging from 2 to 20 m and diameters between 10 and 120 m. These features can appear either individually or in dense clusters, with more than 50 per km^2. Cvijić (1893) distinguished three main types of ordinary dolines based on the ratio of depth to diameter and slope inclination. These types are: bowl-shaped or basin-shaped dolines, which have a small depth relative to their diameter, with the diameter being approximately ten times the depth. The slopes of these dolines are generally gentle, ranging from 10° to 12°. Funnel-shaped dolines, on the other hand, have a diameter about two to three times greater than the depth, with steeper slope inclinations, mostly between 30° and 45°. Well-shaped dolines are characterised by depths that are roughly equal to or even greater than their diameter, with slope inclinations exceeding 45°, resulting in very steep sides.

Cvijić (1893) also identified a special type known as elongated dolines, which he described as valley-like depressions typically found at higher altitudes, though he did not provide specific morphometric criteria for these elongated forms.

Gams et al. (1962) developed a second morphographic typology of dolines, largely based on the work of Cvijić (1893) as seen in Table 1. They characterised well-shaped dolines as having steep, sometimes vertical walls, and a flat floor. Kettle-shaped dolines were also noted for their steep slopes, but with a concave floor. While they acknowledged the existence of bowl-shaped and funnel-shaped dolines due to their distinctive cross-sectional profiles, they did not provide detailed descriptions of these types.

The morphometric analysis of dolines by Gams (1974) did not provide specific morphometric values for each type of doline but instead offered their general dimensions. He found that the depth-to-diameter ratio at the upper edge of dolines typically ranges from 1:6 to 1:10. He also identified regional variations, observing that some areas are characterised by small dolines only a few meters wide, while others contain larger dolines with diameters ranging from 50 to over 100 m.

Péntek et al. (2007) provided a morphodynamic typology of solution dolines based on their morphometric properties. They used depth, horizontal extension and slope shape as the three main morphometric parameters. The solution dolines were classified as dolines widening at rim and base, dolines widening at base, dolines widening at rim and dolines, that are deepening, but not widening.

Jeanpert et al. (2016) developed a morphometric typology based on their analysis of a pseudokarstic environment on ultramafic rocks in New Caledonia. They identified several types of dolines: collapse dolines, which are characterised by an average slope exceeding 30°; bowl-shaped dolines, where the average slope ranges between 15° and 30°; and flat-bottomed dolines, defined by an average slope of less than 15°. The flat-bottomed dolines are further classified into large and small, depending on whether their diameter is greater or less than 10 m.

Sauro (2019) categorised dolines into three distinct types based on their shape: the most common are bowl-shaped dolines, followed by funnel-shaped dolines, which are also fairly common, and the least common are well-shaped dolines. He uniquely linked the shape of dolines to their formation processes, identifying funnel-shaped and bowl-shaped dolines as typical forms of suffosion processes in covered karst areas. He suggested that funnel-shaped dolines may result from either suffosion or collapse processes, making their precise morphogenetic origin challenging to determine. He refers to these as drawdown corrosion dolines.

Cvijić (1893) also classified dolines based on **morphostructural characteristics**, distinguishing them by the presence of sediment or water at the bottom, including »empty dolines« and those that are occasionally or permanently flooded. Čar (2001) expanded this by categorising dolines according to the structural conditions in which they form, identifying six basic types, which are stratification dolines, fissure dolines, bedded-fissured dolines, broken dolines, near-fault dolines, and fault dolines along with contact and reproduced dolines.

Cvijić (1893) first classified dolines based on **morphogenetic mechanisms**, linking different types to processes like corrosion, collapse, and tectonic influences. Cramer (1941) introduced a systematic typology, categorising dolines into collapse dolines, subsidence, solution, suffosion, and alluvial types. Gams expanded these classifications, adding terms like rocky dolines and fossil dolines, and highlighting compound

Table 1: Most notable morphological doline classifications with the original terms used.

Author, year	Doline shape			
Language	Bowl-shaped	Funnel-shaped	Well-shaped	Additional type
Cvijić, 1893 German	*Schüsselförmige Dolinen*	*Trichterförmige Dolinen*	*Brunnenförmige Dolinen*	*Dolinen mit großen Durchmessern (Dolines with large diameters)*
Cvijić, 1895 Serbian	*Karličaste vrtače*	*Levkaste vrtače*	*Oknaste vrtače*	*Nepravilne vrtače (Irregular dolines)*
Gams et al., 1962 Slovenian	*Skledaste vrtače*	*Lijakaste vrtače*	*Vodnjakaste vrtače*	*Kotlaste vrtače (Cauldron-shaped)*
Sauro, 2019 English	Bowl-shaped	Funnel-shaped	Well-shaped	/

and double dolines (Gams et al. 1962; Gams et al. 1973; Gams 1974). Maksimovič (1963) classified dolines by the dominant formation processes as solution dolines, suffosion dolines, subsidence dolines and erosion dolines, including polygenetic types, that are a combination of these processes, while Gams (2003) described the morphological evolution from funnel-shaped to bowl-shaped forms. Sauro (2003) further refined classifications, adding categories like accelerated solution dolines and intersection dolines. Waltham and Fookes (2003) provided a widely accepted typology in engineering geology, focusing on collapse dolines and suffosion dolines. De Waele and Gutiérrez (2022) simplified the typology to solution dolines and subsidence dolines, while Stepišnik (2020; 2024) categorised different dolines based on their formation processes and emphasised the difficulty in distinguishing late-stage collapse dolines from solution dolines. He categorized dolines as collapse dolines, suffosion dolines and solution dolines.

A review of morphometric and morphographic typologies shows that dolines are typically categorized based on parameters such as the extent of the flat floor, the ratio between depth and diameter, and slope inclination. These approaches often classify dolines based on their qualitative descriptions rather than based on morphometric properties, frequently without establishing specific morphometric criteria for different groups. Our analysis builds upon these existing typologies by integrating morphometric parameters to classify dolines more objectively. By applying quantitative criteria, we aim to bridge the gap between existing descriptive typologies and measurable geomorphological characteristics, providing a more consistent and reproducible classification framework.

3 Data and methods

3.1 Data

For the delineation of dolines, we used data from Stefanovski et al. (2024) and feature layers from recent studies on the Slovenian karst (Gostinčar and Stepišnik 2023; Stepišnik and Ferk 2023; Čonč et al. 2024; Mazej 2024; Stepišnik 2024). For this study, we delineated dolines in Slovenia using a DTM with 1 × 1 m spatial resolution. The visual results are only shown for southern Slovenia, as karst prevails in those regions.

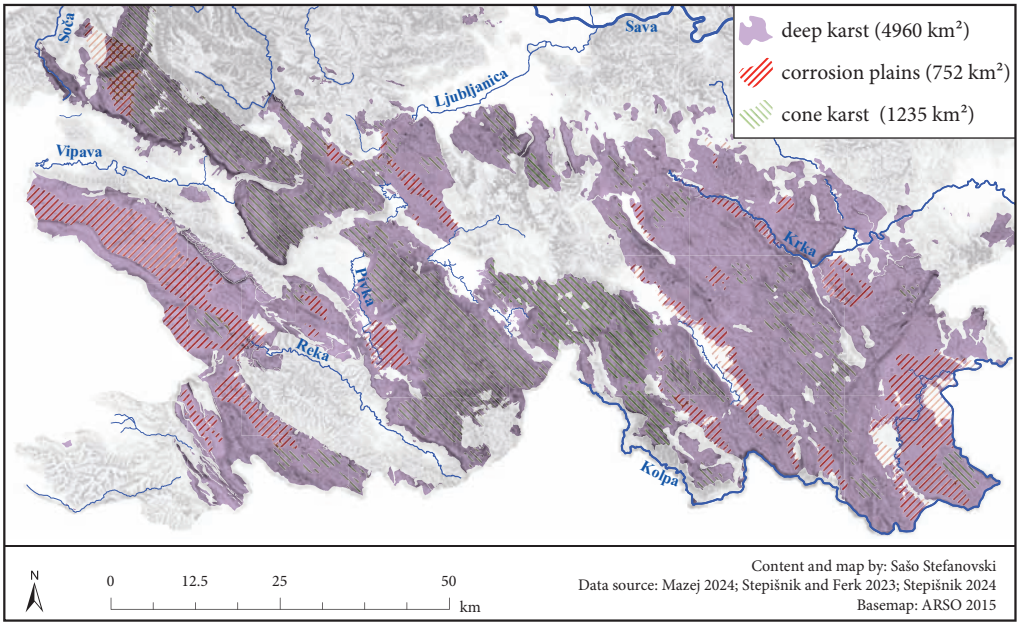

Figure 1: Extent of corrosion plains and cone karst in Slovenia.

Karstic regions in southern Slovenia are less fragmented, which simplified the interpretation of spatial patterns and the relationship between doline types and the characteristics of the karst landscape. Two main types of surface topography in deep karst where dolines are most common were identified: **corrosion plains** and **cone karst** (Figure 1). Corrosion plains are broad, flattened bedrock surfaces that cut horizontally across geological structures and are typically dotted with dolines and occasional conical hills (Stepišnik and Ferk 2023). In contrast, cone karst is a highly dissected terrain dominated by steep, conical hills and uvalas, formed by uneven vertical chemical denudation and the absence of surface water flow (Mazej 2024). The division into these two types of surface topography was chosen to investigate whether the types of dolines are influenced by the type of deep karst. These are currently the only two types of deep karst topography with precisely defined spatial extents, making them the sole input data for the analysis. The spatial extent of corrosion plains was obtained from Stepišnik and Ferk (2023) while cone karst extent was determined by Mazej (2024). For areas that do not fall into either category, there is currently insufficient information available to include them in the study. These areas are mostly karst slopes and areas with limited cone karst features that are not flat, based on the extent of cone karst and corrosion plains in Figure 1.

The general surface topography of karst in Slovenia is characterised by significant barren surfaces, though some areas are entirely covered by fine sediments (Gostinčar and Stepišnik 2023), referred to as uncovered and covered karst, respectively (Ford and Williams 2007). The extent of **uncovered karst** features in deep karst was calculated using the outcrop feature layer presented by Čonč et al. (2024). Outcrops were identified based on Topographic Position Index (TPI) values equal to or greater than 1 standard deviation, combined with slope thresholds that varied according to lithology. Our analysis aimed to explore whether the types of dolines are influenced by the distribution of sediments.

3.2 Doline delineation and classification

For the delineation of dolines, we applied the method presented by Stefanovski et al. (2024). Firstly, we identified dolines based on hydrological filling of sinks (Obu and Podobnikar 2013; Kobal et al. 2015; Ciglič et al. 2022; Čonč et al. 2022). Then their boundary was determined using Sky-View Factor (SVF) (Zakšek et al. 2011; Kokalj and Somrak 2019; Stefanovski et al. 2024). Since the goal was to classify standalone dolines, we excluded compound features and did not delineate dolines near roads, other routes, or buildings (within 5 meters). We removed all collapse dolines, that form with undermining in the subsurface, with the use of the collapse doline registry (Stepišnik 2010; Stepišnik 2024). The perimeters were smoothed by first shrinking each doline by ¼ of its width and then expanding it by the same factor. Features where the length exceeded the width by more than a factor of 2 were removed, as dolines are generally circular or slightly elongated (Gams et al. 1973; Gams 2003). These elongated features can be considered as other landforms, such as unroofed caves or landforms of fluvial origin. This process resulted in 179,288 standalone dolines used for classification.

We then calculated the basic morphometric properties of the dolines. Existing typologies typically differentiate doline types based on slope steepness and the extent of the doline floors, so we focused on these basic parameters for classification (Table 2). To calculate slope, we first applied a low-pass 3×3 mean filter to the DTM to smooth the surface. We used a value of 30° as the threshold for steep slopes. The threshold value for steep slopes was chosen as a previous study discussed this value as a threshold for active slopes, which indicate slopes where mass wasting is present (Stepišnik and Kosec 2011). Gently sloped terrain primarily indicates the doline floors. The 7° threshold was determined through testing on various examples to effectively capture doline floors, as lower values often failed to identify rugged floors. This value proved to be reliable for distinguishing doline floors from surrounding slopes, despite their gradual transitions, as floor morphology plays a crucial part in doline classifications (Cvijić 1893). The calculated value represents the share of a doline's surface area that meets the specified slope threshold used for classification. The perimeter axial ratio was also included, as elongation may indicate specific morphogenetic processes, such as horizontal cave denudation or the influence of fluvial activity (Sauro 2003; Grlj and Grigillo 2014; Stepišnik 2024). Perimeter axial ratio value of 100 represents dolines, where both axes are the same distance. A value of 50 represents dolines with lengths twice their width. Importantly, the classification lacks clearly defined morphometric thresholds, as the classes are continuous and gradually transition into one another.

Table 2: Morphometric parameters used in the process of classification.

Morphometric parameter	Description	Value
Percentage of steep slopes	Percentage of area with steep slopes (30° or more)	0–100
Percentage of gently sloped terrain	Percentage of area of gently sloped terrain (7° or less)	0–100
Perimeter axial ratio	Ratio between width and length	50–100

The classification was performed using ArcGIS Pro 3.0.0 software. Since the classification is raster-based, the morphometric parameters had to be rasterised. First, the polygon feature layer was converted into a point layer, so each doline was represented by a single 10 m^2 cell during rasterization. The point layer was then rasterised three times, once for each parameter. These layers were merged using the composite function and classified using ISO (Iterative Self-Organising) clustering, an unsupervised method ideal for identifying natural groupings without prior knowledge and suitable for parameters lacking a normal distribution (Jensen 2016). We defined a maximum of four classes, based on a literature review of typologies (Cvijić 1893; Cramer 1941; Gams 2003; Sauro 2003; Sauro 2019). While the results were homogeneous, it was not immediately clear which doline type each class, based on the literature, corresponded to. This was determined through class interpretation, where an observer identifies the existing classes and assigns them appropriate labels or descriptions (Oštir 2006).

3.3 Class interpretation

Class interpretation is a crucial step in unsupervised classification, transforming data-driven clusters into actionable insights by assigning meaningful labels. This ensures practical and relevant results. This was done by analysing the correlation between doline classes, extent of cone karst or corrosion plain and the presence of sediment cover. We began by interpreting the classification results, examining parameter distribution by class and analysing class distribution within corrosion plains and cone karst areas. The chi-square

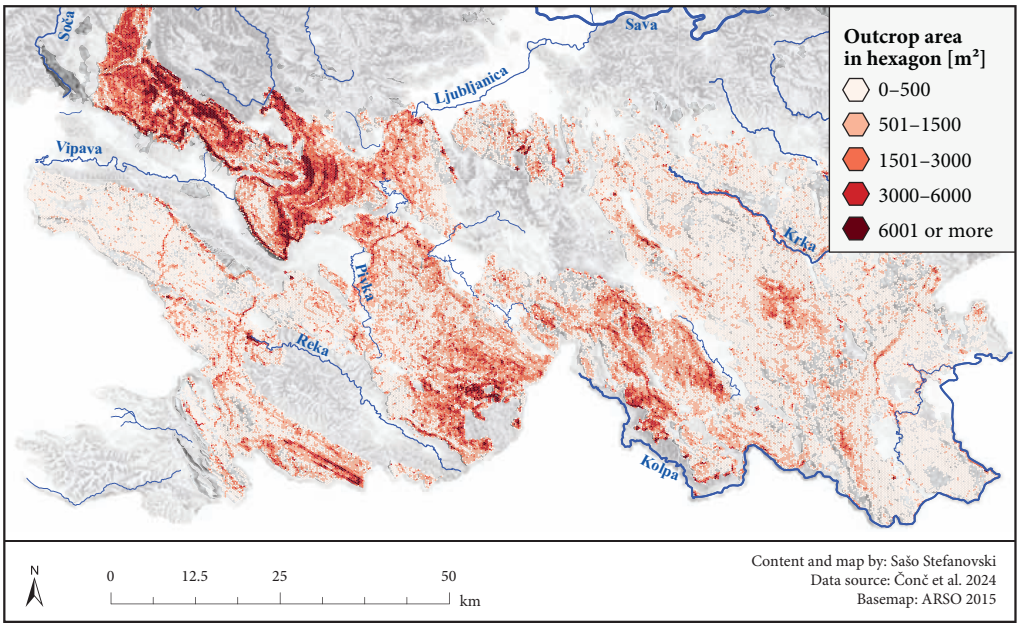

Figure 2: Extent of uncovered karst in 10 ha hexagons.

test was used to assess correlations between these deep karst types and doline classes, identifying significant relationships. The analysis was conducted in two steps: first, by comparing the classification (4 classes) with the presence or absence of corrosion plains, and second, by comparing the same classification with the presence or absence of cone karst areas.

To interpret the results, we also created density maps for each doline class using a 570 m radius in the point density tool, covering about 1 km² per calculation. These layers were standardised to a 0–1 scale using the fuzzy membership tool and displayed with a minimum-maximum stretch. The proportion of uncovered karst features in deep karst was calculated using a feature layer from Čonč et al. (2024) with the study area divided into 10 ha hexagons. The Summarise Within tool calculated the extent of uncovered karst per hexagon (Figure 2). We used IBM SPSS Statistics 26 for correlation analysis and the Mann-Whitney U test for comparing two independent groups. Both tests were chosen for their suitability with non-normally distributed data (Sheskin 2007).

4 Results

4.1 Morphometric properties of classified dolines

Figure 3 shows that the distribution of active slope percentages in dolines is strongly left-skewed, which means that dolines with a smaller share of steep slopes are more common. Specifically, 57,504 dolines feature steep slopes that account for 1% or less of their total area. The distribution of gently sloping terrain is similar, showing that dolines with a smaller percentage of gently sloped terrain are more common. This suggests that, on average, dolines have a small proportion of steep slopes and gently sloping terrain, with slope inclinations between 7° and 30° being most common. These dolines make up approximately 85% of doline cases analysed. The axial ratio distribution is peaking around the interval between 82 and 84, indicating a more normal distribution. This suggests that most dolines have a slightly elongated shape rather than being perfectly circular. Table 3 shows the mean, median and 95th percentile of morphometric parameters used in the classification.

Table 3: Basic descriptive statistics of morphometric parameters used in the process of classification.

Morphometric parameter	Mean	Median	95th Percentile
Percentage of steep slopes	8	3	29
Percentage of gently sloped terrain	15	9	51
Perimeter axial ratio	78	80	92

4.2 Classification results

In this study, dolines were classified into four classes using the ISO clustering method, an unsupervised classification approach where the number of classes was set by the user according to literature suggesting three to four doline types. The classification criteria included the proportion of steep slopes, gently inclined slopes, and axial ratio (Table 4; Figure 4).

Class 0 is characterised by a small proportion of steep slopes and gently sloping terrain, with approximately 85% dolines having slope inclinations between 7° and 30° and being slightly elongated but rounder than the average of all the dolines in the study area, which is 78. Class 1 differs from other classes primarily in having a large area of steep slopes (Figure 4), with most dolines featuring over 10% active slopes and being more elongated than those in Class 0. Class 2 typically lacks extensive areas of steep slopes, is characterised by gently sloping terrain, and includes dolines that are more elongated compared to Class 0 and 1, as indicated by a right-skewed axial ratio histogram. In contrast to Class 2, Class 3 shows a decrease in steep slopes and gently sloping terrain, with a left-skewed slope inclination histogram, and these dolines are distinctly elongated, as reflected by their axial ratio.

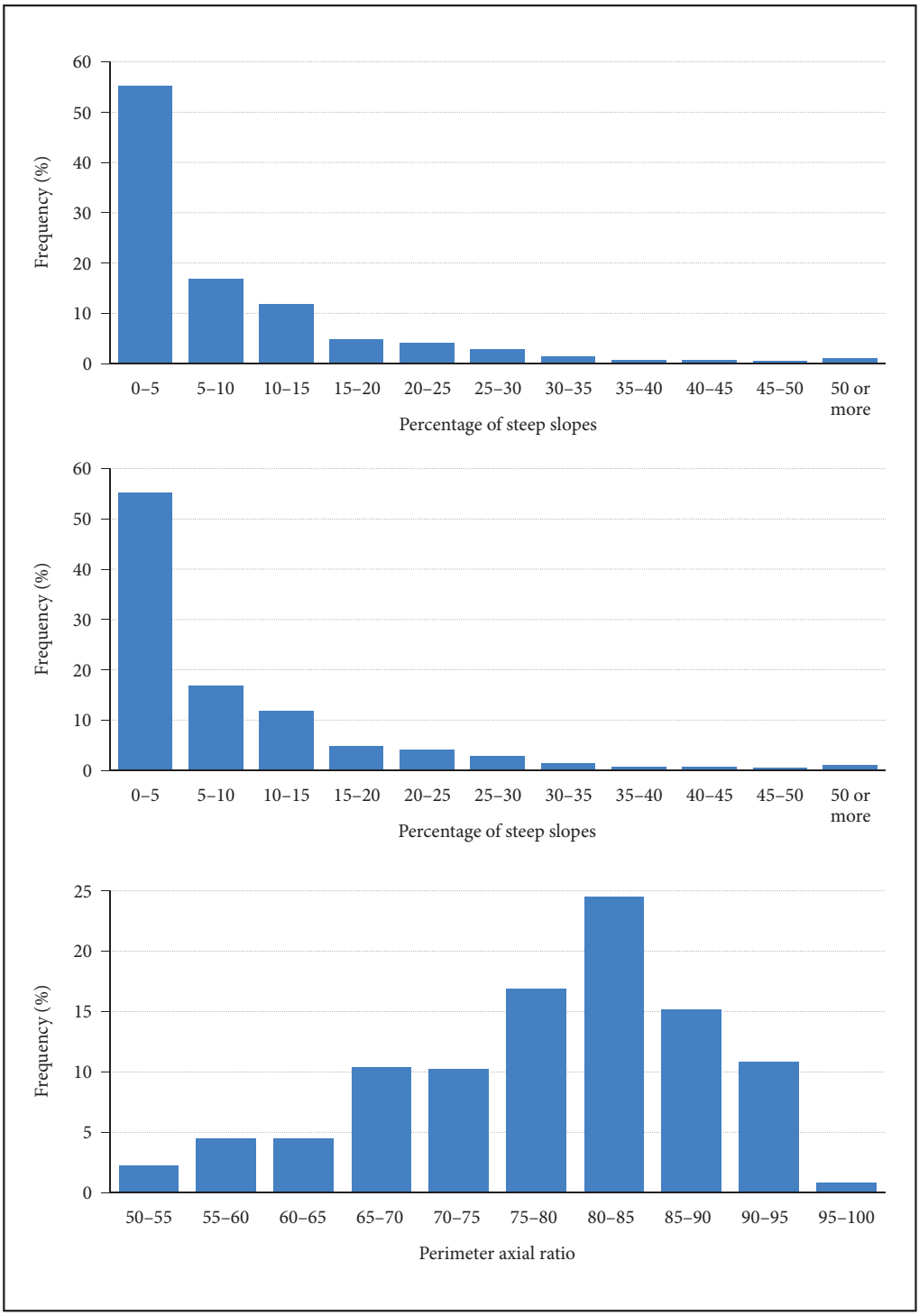

Figure 3: Histograms of morphometric parameters of dolines with descriptive statistics.

Table 4: Basic descriptive statistics of morphometric parameters used in the process of classification based for each class.

Morphometric parameter	Statistic	Class 0	Class 1	Class 2	Class 3	All classes
Percentage of steep slopes	Mean	3	23	1	7	8
	Median	2	19	0	4	3
	95th Percentile	9	50	4	23	29
Percentage of gently sloped terrain	Mean	11	4	52	12	15
	Median	9	4	47	9	9
	95th Percentile	27	12	89	29	51
Perimeter axial ratio	Mean	84	83	75	66	78
	Median	84	83	75	67	8
	95th Percentile	92	93	90	74	92

4.3 Spatial distribution of doline classes

Class 0 dolines are the most numerous in Slovenian deep karst, followed by Class 3 (Figure 5). Class 1 is only slightly less common, being 4% behind Class 3, while Class 2 is the rarest. In corrosion plains, the proportion of Class 0 dolines is even higher than the general distribution, with a notable increase in the percentage of Class 2 dolines, suggesting that Class 2 dolines may be typical of corrosion plains. Class 1 dolines are the least common in these areas. In contrast, cone karst areas show a different pattern, where Class 1 dolines are more prevalent, and Class 2 dolines are the least common. The percentage of Class 3 dolines also is higher in cone karst areas, though Class 0 dolines remain the most common type in these regions.

The chi-square results are indicating a strong correlation between class distribution and whether the area is a corrosion plain or a cone karst area (Table 5). The p-values, all below 0.05, further confirm a significant correlation. This suggests that the distribution of doline classes is not random but is instead related to the specific type of karst, meaning certain classes are more likely to be found in particular karst environments.

The highest density of **Class 0 dolines** is found in corrosion plains of all types, with the Logatec-Begunje dry polje having the highest concentration. Lower densities are observed on high karst plateaus such as Nanos, Snežnik, and Trnovski Gozd, although Class 0 dolines still occur in these areas. Overall, Class 0 dolines are present across nearly all deep karst regions in Slovenia (Figure 6).

Class 1 dolines show a markedly different spatial distribution compared to Class 0. The highest density of Class 1 dolines is found in the cone karst area of Kočevski Rog. Some parts of the corrosion plains also exhibit higher concentrations of Class 1 dolines. Additionally, there are localised areas of high density in the Ljubljanica River catchment, particularly in the hinterland of major ponors and springs.

Class 2 dolines rarely exhibit high densities, and when they do, these are very localised. Notably, higher densities are observed in areas of corrosion plains, with the highest densities found in the Karst corrosion plain, as well as Kočevje corrosion plain and Bela Krajina corrosion plain.

Class 3 dolines are more densely concentrated in areas with greater slopes, such as the sloping terrain between Nanos and Hrušica. Menišija also exhibits a high density of Class 3 dolines. These dolines are more frequently observed in cone karst areas and especially in dolostone karst.

Table 5: Chi-square test results for correlation between doline classes and the two karst types.

Karst type	Chi-square value	P-value	Null hypothesis
Corrosion plain	7873.3	0.00	Rejected
Cone karst	3375.5	0.00	Rejected

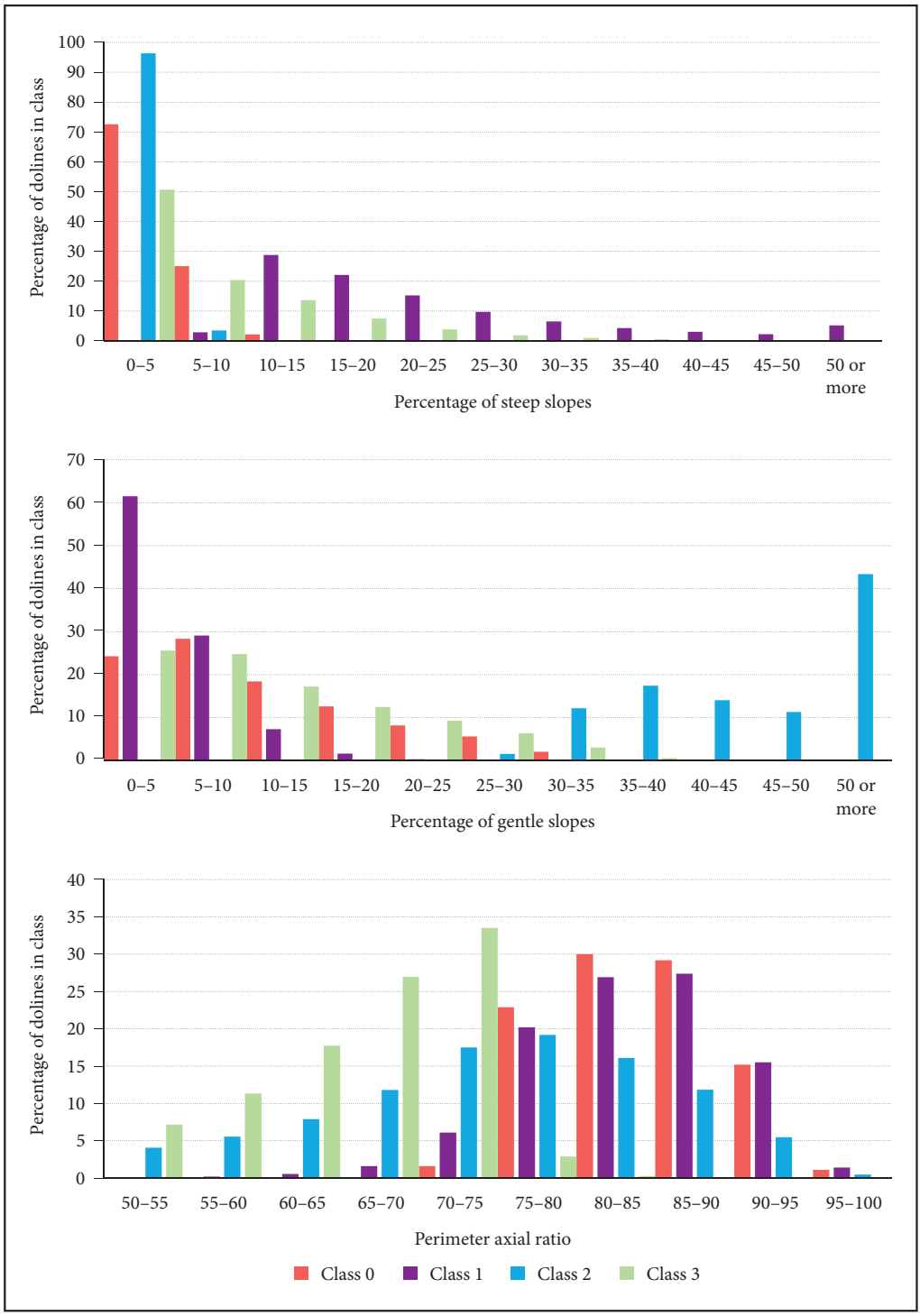

Figure 4: Histograms of dolines ISO classification parameters.

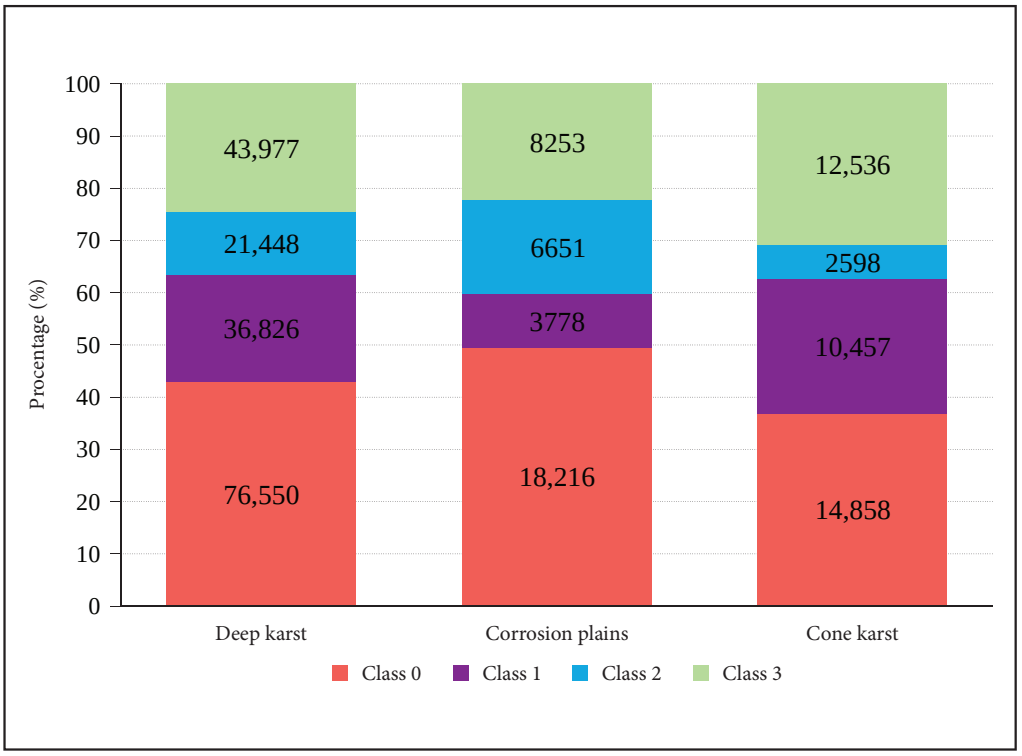

Figure 5: Distribution of doline classes across different karst types.

4.4 Doline classes and sediment cover

Some doline classes are more prevalent in karst environments extensively covered by sediment (Figure 7). Notably, Class 2 stands out, with approximately three quarters of its dolines in covered karst with 5 m^2 or less outcrops in their surroundings, and it also has the lowest mean and median values. In contrast, Class 1 shows the opposite trend, having the fewest dolines that are completely covered by sediments compared to other classes. Class 1 dolines are the most frequent class in areas with 25 m^2 or more outcrops in their surroundings, and they exhibit the highest mean and median values, indicating a preference for rocky terrain. Nearly half of the Class 0 dolines have little to no outcrops nearby, with the remainder mostly showing low values. Class 3 is similar to Class 1 regarding covered karst area, with the second-highest mean and median values and a high percentage of dolines with more than 25 m^2 of outcrops in their surroundings.

Table 6 displays the results of the Mann-Whitney U test. The differences in the share of uncovered karst between the classes are statistically significant, since the p-value does not exceed 0.05. Thus, we can reject all null hypotheses. This suggests that some doline types are linked to areas with continuous sediment cover, while others occur in regions with sparse or minimal sediment.

Figure 6: Doline density by class. ➤ p. 20

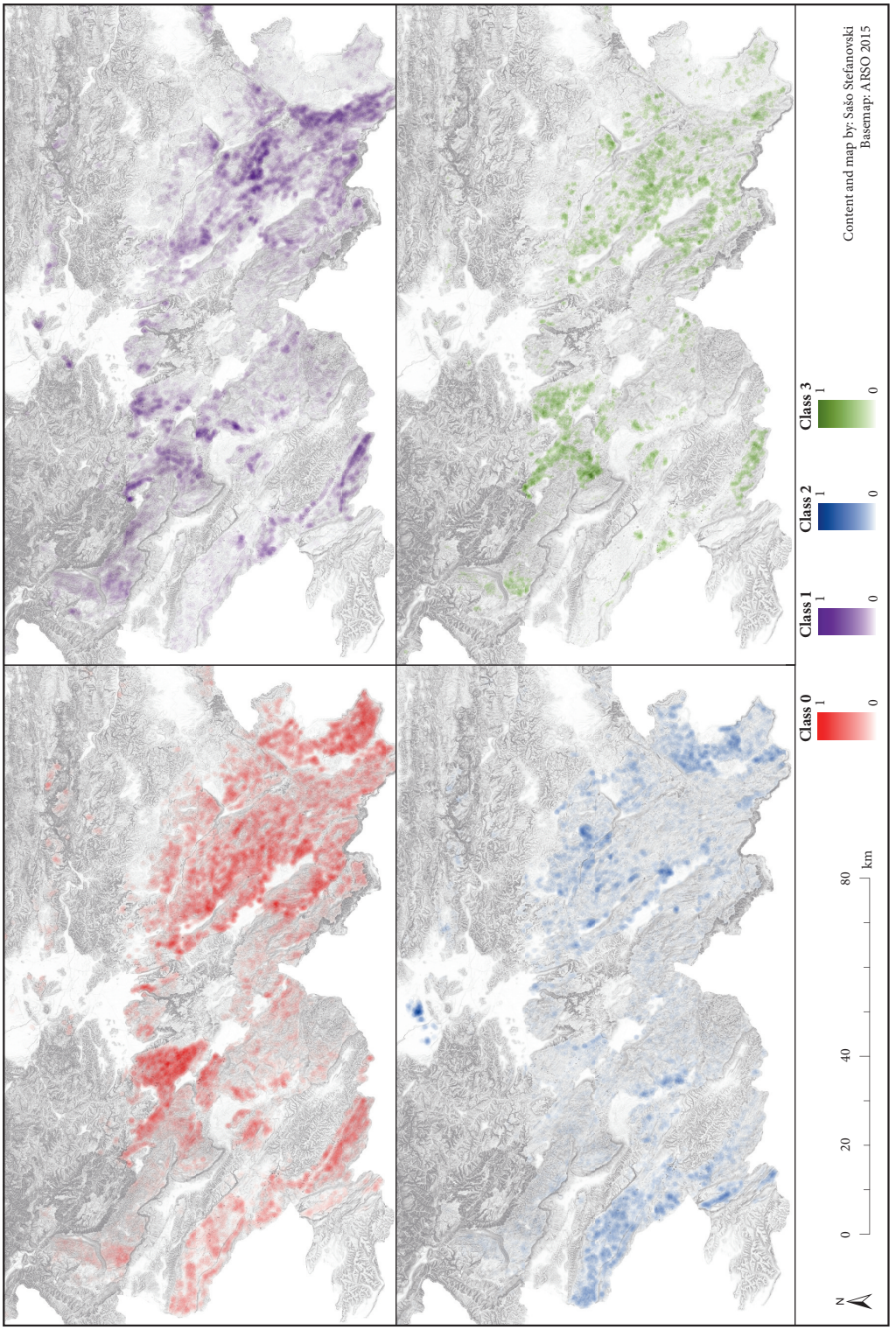
Class 0
1
0
Class 1
1
0
Class 2
1
0
Class 3
1
0
Content and map by: Sašo Stefanovski
Basemap: ARSO 2015
N
0
20
40
80
km

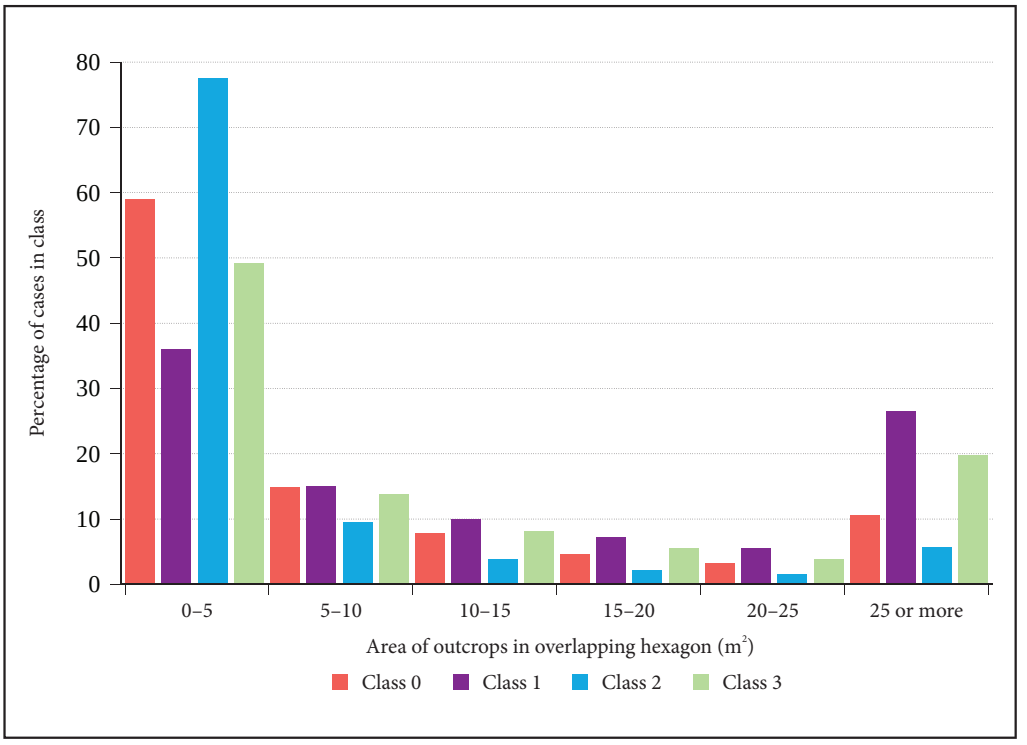

Figure 7: Area of outcrops in doline surroundings.

Table 6: Results of Mann-Whitney U test.

Classes	U-statistic	P-value	Null hypothesis
(0, 3)	$1.47x10^9$	0.00	Rejected
(0, 2)	$1.04x10^9$	0.00	Rejected
(0, 1)	$0.99x10^9$	0.00	Rejected
(3, 2)	$0.64x10^9$	0.00	Rejected
(3, 1)	$0.68x10^9$	0.00	Rejected
(2, 1)	$0.19x10^9$	0.00	Rejected

5 Discussion

Using parameters such as steep slopes, gently sloping terrain, and perimeter axial ratio, we conducted an unsupervised ISO classification with four doline classes, based on literature. The results were then linked to morphographic typologies. We applied established doline terms from the literature, clearly defining them both morphographically and morphometrically. This is visible in Figure 8.

Figure 8: Morphological types of dolines and their main features. ➤ p. 22

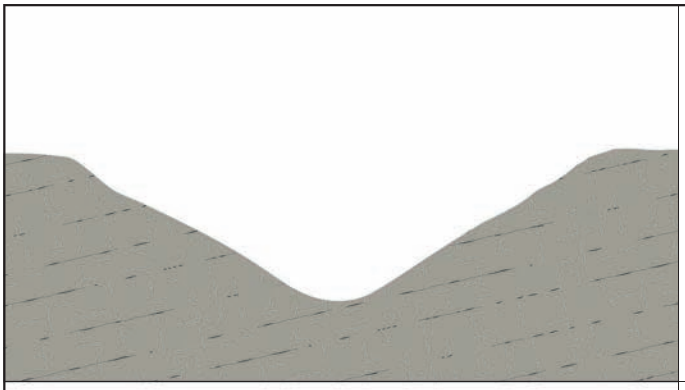

Funnel–shaped doline
- usual presence of active slopes
- narrow concave floors
- slightly elongated
- typical for cone karst and corrosion plains
- typical for covered and semi–covered karst

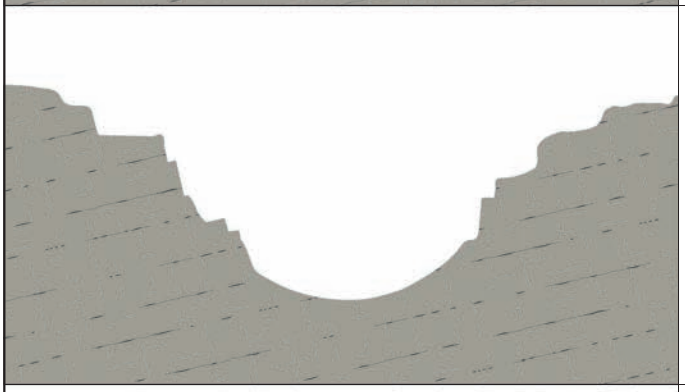

Well–shaped doline
- large proportion of active slopes
- narrow to semi–narrow concave floors
- typical for cone karst
- typical for semi–covered karst

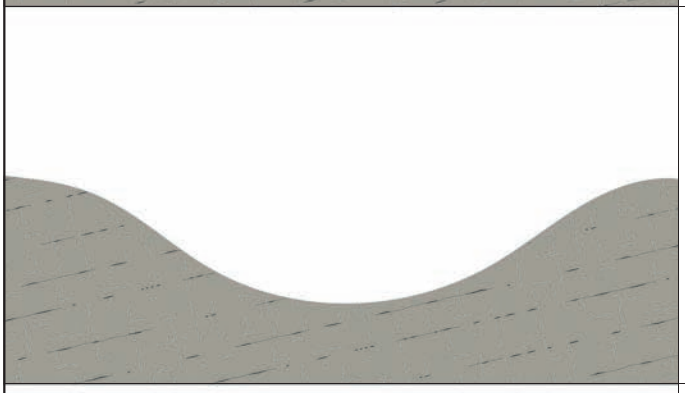

Bowl–shaped doline
- near absence of active slopes
- extensive flat floors
- moderately elongated
- typical for corrosion plains
- typical for covered karst

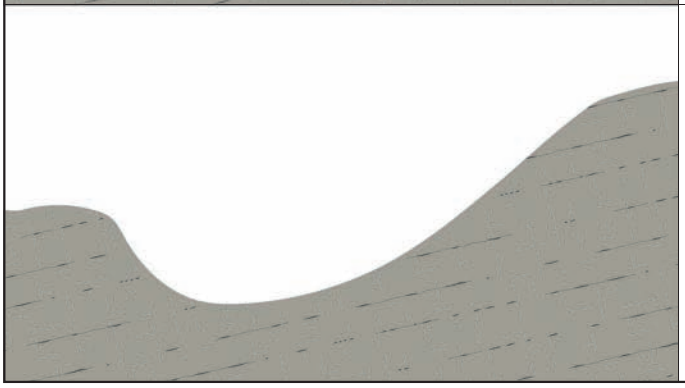

Elongated doline
- near absence of active slopes
- narrow to semi–narrow concave floors
- length greatly exceeds width
- typical for dolostone cone karst
- typical for covered karst

Class 0 dolines are characterised by the presence of steep slopes, though these constitute only a small portion of the doline. The slope inclination between 7° and 30° prevails in this class, with a low proportion of gently sloping terrain. Majority of Class 0 dolines have an axial ratio between 80 and 90. Morphologically, they get narrower with depth and have narrow floors, with a slightly elongated ground plan. Cvijić (1893) first described these as funnel-shaped dolines, wide at the top and narrow at the bottom. Gams et al. (1973) also used the term funnel-shaped based on their cross-sectional profile. As this term is still widely used (Gams 2000; Gams 2003; Sauro 2019) we propose maintaining the usage of »**funnel-shaped dolines**« (sl. *lijakaste vrtače*) for this type.

Class 1 dolines are characterised by a large proportion of steep slopes, with most having an area of 10% or more. Gently sloping terrain is rare, with 68% of these dolines having 5% or less of such terrain. The axial ratio is slightly lower than in Class 0 dolines, but they remain only slightly elongated. These dolines have steep slopes, often with walls, and narrow floors are more common than larger ones. Cvijić (1893) first described dolines with steep, vertical, or inclined slopes, which he termed well-shaped. Gams' descriptions (Gams et al. 1962; Gams et al. 1973; Gams 2000; Gams 2003) align Class 1 dolines with well-shaped and kettle-shaped dolines, though the term kettle-shaped is problematic, as it is typically used for glaciokarst features (Kunaver 1983; Žebre and Stepišnik 2015; Ferk et al. 2017). Therefore, we recommend using the term »**well-shaped dolines**« (sl. *vodnjakaste vrtače*) for those with a high proportion of steep slopes, regardless of floor morphology.

Class 2 dolines are characterised by the near absence of steep slopes, with almost all having less than 5% of their area comprising steep slopes. Conversely, these dolines have the largest percentage of gently sloped terrain, with nearly all having at least 30% gently sloped terrain. The axial ratio varies, but most dolines fall between 70 and 80, indicating slight elongation. These dolines rarely experience mass wasting processes and typically feature extensive, flat floors, often due to anthropogenic alterations. Given their gentle slopes and broad floors, these dolines are generally shallow. Cvijić (1893) first described such dolines as bowl-shaped, noting their small depth relative to their diameter and lack of steep slopes. The term »**bowl-shaped doline**« (sl. *skledaste vrtače*) remains widely used (Gams 2003; Sauro 2019; De Waele and Gutiérrez 2022), making it an appropriate term for this class.

Class 3 dolines exhibit a wide range of morphometric characteristics, with their number decreasing as the proportion of steep slopes and gently sloping terrain increases. The most distinguishing feature of these dolines is their axial ratio, which typically ranges from 50 to 75, indicating significant elongation. This elongation is the primary characteristic that sets these dolines apart from other types. Cvijić (1893) was the first to identify such elongated dolines, referring to them as valley-shaped dolines, though he did not provide detailed morphological descriptions. While elongation in dolines is sometimes associated with compound features (Gams et al. 1962; Gams et al. 1973; Gams 2003), this study focuses exclusively on standalone dolines. Previous research on karst anisotropy, also identified elongated dolines as significant geomorphological features in karst landscapes (Verbovšek 2024). The term »valley-shaped doline« can be misleading due to its derivation from the Slavic word for valley (dolina), which could cause confusion. As elongation is the main parameter defining the shapes of these dolines, we propose the term »**elongated dolines**« (sl. *podolgovate vrtače*), as it accurately reflects their defining morphometric characteristic. By »elongated«, we refer to dolines, that are distinctly elongated, somewhat linear depressions with a profile resembling a shallow channel or trough, rather than a circular or bowl-like pit.

We then analysed their spatial distribution in Slovenia and investigated the correlation between doline types and morphogenetic karst types (Stepišnik and Ferk 2023; Stefanovski et al. 2024; Stepišnik 2024). The distribution of doline types and karst types shows a strong correlation, with certain doline types being more characteristic of specific deep karst environments.

Bowl-shaped dolines (Class 2) are mainly found on corrosion plains, with the highest densities on covered karst areas (Figure 9). Well-shaped dolines (Class 1) are most common in cone karst areas with greater elevation changes, though they also appear less frequently on corrosion plains and are more common in semi-covered karst areas. Funnel-shaped dolines (Class 0), the most prevalent type in Slovenian deep karst, occur in both cone karst regions and corrosion plains, with higher densities in covered and semi-covered karst. Elongated dolines (Class 3) are found in cone karst areas, corrosion plains, and covered and semi-covered karst regions. They fall into two distinct groups. The first group is located in the hinterland, where high-discharge watercourses contribute to allogenic recharge in karst systems, and their shape can be linked to the gradual collapse of horizontal cave passages (Bahun 1969; Mihevc and Zupan Hajna 2007; Hajna et al. 2024). The second group is found on slopes, particularly on covered karst slopes in dolostone cone karst areas, where elongated dolines are especially characteristic.

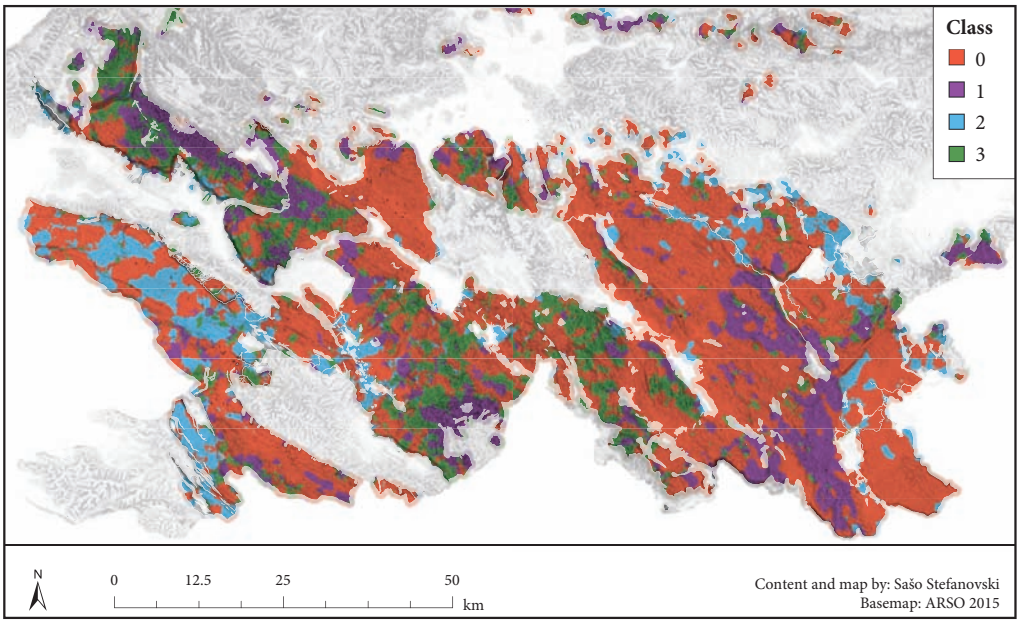

Figure 9: A map of deep karst in southern Slovenia based on the predominant type of dolines.

Although this article does not focus on the morphogenetic interpretation of doline formation, the discussion reveals that doline distribution is closely linked to the prevailing karst type. Deep karst types, shaped by varying denudational processes and sediment presence, suggest that doline types are also accredited to distinct morphogenetic and morphodynamic processes. Sauro (2019) noted that funnel-shaped and bowl-shaped dolines are typical of suffosion dolines, and our study confirms that bowl-shaped dolines are common in covered karst, where suffosion dolines predominate. Well-shaped dolines correspond to earlier stages of collapse dolines, gradually becoming more funnel-shaped as the slope angle decreases (Šušteršič 1973; Šušteršič 1994; Šušteršič 2000; Waltham et al. 2005; Sauro 2012; Lipar et al. 2019; Sauro 2019). Their spatial distribution indicates this, with higher densities found in areas with collapsed dolines due to denser cave systems (Stepišnik 2010). Funnel-shaped dolines may represent a morphogenetic convergence of both collapse and suffosion types, making their exact origin difficult to determine in later stages. Elongated dolines, appear in areas where high-discharge watercourses contribute to allogenic recharge in karst systems, linked to the gradual collapse of horizontal cave passages, and on slopes, particularly covered karst slopes in dolostone cone karst areas, where they are especially characteristic.

6 Conclusion

In this study, we classified dolines in Slovenian deep karst based on their morphometric characteristics and studied their spatial distribution in southern Slovenia. We focussed on classifying dolines based on the extent of steep slopes, floor extent and perimeter elongation, as previous morphographic descriptions of dolines was mainly centred on describing these characteristics. Development in GIS now enables precise morphometric analyses. We defined four different morphometric types of dolines that are consistent with existing typologies. These include funnel-shaped dolines, which narrow with increasing depth; well-shaped dolines, characterised by steep slopes that often form walls; bowl-shaped dolines, characterised by a low slope inclination and a flat, extensive floor; and elongated dolines, which are notable for their significant elongation of the ground plan. The results show that the shape of dolines is closely related to different karst types, suggesting that their formation is driven by processes characteristic of specific karst types.

ACKNOWLEDGEMENT: The authors would like to thank the anonymous reviewers and the editorial board for their constructive comments and suggestions, which greatly contributed to improving the quality of this article. The research was financially supported by the Slovenian Research and Innovation Agency: P6-0229, P6-0101, I0-0031, P1-0195, J6-50213.

RESEARCH DATA: For information on the availability of research data related to the study, please visit the article webpage: https://doi.org/10.3986/AGS.13940.

7 References

Bahun, S. 1969: On the formation of dolines. *Geološki vjesnik* 22-1.

Bögli, A. 1980: Karst hydrology and physical speleology. Springer-Verlag.

Bondesan, A., Meneghel, M., Sauro, U. 1992: Morphometric analysis of dolines. *International Journal of Speleology* 21-1. https://doi.org/10.5038/1827-806X.21.1.1

Ciglič, R., Čonč, Š., Breg Valjavec, M. 2022: The impact of digital elevation model preprocessing and detection methods on karst depression mapping in densely forested Dinaric mountains. *Remote Sensing* 14-10. https://doi.org/10.3390/rs14102416

Cramer, H. 1941: Die Systematik der Karstdolinen. *Neues Jahrbuch für Mineralogie, Geologie und Paläontologie* 85-1.

Cvijić, J. 1893: Das karstphänomen: Versuch einer morphologischen monographie. Hölzel.

Cvijić, J. 1895: Karst: Geografska monografija. Srpska akademija nauka i umetnosti.

Čar, J. 1982: Geološka zgradba požiralnega obrobja Planinskega polja. *Acta Carsologica* 10-1.

Čar, J. 2001: Structural bases for shaping of dolines. *Acta Carsologica* 30-2.

Čar, J. 2018: Geostructural mapping of karstified limestones. *Geologija* 61-2. https://doi.org/10.5474/geologija.2018.010

Čonč, Š., Oliveira, T., Belotti, E., Bufka, L., Černe, R., Heurich, M., Breg Valjavec, M., Krofel, M. 2024: Revealing functional responses in habitat selection of rocky features and rugged terrain by Eurasian Lynx (Lynx lynx) using LiDAR data. *Landscape Ecology* 39-7. https://doi.org/10.1007/s10980-024-01923-y

Čonč, Š., Oliveira, T., Portas, R., Černe, R., Breg Valjavec, M., Krofel, M. 2022: Dolines and cats: Remote detection of karst depressions and their application to study wild felid ecology. *Remote Sensing* 14. https://doi.org/10.3390/rs14030656

De Waele, J., Gutiérrez, F. 2022: Karst hydrogeology, geomorphology and caves. Wiley. https://doi.org/10.1002/9781119605379.fmatter

Ferk, M., Gabrovec, M., Komac, B., Zorn, M., Stepišnik, U. 2017: Pleistocene glaciation in Mediterranean Slovenia. In: Quaternary glaciation in the mediterranean mountains. Geological Society of London. https://doi.org/10.1144/sp433.2

Ford, D., Williams, P. D. 2007: Karst hydrogeology and geomorphology. Wiley.

Frelih, M. 2014: Gostota, razporeditev in morfološke značilnosti vrtač na izbranih primerih v Sloveniji. *Ph.D. thesis*. Univerza v Ljubljani.

Gams, I. 1974: Kras: zgodovinski, naravoslovni in geografski oris. Slovenska matica.

Gams, I. 2000: Doline morphogenetic processes from global and local viewpoint. *Acta Carsologica* 29-2.

Gams, I. 2003: Kras v Sloveniji v prostoru in času. Založba ZRC.

Gams, I., Kunaver, J., Novak, D., Jenko, F., Savnik, R. 1962: Kraška terminologija. *Geografski vestnik* 34-1.

Gams, I., Kunaver, J., Radinja, D. 1973: Slovenska kraška terminologija. Univerza v Ljubljani.

Gostinčar, P., Stepišnik, U. 2023: Extent and spatial distribution of karst in Slovenia. *Acta geographica Slovenica* 63-1. https://doi.org/10.3986/AGS.11679

Grlj, A., Grigillo, D. 2014: Uporaba digitalnega modela višin in satelitskega posnetka RapidEye za zaznavanje kraških kotanj in brezstropih jam Podgorskega krasa. *Dela* 42-1. https://doi.org/10.4312/dela.42.7.129-147

Habič, P. 1986: Površinska razčlenjenost dinarskega krasa. *Acta Carsologica* 14-15.

Hajna, N. Z., Pruner, P., Bosák, P., Mihevc, A. 2024: Temporal insights into karst system evolution: A case study of the unroofed cave above Škocjanske jame, NW Dinarides. *Geomorphology* 461. https://doi.org/10.1016/j.geomorph.2024.109282

Jeanpert, J., Genthon, P., Maurizot, P., Folio, J.-L., Vende-Leclerc, M., Sérino, J., Join, J.-L., Iseppi, M. 2016: Morphology and distribution of dolines on ultramafic rocks from airborne LiDAR data: The case of southern Grande Terre in New Caledonia (SW Pacific). *Earth Surface Processes and Landforms* 41-1. https://doi.org/10.1002/esp.3952

Jennings, J. N. 1985: Karst geomorphology. Basil Blackwell.

Jensen, J. R. 2016: Introductory digital image processing: A remote sensing perspective. Pearson Education, Incorporated.

Kobal, M., Bertoncelj, I., Pirotti, F., Dakskobler, I., Kutnar, L. 2015: Using LiDAR data to analyse sinkhole characteristics relevant for understory vegetation under forest cover – case study of a high karst area in the Dinaric mountains. *PLOS ONE* 10-3. https://doi.org/10.1371/journal.pone.0122070

Kokalj, Ž., Somrak, M. 2019: Why not a single image? Combining visualizations to facilitate fieldwork and on-screen mapping. *Remote Sensing* 11-7. https://doi.org/10.3390/rs11070747

Kunaver, J. 1983: Geomorphology of the Kanin mountains with special regard to the glaciokarst. *Geografski zbornik* 12-1.

Lipar, M., Stepišnik, U., Ferk, M. 2019: Multiphase breakdown sequence of collapse doline morphogenesis: An example from Quaternary aeolianites in Western Australia. *Geomorphology* 327. https://doi.org/10.1016/j.geomorph.2018.11.031

Maksimovič, G. 1963: Osnovi karstovedenia.

Mazej, T. 2024: Geomorfološke značilnosti kopastega krasa v sloveniji. *Master thesis*. Univerza v Ljubljani.

Mihevc, A., Zupan Hajna, N. 2007: Sestava in izvor klastičnih sedimentov iz vrtač in brezstropih jam pri Divači. In: Kraški pojavi, razkriti med gradnjo slovenskih avtocest. Založba ZRC.

Mihevc, A., Mihevc, R. 2021: Morphological characteristics and distribution of dolines in Slovenia, a study of a lidar-based doline map of Slovenia. *Acta Carsologica* 50-1. https://doi.org/10.3986/ac.v50i1.9462

Obu, J., Podobnikar, T. 2013: Algorithm for karst depression recognition using digital terrain models. *Geodetski vestnik* 57-2. https://doi.org/10.15292/geodetski-vestnik.2013.02.260-270

Oštir, K. 2006: Daljinsko zaznavanje. Založba ZRC.

Pavlopoulos, K., Evelpidou, N., Vassilopoulos, A. 2009: Mapping geomorphological environments. Springer. https://doi.org/10.1007/978-3-642-01950-0

Péntek, K., Veress, M., Lóczy, D. 2007: A morphometric classification of solution dolines. *Zeitschrift für Geomorphologie* 51-1.

Sauro, U. 2003: Dolines and sinkholes: Aspects of evolution and problems of classification. *Acta Carsologica* 32-2.

Sauro, U. 2012: Closed depressions in karst areas. In: Encyclopedia of caves. Academic Press.

Sauro, U. 2019: Chapter 33 – Closed depressions in karst areas. In: Encyclopedia of caves. Academic Press.

Sheskin, D. J. 2007: Handbook of parametric and nonparametric statistical procedures. Chapman & Hall/CRC.

Stefanovski, S., Kokalj, Ž., Stepišnik, U. 2024: Sky-view factor enhanced doline delineation: A comparative methodological review based on case studies in Slovenia. *Geomorphology* 465. https://doi.org/10.1016/j.geomorph.2024.109389

Stepišnik, U. 2010: Udornice v Sloveniji. Znanstvena založba Filozofske fakultete.

Stepišnik, U. 2020: Fizična geografija krasa. Znanstvena založba Filozofske fakultete.

Stepišnik, U. 2024: Geomorfologija krasa Slovenije. Znanstvena založba Filozofske fakultete. https://doi.org/10.4312/9789612973131

Stepišnik, U., Ferk, M. 2023: Morphogenesis and classification of corrosion plains in Slovenia. *Acta geographica Slovenica* 64-1. https://doi.org/10.3986/AGS.11774

Stepišnik, U., Kosec, G. 2011: Modelling of slope processes on karst. *Acta Carsologica* 40-2. https://doi.org/10.3986/ac.v40i2.11

Sweeting, M. M. 1973: Karst landforms. Columbia University Press.

Šegina, E., Benac, Č., Rubinić, J., Knez, M. 2018: Morphometric analyses of dolines – the problem of delineation and calculation of basic parameters. *Acta Carsologica* 47-1. https://doi.org/10.3986/ac.v47i1.4941

Šerko, A. 1947: Kraški pojavi v Jugoslaviji. *Geografski vestnik* 19-1.

Šušteršič, F. 1973: K problematiki udornic in sorodnih oblik visoke Notranjske. *Geografski vestnik* 45-1.

Šušteršič, F. 1994: Classic dolines of classical site. *Acta Carsologica* 23-1.

Šušteršič, F. 2000: Are collapse dolines formed only by collapse? In: 8th International Karstological School – Collapse Dolines, Postojna, June 26-29th, 2000. Slovenska akademija znanosti in umetnosti.

Šušteršič, F. 2006: A power function model for the basic geometry of solution dolines: Considerations from the classical karst of south-central Slovenia. *Earth Surface Processes and Landforms* 31-3.
Šušteršič, F. 2017: A conceptual model of dinaric solution doline dynamics. *Cave and Karst Science* 44.
Telbisz, T. 2021: Lidar-based morphometry of conical hills in temperate karst areas in Slovenia. *Remote Sensing* 13-14. https://doi.org/10.3390/rs13142668
Telbisz, T., Dragvaica, H., Nagy, B. 2009: Doline morphometric analysis and karst morphology of Biokovo mt (Croatia) based on field observations and digital terrain analysis. *Hrvatski geografski glasnik* 71-2.
Verbovšek, T. 2024: Analysis of karst surface anisotropy using directional semivariograms, Slovenia. *Pure and Applied Geophysics* 181. https://doi.org/10.1007/s00024-023-03411-x
Verbovšek, T., Gabor, L. 2019: Morphometric properties of dolines in Matarsko podolje, SW Slovenia. *Environmental Earth Sciences* 78-14. https://doi.org/10.1007/s12665-019-8398-6
Waltham, T., Bell, F., Culshaw, M. 2005: Sinkholes and subsidence: Karst and cavernous rocks in engineering and construction. Springer, Praxis. https://doi.org/10.1007/b138363
Waltham, T., Fookes, P. G. 2003: Engineering classification of karst ground conditions. *Quarterly Journal of Engineering Geology and Hydrogeology* 36-2. https://doi.org/10.1144/1470-9236/2002-33
White, W. B. 1988: Geomorphology and hydrology of karst terrains. Oxford University Press.
Zakšek, K., Oštir, K., Kokalj, Ž. 2011: Sky-view factor as a relief visualization technique. *Remote Sensing* 3-2. https://doi.org/10.3390/rs3020398
Zumpano, V., Pisano, L., Parise, M. 2019: An integrated framework to identify and analyze karst sinkholes. *Geomorphology* 332. https://doi.org/https://doi.org/10.1016/j.geomorph.2019.02.013
Žebre, M., Stepišnik, U. 2015: Glaciokarst geomorphology of the Northern Dinaric Alps: Snežnik (Slovenia) and Gorski Kotar (Croatia). *Journal of Maps* 12-5. https://doi.org/10.1080/17445647.2015.1095133

Acta geographica Slovenica, 65-2, 2025, 29–45

RECONSTRUCTION OF PALAEOFLOW AND DEPOSITIONAL DYNAMICS FROM THE MERJASEC UNROOFED CAVE, LAZE PLAIN (CENTRAL SLOVENIA)

Primož Miklavc, Matej Lipar, France Šušteršič, Andrej Šmuc

ANDREJ ŠMUC

Merjasec unroofed cave deposits.

DOI: https://doi.org/10.3986/AGS.14446
UDC: 551.435.84:551.3.051(497.4)

Primož Miklavc[1], Matej Lipar[2], France Šušteršič[1], Andrej Šmuc[1]

Reconstruction of palaeoflow and depositional dynamics from the Merjasec unroofed cave, Laze Plain (central Slovenia)

ABSTRACT: Sparsely preserved unroofed cave deposits are ancient remains of cave systems. The Merjasec unroofed cave is a perfect example of poorly preserved cave deposits where conventional sedimentological study revealed a greater potential for the reconstruction of local to regional palaeoenvironmental conditions. Cave deposits are characterised by polymictic conglomerates, pebbly sandstones and flowstone belonging to five distinct sedimentary facies. Sedimentary features indicate deposition of channel-related bedforms in a narrow cave-connecting conduit, activated only during extreme pulsating floods under epiphreatic conditions. In this sense, it mimics the current hydrology of the regional system and shows that the hydrological history of the cave system is strongly dependent on climatic conditions. Moreover, this study demonstrates a methodological approach that can be successfully applied to similary exposed cave deposits elsewhere, showing that even fragmentary or eroded remnants, when analysed in detail, can significantly contribute to understanding of karst palaeohydrology.

KEYWORDS: karst, denuded cave, clastic cave deposits, facies, fluvial, depositional dynamics, palaeoenvironment

Rekonstrukcija paleotoka in dinamike zapolnjevanja brezstrope jame Merjasec, Laški ravnik (osrednja Slovenija)

POVZETEK: Redkeje ohranjeni sediment brezstropih jam so ostanki starejših jamskih sistemov. Brezstropa jama Merjasec je odličen primer slabo ohranjenih jamskih sedimentov, kjer so konvencionalne sedimentološke študije pokazale velik potencial za rekonstrukcijo lokalnih do regionalnih paleookoljskih razmer. Jamske sedimente predstavljajo polimiktični konglomerati, prodnati peščenjaki ter sige in so organizirani v pet različnih sedimentnih faciesov. Sedimentne značilnosti kažejo na odlaganje v ozkem, povezujočem kanalu aktiviranem le med ekstremnimi pulzirajočimi poplavami pod epifreatičnimi pogoji. V tem smislu posnema sedanjo hidrologijo regionalnega sistema in kaže, da je hidrološka zgodovina jamskega sistema močno odvisna od podnebnih razmer. Poleg tega ta študija prikazuje metodološki pristop, ki ga je mogoče uspešno uporabiti za podobno razgaljene jamske sedimente drugje, in kaže, da lahko celo fragmentirani ali erodirani ostanki, če jih podrobno analiziramo, pomembno prispevajo k razumevanju kraške paleohidrologije.

KLJUČNE BESEDE: kras, brezstropa jama, klastični jamski sedimenti, faciesi, fluvialno, dinamika odlaganja, paleookolje

The article was submitted for publication on May 8th, 2025.
Uredništvo je prejelo prispevek 8. maja 2025.

[1] University of Ljubljana, Faculty of Natural Sciences and Engineering, Department of Geology, Ljubljana, Slovenia
primoz.miklavc@ntf.uni-lj.si (https://orcid.org/0000-0002-6140-4020), andrej.smuc@ntf.uni-lj.si (https://orcid.org/0000-0002-7883-4676), france.sustersic@siol.net (Retired)

[2] Research Centre of the Slovenian Academy of Sciences and Arts, Anton Melik Geographical Institute, Ljubljana, Slovenia
matej.lipar@zrc-sazu.si (https://orcid.org/0000-0003-4414-0147)

1 Introduction

Caves are natural archives which contain a wide spectrum of clastic, chemical, and organic deposits that preserve valuable information about surface and subsurface palaeoenvironmental conditions (White 2007; Laureano et al. 2016; Caldeira et al. 2021; De Waele and Gutiérrez 2022). Volumetrically most abundant cave deposits are clastic autochthonous and allochthonous sediments; the former originate locally in the cave due to mechanical and chemical weathering of the host rock, whilst the latter were transported into the cave from outside (White 2007; Herman et al. 2012). The composition of clastic cave sediments depends mainly on their provenance, while their textures and structures relate on transportation and depositional processes (De Waele and Gutiérrez 2022). Cave sedimentary environments closely resemble surface fluvial systems, however, subterranean waterflows are strongly influenced by the resistant nature of the bedrock morphology and prone to dramatic changes in flow velocities, resulting in rapid local variations in transport and deposition processes (Trappe 2010; Bella et al. 2020; De Waele and Gutiérrez 2022). In this context, understanding the sedimentological processes, their depositional dynamics, and the facies concepts of clastic cave sediments (Bosch and White 2007; Trappe 2010; Campaña et al. 2017; Campaña et al. 2023) is crucial for reconstructing the hydrological history of cave systems, which is the starting point for advanced studies of palaeoclimate and land evolution in karst areas. Clastic cave sediments are found in recent cave systems and also unroofed caves exposed by denudation or human activity. These are of special importance for the reconstruction of temporal and spatial geomorphologic evolution of the area spanning over millions of years.

Unroofed caves, are ancient cave conduits that underwent a transition from phreatic or epiphreatic to vadose conditions until they were surface-exposed due to denudation (Mihevc 1996; Mihevc and Zupan Hajna 1996; Šušteršič 1998; Šebela 1999; Bosák et al. 2000; Šebela and Sasowsky 2000; Zupan Hajna et al. 2020). They can be identified by elongated, shallow depressions such as trenches or dolines, and by the sediment characteristics for caves (Mihevc 1999). They resemble the oldest still identifiable fragments of cave systems, which emphasises their value as they store the only preserved information on regional underground palaeohydrology. The preservation of unroofed cave deposits is often very sparse, so their interpretation can be very challenging as their sedimentary characteristics may be blurred or even unrecognisable. In this case, the study of such deposits requires a very comprehensive sedimentary analytical approach and diverse knowledge of various surface and underground processes (Caldeira et al. 2021), allowing the identification of sedimentary facies and their vertical and lateral distribution, which provide information about processes and the environment of the deposition (Reading 2001).

In this paper we reconstruct the cave palaeoenvironment and its palaeohydrological regime from the sparsely preserved Merjasec unroofed cave deposits from Laze Plain (slv. *Laški ravnik*), also known as Logatec-Begunje Plain (slv. *Logaško-Begunjski ravnik*), in central Slovenia using a conventional sedimentological methodology. This study demonstrates that even fragmentary remnants of unroofed cave deposits can yield valuable insights into karst palaeohydrology, highlighting the importance of applying similarly detailed methodologies to palaeocave deposits in other regions.

2 Geological and geomorphological setting of the research area

The low-relief elevated plain of Laze Plain structurally belongs to the NW part of the External Dinarides (Placer 2008) (Figure 1A) and was in the Mesozoic part of the Adriatic Carbonate platform (Vlahović et al. 2005). During the Cenozoic, a complex northwest - southeast trending thrusting, divided the area into several thrusts and nappes (Placer 2008; Korbar 2009). The area was later in Neogene cut by dextral strike-slip faults with the most significant structural element represented by the Idrija Fault zone (Figure 1A). The Idrija Fault zone is characterised by chaotically displaced blocks separated by minor faults (Šušteršič 1996; Čar 2010) and plays an important role in the development of surface and subsurface karst forms and in determining the regional hydrological network (Šušteršič 1996; Čar 2018; Gabrovšek et al. 2022). The karst of Laze Plain is mainly formed in Jurassic, well-bedded limestone (micritic and oolithic) and coarse-crystalline dolomite (Buser 1978; Borenović 1993), as well as in Cretaceous, bedded limestone (micritic, bioclastic) and crystalline dolomite (Jež and Otoničar 2018), and the Upper Triassic bedded dolomites. The latest have proven to be the least permeable and are therefore less susceptible to karstification (Figure 1B).

Geomorphologically, the Laze Plain is a corrosion plain (Figure 1B), defined as a dry polje (Stepišnik and Ferk 2023), which extends parallel to the Planina Polje (i.e., a karst polje) in the NW-SE (Dinaric) direction

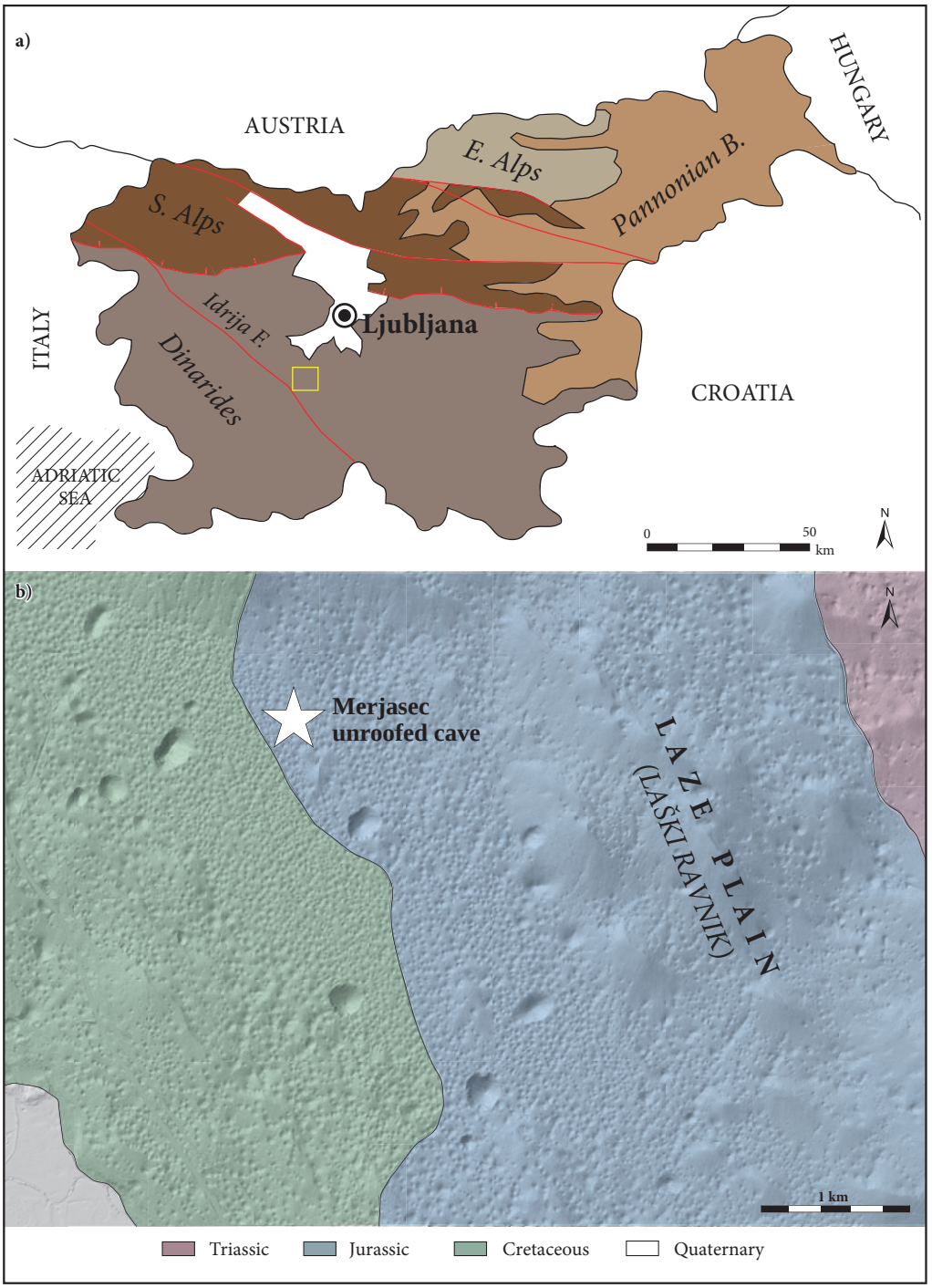

Figure 1: Location and geological characteristics of the investigated area. A) Structural map of Slovenia (Placer 2008). The yellow rectangle marks the investigated area. B) Geological map (Pleničar et al. 1970) of the investigated area with the exact location of the Merjasec unroofed cave (45º52′57.90″N; 14º17′23.34″E).

and is extremely rich in surface and subsurface karst forms (Figure 1B), especially solution dolines and caves (Šušteršič 1994; Šušteršič 2002). Laze Plain is a part of the Ljubljanica river recharge area and has a very complex structure of epiphreatic and vadose zones, where caves occupy multiple levels and are characterised by a very irregular geometry (Blatnik et al. 2019). The thickness of the vadose zone ranges from a few dozen to more than hundred metres, which allows a very dynamic epiphreatic zone in which water can rise up to 60 m during flood events (Gabrovšek and Turk 2010). A very complex organisation of the cave system is also detectable on the surface, where several cave conduits of phreatic or epiphreatic origin and outcrops of clastic cave sediments are exposed (Šušteršič 1998).

3 Methods

The unroofed cave sediment represents a unique archive of ancient cave system. Unfortunately, the exposed cave deposits are predominantly composed of fine-grained clays and silts that have been completely or partially transformed by pedogenetic processes. In this study we therefore focussed on coarse-grained cave sediments (conglomerates and pebbly sandstones) of Laze Plain, which are much rarer but can hold a rich archive of the past environmental events. Even though the exposed conglomerate outcrops are often highly eroded, understanding their sedimentary characteristics, facies types and architectural elements is crucial for reconstructing the depositional environment and interpreting the evolution of individual cave conduit, which, due to their inherent connectivity within the cave network, provide essential insights into the wider ancient cave system.

The investigated Merjasec unroofed cave represents one of the best preserved outcrops of cave deposits of Laze Plain. These deposits were analysed using conventional methods for clastic sedimentary rocks (Boggs 2009). The sedimentary succession was logged on a scale of 1:10 using a standard sedimentological procedure. A total of 22 samples were collected to prepare polished slabs, which were used to determine and interpret the sedimentary structures and textures. The main criteria for determining the facies types and architectural elements was based on Miall (1977; 1996 in conjunction with existing facies classifications for clastic cave sediments (e.g., Bosch and White 2007; Ghinassi et al. 2009; Trappe 2010; Laureano et al. 2016; Campaña et al. 2017; Campaña et al. 2022). The identified facies types and sedimentary bodies (architectural elements) were used to reconstruct the depositional dynamics and evolution of the conduit.

4 Results

4.1 Unroofed cave

The Merjasec unroofed cave is characterised by its unique deposits, which are the only clear indicators of the cave´s existence. The surface around the cave is mostly flat and characterised by solution dolines. The cave was formed in Late Jurassic shallow-marine, well-bedded carbonates and is now surface-exposed on the southern slope of the doline. The cross-section of the cave conduit (Figure 2) is irregular and elliptical, at least 500 cm wide and 110 cm high. The cave conduit was most probably of phreatic origin and later modified by epiphreatic and alluviation processes. The outcrop is characterised by eight clearly detectable cave deposit remnants (Figure 2). The best preserved and most exposed is remnant 7 (Figure 2), where a detailed cross-section was recorded. Other remnants (Figure 2), on the other hand, are poorly preserved polymictic conglomerates, that are mostly covered by soil.

4.2 Merjasec section

The investigation of the Merjasec section (Figure 3A) in remnant 7 (Figure 2) of the unroofed cave outcrop revealed that it is a completely filled palaeocave conduit characterised by well-stratified polymictic conglomerates, pebbly sandstones and flowstone (Figure 3A; Table 1). The basal contact with the hostrock is covered. The cave deposits are organised into five sedimentary units (Figure 3C; Table 1) separated by major erosional contacts, representing five cut-and-fill sequences in which five distinct facies (Gh, Gp, Sp, Ss and Flowstone; see Table 1 for full names) and three architectural elements (CH, SB, GB; see Table 1 for full names) were identified (Figure 3A, B). Conglomerate (Gh, Gp) and sandstone (Sp, Ss) facies are

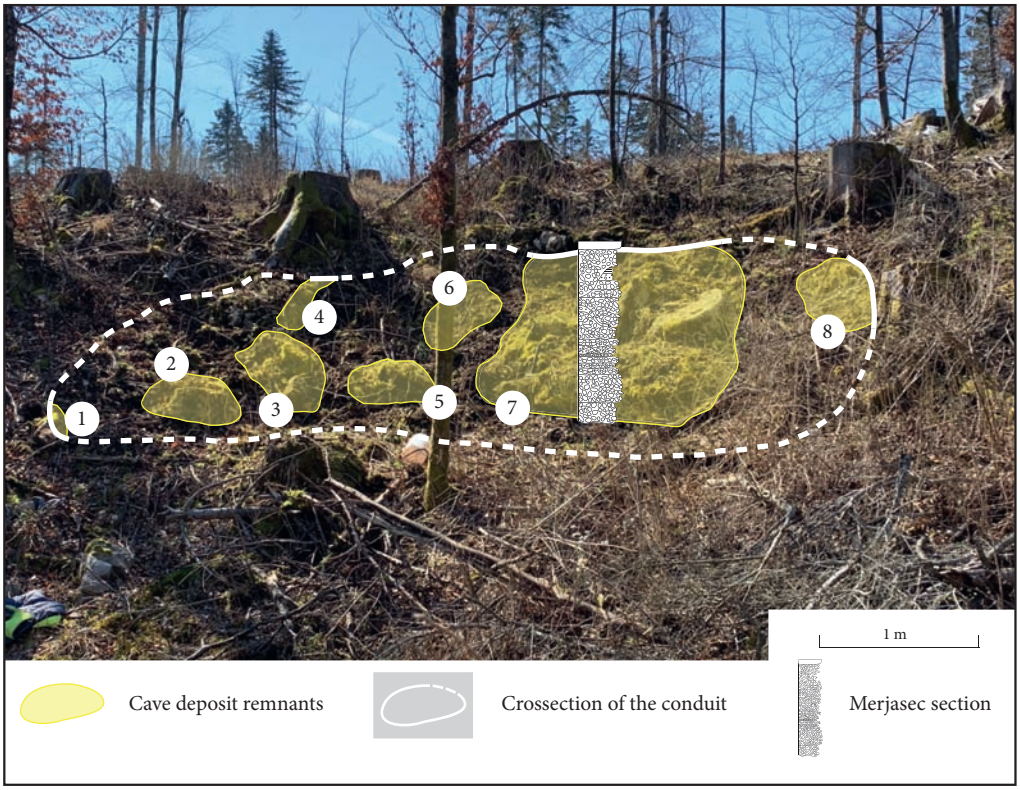

Figure 2: The cross-section of the Merjasec unroofed cave. White line marks the clearly detectable cross-section, white dashed line marks the possible cross-section of the conduit with no clear contact between the hostrock and cave deposits.

Table 1: List of facies, depositional environments, characteristics of depositional units, architectural elements and interpretation.

Facies	Facies characteristics	Depositional environment	Depositional unit	Architectural elements	Interpretation
Gh – clast-supported conglomerate	Bedded, graded, imbricated	Fluvial	I, II, III, IV, V	GB - gravel bars and bedforms, CH – channel	Channel lags or low relief longitudinal bars
Gp – cross-stratified clast-supported conglomerate	High-angle, cross-stratified	Fluvial	II	GB - gravel bars and bedforms	Migration of longitudinal and transverse bars
Sp – cross-stratified pebbly sandstone	High-angle, cross--stratified, imbricated	Fluvial	II	SB - sand bars and bedforms	Migration of longitudinal and transverse bars
Ss – pebbly sandstone	Non-stratified, imbricated	Fluvial	IV	CH - channel, SB - sand bars and bedforms	Rapid channel-fill of coarse bedload or final deposit during flood's waning stage
Fl – flowstone	Laminated	Precipitation	IV	/	Weak supersaturated sheet flows under sub-aerial conditions

Figure 3: Merjasec unroofed cave. A) Merjasec section with distribution of sedimentary units and facies. B) Architectural elements and their bounding surfaces. C) Outcrop of the Merjasec section and the sedimentary unit distribution (white dashed lines mark the erosional contacts; the length of the measuring rod is 80 cm). ► p. 35

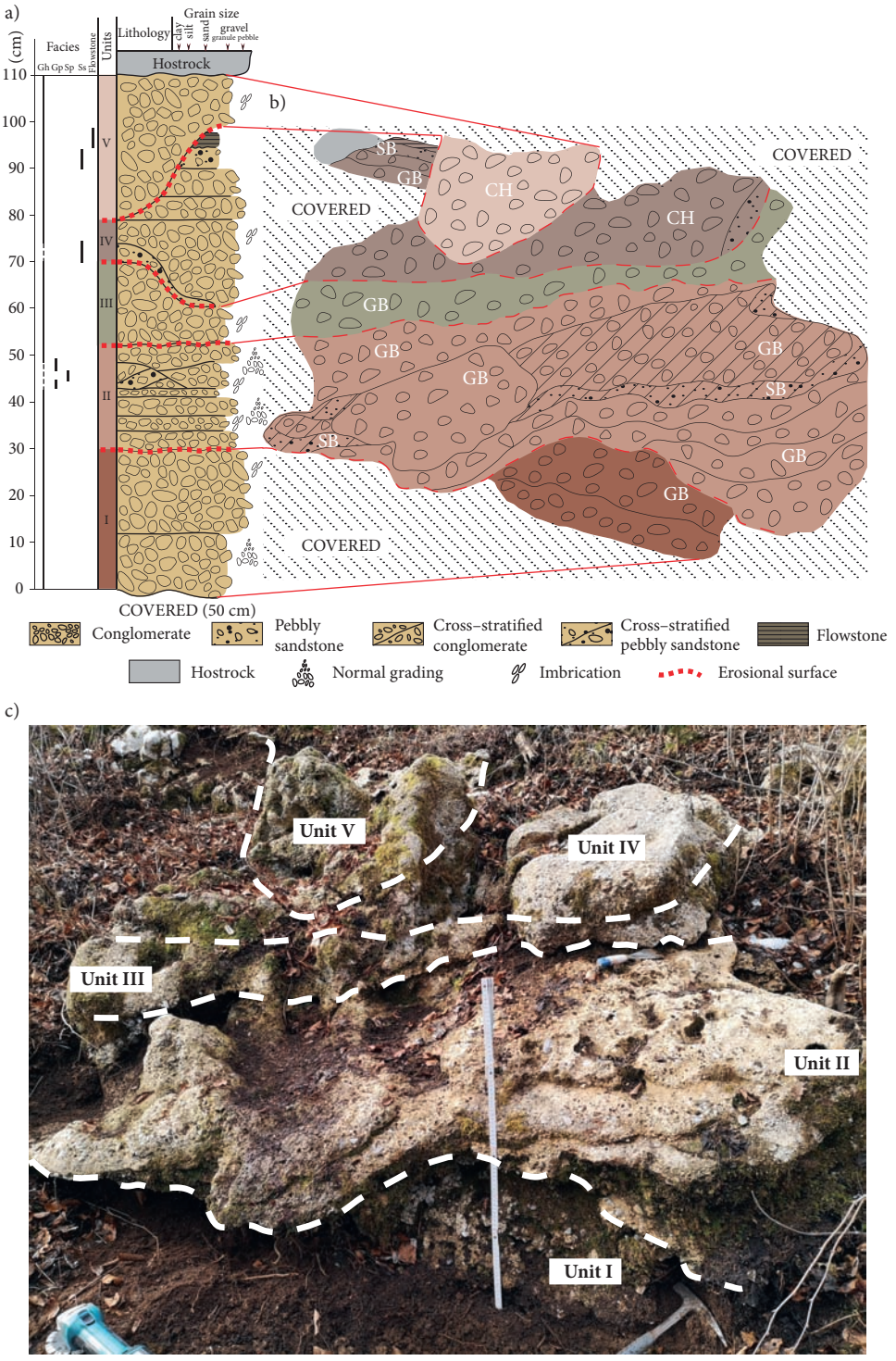
a)
(cm)
Facies
Gh Gp Sp Ss Flowstone
Units
Lithology
Grain size
clay
silt
sand
gravel
granule pebble
Hostrock
110
100
90
80
70
60
50
40
30
20
10
0
V
IV
III
II
I
COVERED (50 cm)
b)
SB
GB
CH
COVERED
GB
GB
GB
GB
SB
SB
GB
GB
COVERED
COVERED
Conglomerate
Pebbly sandstone
Cross–stratified conglomerate
Cross–stratified pebbly sandstone
Flowstone
Hostrock
Normal grading
Imbrication
Erosional surface
c)
Unit V
Unit IV
Unit III
Unit II
Unit I

characteristic for fluvial environment, while flowstone facies (Fl) represents autochthonous sediment accumulation. Clast composition is very similar throughout the entire section. Most abundant are coarse-grained dolomite clasts and various types of limestone clasts, while quartz, chert, iron oxide/hydroxide and speleothem clasts are less common.

4.3 Description of sedimentary facies

Facies Gh (clast-supported conglomerate) is the most abundant and is present in every unit of the section (Figure 4A, B). This facies forms 2–31 cm thick beds, which are graded and imbricated (Figure 5A, B) or may locally express plane-parallel stratification (Figure 4B). The contact between beds is usually irregular or erosional. The conglomerate is characterised by a clast-supported texture and consists of moderately to well-sorted, mostly subangular to rounded granule- to pebble- sized clasts and a fine-grained carbonate matrix.

Facies Gp (cross-stratified clast-supported conglomerate) is represented in unit II of the section (Figure 4C). This facies forms up to 3 cm thick lenticular beds, which underlie and overlie sandstones of Facies Sp. The high-angle cross-stratified conglomerate is moderately sorted, clast-supported and consists of angular to subrounded granules and rarely pebbles. Matrix is fine grained carbonate.

Facies Sp (cross-stratified pebbly sandstone) is present in Unit II of the section (Figure 4B, C). This facies forms a high-angle cross-stratified, up to 2 cm thick lenticular bodies with weakly developed imbri-

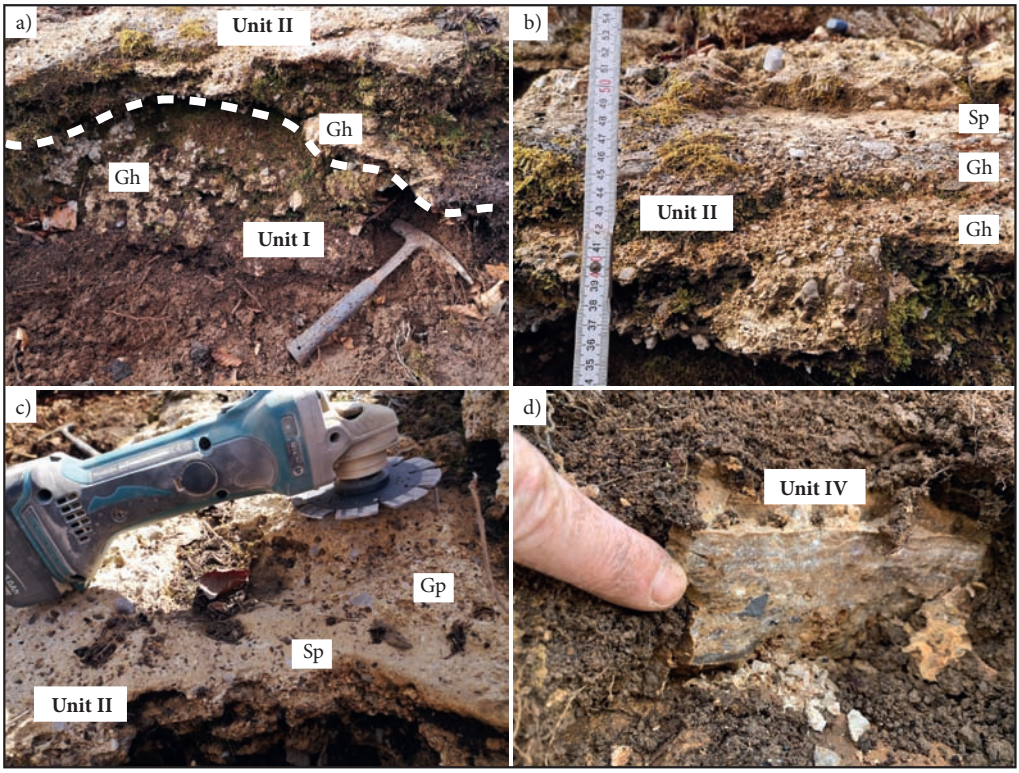

Figure 4: Details from the Merjasec unroofed cave deposits. A) Basal part of the section. Erosional contact (white dashed line) between conglomerate (facies Gh) of Unit I and conglomerate (facies Gh) of Unit II. B) Pebbly-sandstone (facies Sp) overlaying plane-parallel bedded conglomerate (facies Gh) of Unit II. C) Pebbly-sandstone (facies Sp) and conglomerate (facies Gp) from Unit II. D) Flowstone layer covering the irregular surface pebbly-sandstone of Unit IV.

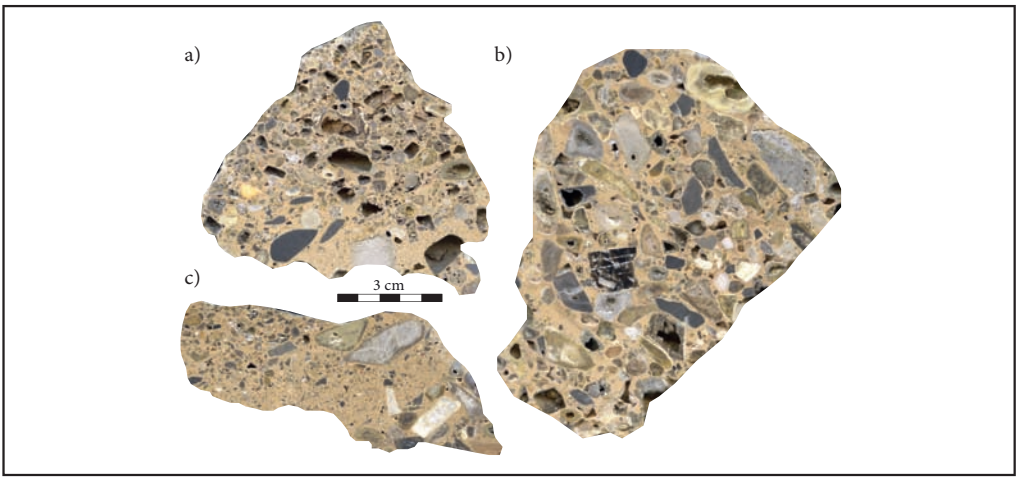

Figure 5: Polished slabs of Merjasec unroofed cave deposits. A) Graded and imbricated conglomerate (facies Gh) of Unit II. B) Imbricated conglomerate (facies Gh) of Unit IV. C) Cross-stratified pebbly-sandstone (facies Sp) of Unit II.

cation (Figure 5C), that are present as insets in conglomerates of facies Gp. The cross-stratified pebbly sandstone is characterised by a clast-supported texture and is poorly to moderately sorted. It consists of angular and rounded medium to coarse sand sized clasts and rare granules and pebbles. Matrix is mostly composed of fine-grained carbonate.

Facies Ss (pebbly sandstone) is present in Unit IV of the Merjasec section. This facies forms lenticular shaped or sheet-like beds up to 5 cm thick, which are overlying erosional bounding surfaces or gravel lags of facies Gh. The pebbly sandstone is clast-supported and moderately to poorly sorted. It consists of mostly subrounded to subangular medium to coarse sand clasts and rare granules and pebbles that exhibit moderate imbrication. The matrix is mostly fine-grained carbonate.

Facies Fl (flowstone) is present in Unit IV of the section (Figure 4D). The facies forms a 3 cm thick bed precipitated over an irregular bed surface of pebbly sandstone (facies Ss). The flowstone is characterised by the alternation of thin microcrystalline laminae and thicker laminae of sparry calcite crystals covered by columnar calcite.

4.4 Description of sedimentary architectural elements

Gravel bars and bedforms (GB) are represented by coarse-grained facies Gh and Gp (Figure 3B). GB deposits characterised by sheet-like bed geometry or rarely lenticular geometry. Irregular, low-relief scoured bases are common. These gravels mostly occur as conduit-wide conglomerate deposits.

Minor channel deposits (CH) (Figure 3B) are represented by deposits of facies Gh and Ss and are characterised by sharp, high-relief erosional base. The channel infills consist of massive conglomerates or conglomerates and lenticular bodies of pebbly sandstones. The channel deposits are covered by sheet-like, bedded conglomerates of the element previously described.

Sand bar and bedform (SB) (Figure 3B) are represented by deposits of facies Sp and Ss and are characterised by a lenticular geometry. They occur as interbeds in gravel bedforms (facies Sp) or minor channel fills (facies Ss).

5 Discussion

The sparsely preserved Merjasec unroofed cave deposits were deposited in a very dynamic, high-energy underground environment, mainly characterised by channel-related bedforms with a multistorey architecture

controlled by fluvial forces and the resistant nature of the hostrock. The coarse-grained clastic cave material mostly consists of carbonates, which means that it is a product of underground erosion of the conduit walls – the corrosion of caves is much more intense during flood waters than during low waters (Palmer 2007) or is related to collapse of the tectonically weakened zones (Zupan Hajna et al. 2024) or a combination of both processes. The presence of channel-related bedforms, erosional surfaces and the complete absence of fine-grained overbank flood sheets, crevasses and levées indicates that deposition took place in a narrow cave-connecting conduit, where the open channel flow may become a pipe-full flow during floods (Ghinassi et al. 2009; Trappe 2010; Herman et al. 2012; Laureano et al. 2016; Bella et al. 2020). During these flood events, a conduit-wide stream channel was formed, in which the mobilisation of the riverbed generated bedforms similar to those in surface rivers (Trappe 2010; Bella et al. 2020).

5.1 Facies interpretation

Conglomerate facies Gh is present in every unit and is characterised by sheet-like bedded or minor channel-fill, clast-supported conglomerates. The abundant clast-supported framework, graded bedding, clast imbrication, and scoured erosive surfaces indicate deposition in a bedload-dominated fluvial system in which the flow conditions change rapidly from high-energy to waning-energy flows. Therefore, the facies is interpreted as a channel lag deposit or low relief longitudinal bars developed by ephemeral high-energy dynamic events (seasonal floods) (Miall 1977; Miall 1996. In this scenario, gravels are moving and accumulating along the riverbed, while fine-grained sediments are washed downstream, forming openwork conglomerates in which pores were filled by filtration of suspended load during the waning phase of the flood event (Ramos and Sopeña 1983; Zhang et al. 2020).

Conglomerate facies Gp occurs in Unit II in lenticular beds of high-angle, cross-stratified and clast-supported conglomerate. Facies is in direct contact with cross-stratified sandstones, which indicates channel deposition and migration of longitudinal and transverse bar forms (Miall 1981; Miall 1996).

In general, the Merjasec cave conglomerate facies exhibit similar characteristics to other cave environments. Ghinassi et al. (2009) described the clast-supported gravels of the channel-lag deposits (facies Gh in the present study) as a result of the erosive and rising phases of the stream floods and cross-bedded gravels (facies Gp in the present study) as alternate or side bars. Campaña et al. (2017) and Laureano et al. (2016) interpreted clast-supported gravels (facies Gh in the present study) as deposits of water flow in fluvial channels, while according to the classification of Bosch and White (2007), investigated deposits are mainly characteristic for the thalweg facies, although they could also be determined as »gravelly« channel facies deposits due to the presence of fabrics (imbrication, normal grading) and sedimentary structures (horizontal bedding, cross-stratification).

Sandstone facies Sp occurs in Unit II as lenticular bodies of high-angle, cross-stratified coarse-grained sandstone with a weakly imbricated pebbly admixture. Facies is imbedded in channel lag/bar conglomerates and was deposited from traction by a unidirectional current, which indicates a downstream migration of longitudinal and transverse bar forms (Miall 1977; Miall 1981; Miall 1996; Opluštil et al. 2005).

Sandstone facies Ss occurs in unit IV as a lenticular or sheet-like bodies of non-stratified mainly coarse-grained sandstone with abundant granule- to pebble-sized clasts that exhibit moderate imbrication. Facies directly overlies scoured basal surface of channel lag conglomerates, indicating rapid channel-fill deposition of coarse bedload (Miall 1996), or it covers conglomerate lags as a final deposit during the flood's waning stage.

Compared to other investigated caves (Ghinassi et al. 2009; Laureano et al. 2016), similar sandstone facies were mostly described as channel bedforms (bars, side-bars, dunes) formed as a result of localised sediment deposition related to channel floor irregularity, channel widening, channel migration or as channel-fill deposits accumulated by vertical accretion.

Flowstone facies Fl occurs in Unit IV as laminated bed precipitated over conglomerate. Facies indicates a cessation of fluvial sedimentation and beginning of flowstone formation under sporadic or weak supersaturated sheet flows under sub-aerial conditions with typically slow accretion (Fairchild et al. 2007; Ford and Williams 2007; De Waele and Gutiérrez 2022). Flowstone indicates a hiatus in the stratigraphic sections, which means that during its precipitation, other sediments should not be deposited (Gillieson 1986).

Flowstones, which are very common authigenic deposits in caves are described as a very useful indicator for palaeoenvironmental conditions (Fairchild and Baker 2012; Nehme et al. 2015) and geochronology (Bosák 2002; Fairchild et al. 2006; Laureano et al. 2016; Ferk et al. 2019; Sierpień et al. 2021; Zupan Hajna et al. 2021).

5.2 Architectural interpretation

The Merjasec cave conduit represents a complex, channel-fill sequence consisting of various types of intra-channel bars and minor channel deposits, mostly separated by erosional bounding surfaces (Figure 3). Investigated cave deposits have been recognised as three distinct architectural elements defined by their geometries, bounding surfaces and sediment fills. The most common are deposits of gravel bars and bedforms (GB) interbedded with rare deposits of minor channels (CH) and sand bars and bedforms (SB).

Gravel bars and bedforms (GB) form multistory sheets, rarely lenses composed of facies Gh, and Gp, and represent an intra-channel (conduit-wide) bar (longitudinal, transverse) deposited during pulsating high-water discharge (Miall 1996).

Minor channels (CH) were incised into underlying conglomerate sheets of element GB during the erosional stage of the flood and were filled rapidly after the formation of the channel. Two types of channels were recognised. First is a single channel with a complex fill of pebbly sands (facies Ss) and gravels (facies Gh) and the second is a single channel with a simple fill of gravels (facies Gh) (Ramos and Sopeña 1983; Miall 2014).

Sand bars and bedforms (SB) record intra-channel deposits, which were probably generated by migrating dunes within the shallower part of the conduit (facies Sp) (Opluštil et al. 2005; Miall 1996) or by the flood's wanning stage (facies Ss) (Miall 1996).

5.3 Reconstruction of palaeodepositional dynamics

Stratigraphy and sedimentary characteristics of the exposed cave deposits reveal five cut-and-fill sequences (Figure 6), which describe the local palaeohydrological evolution of the investigated cave conduit and resemble the palaeohydrological conditions of the regional system. The architecture of the sediments indicates ephemeral, high-energy dynamic events terminated by a longer period of subaerial exposure under epiphreatic conditions.

The first **sequence S1** (Figure 6) indicates the deposition of conduit-wide sheet-like gravel lags during the high-energy pulse generated by the rising stage of the stream flood.

Second **sequence S2** (Figure 6) begins with an erosive phase during the rise of the flood, followed by a conduit-wide aggradation of sheet-like gravel beds during the high-energy flow, which were covered by the migration of longitudinal and transverse bars by the pulsating moderate- to low-energy flow during the waning of the flood.

The **sequence S3** (Figure 6) recorded a reactivation of flooding-induced erosion and a subsequent accumulation of gravel lag under high-energy flood flow conditions.

The **sequence S4** (Figure 6) records one of the two major erosional events, forming a channel incised into the underlying gravel pavement, which was filled with a complex-fill of gravels and gravelly sands immediately after the flood´s erosional phase. A conduit-wide aggradation covers the channel deposits under high-energy flow conditions and accumulates gravel lags that were covered by a sheet-like sand bed during the flood's waning stage. The accumulation of flowstone over slightly irregular surface records a break of the fluvial activity in the conduit.

After this quiet period, the **sequence S5** (Figure 6) records an upstream barrage breakthrough and a restoration of epiphreatic flood-induced fluvial activity with a second major, very intensive erosional event that cuts the stream channel through the flowstone into the deposits of the fourth sequence, which was filled with gravel immediately after the flood´s erosional phase and covered by a conduit-wide gravel lag during later phase of the flood that eventually completely filled the conduit. Sequence 5 thus documents the last known erosional and depositional activity in the conduit before it was abandoned.

5.4 Energy fluctations of palaeoflow

Merjasec cave palaeoflow was characterised by high-energy ephemeral flood-flows and intra-channel deposition, as evidenced by upper-flow regime features such as planar bedding, the predominance of coarse-grained material, erosional surfaces and the presence of speleothem debris, indicating also an upstream erosion of older cave deposits.

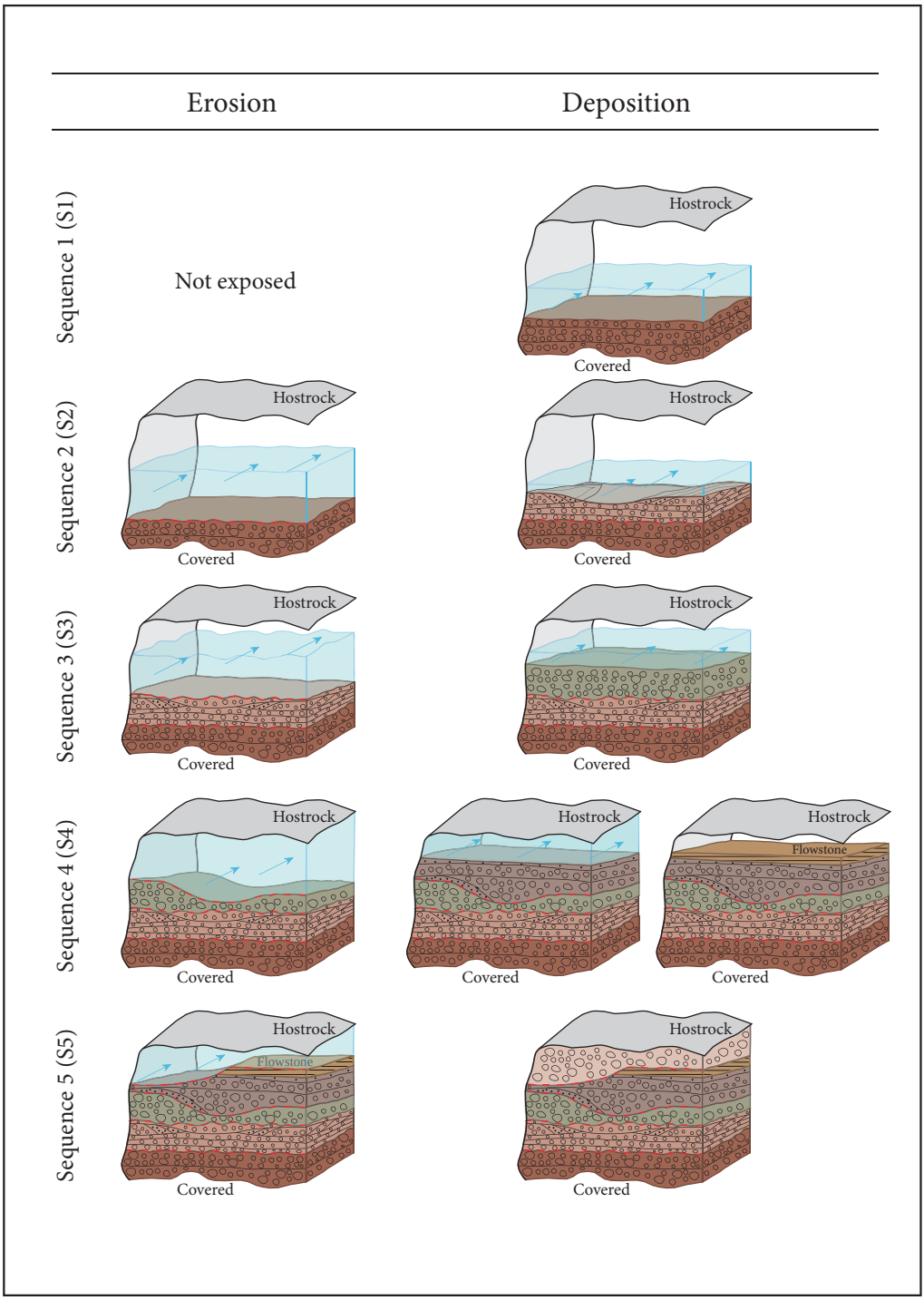

Figure 6: Schematic evolution of depositional dynamics in the Merjasec unroofed cave conduit. Illustration (not to scale) represents erosional and depositional phases in each of the five sequences. A description of each sequence is provided in section 5.3.

All recorded floods in Merjasec cave are characterised by an early erosional and subsequent depositional stage, developing a cut-and-fill sequence (Simms 1994; Adams et al. 2019). However, a detailed analysis of the facies and architecture reveals that the floods differ in their flow energy, resulting in different erosional bounding surfaces and different channel bedforms. The low-relief, conduit-wide erosions indicate a high-energy, laterally stable flow and occur in the early erosional flood stage in sequences 1, 2 and 3. These low-relief erosional surfaces were in the later depositional stage covered by conduit-wide gravel bars of the facies Gh. High-relief erosion with increased localised incisions represents the early flood stages in sequences 4 and 5, indicating thalweg migration within the conduit-wide stream channel, probably associated with oscillations in flow velocity (Collinson 1970). High-relief incisions were later covered by minor channel fills of facies Gh and Ss (also noticed by Miall 1996; Ghinassi et al. 2009; Scherer et al. 2015; Fambrini et al. 2017; Bella et al. 2020).

Low-energy bedforms are rare in Merjasec cave and were only found in the sequence 2. They are characterised by a lenticular geometry and cross-bedded structure composed of facies Gp and Sp. They represent a downstream migration of subaqueous dunes and bars in lower flow regime (Miall 1977; Miall 1996; Miall 1996; Fambrini et al. 2017). Direct stacking of high-energy conglomerates and low-energy sands clearly demonstrate relatively fast changes in the flow energy and consequently depositional dynamics (Ramos and Sopeña 1983). Sequence 2 is therefore the only one that records the flood´s waning stage, while in other sequences the deposits of this stage were probably washed away by the rising and erosive stage of the flood in other sequences (Zupan Hajna et al. 2024).

5.5 Regional implications

The regional underground palaeohydrology, mostly characterised by periodic, pulsating flooding, as evident from the Merjasec section, was probably controlled by climatic conditions (Ghinassi et al. 2009; Hercman et al. 2023; Zupan Hajna et al. 2024), which transferred larger amounts of rainwater into the cave system during storm periods or to processes related to allogenic recharge, leading to a sudden rise in the water table and thus to the reactivation of several levels in the epiphreatic zone of the cave system, including the investigated conduit. Similar conditions are also present in a current hydrological regime of the regional system with variable recharge conditions, characterised by increased discharge of influent rivers, causing pulsating flooding of the system (Prelovšek et al. 2008; Gabrovšek and Turk 2010; Gabrovšek et al. 2014; Blatnik et al. 2019).

The end of sequence 4 record a significant change in the depositional environment and thus in the depositional dynamics. The formation of the flowstone layer over the irregular morphology of the fluvial deposits indicates a break of fluvial activity (Bella et al. 2020; Hercman et al. 2023; Zupan Hajna et al. 2024). It is possible that the irregular contact between the flowstone and the underlying fluvial deposits record yet another flood event with only detectable erosional stage, as conduits can undergo several phases of deposition and removal without leaving clear indicators (Zupan Hajna et al. 2024), but this remains only a conjecture as this part of the section is very sparsely exposed. This sudden change in environmental conditions from repetitive flooding (epiphreatic) to calm, intermittent thin flows in sub-aerial exposed conduit and back again could be explained by the temporary drier conditions or underground flow bypass created by the upstream blockage of the conduit due to cave-roof collapses (Bella et al. 2020).

Sequence 5 records the last active phase in which the conduit was completely filled with clastics. After this phase, the conduit became completely abandoned, which can be related to (a) base level drop and regional uplift that moved the conduit to higher levels of the system, where it became out of reach even for large flood events (b) clogging of the conduit and therefore forcing flood waters through different pathways or (c) the deflection of flood waters by faults that can act as very effective underground flow barriers.

Regarding the morphological features and sedimentary characteristics, the investigated cave was most likely connected to the main regional drainage system and functioned as a bypass conduit that was fully activated only during extreme floods under epiphreatic conditions. Such conduits are usually draining flood waters from the main conduit, a characteristic of a cave systems with a complex, interconnected conduit network.

The detailed sedimentological investigation of the Merjasec section highlights the significant value of unroofed cave deposits in reconstructing past subsurface and surface environmental conditions, despite their typically sparse preservation, poor exposure, and frequent erosion. The present study demonstrates

that, when examined in detail, such deposits can yield far more than just confirmation of ancient fluvial activity; they can provide insights into the provenance, energy, and dynamics of palaeoflow, offering an understanding of past hydrological conditions. The Merjasec case further underscores the potential of unroofed cave deposits to act as key pieces in deciphering the evolution and hydrodynamics of regional cave systems, particularly in areas like Laze Plain where few caves intersect the epiphreatic zone (Blatnik et al. 2019). Importantly, this work also demonstrates a methodological approach that can be successfully applied to similarly exposed deposits elsewhere, showing that even fragmentary or degraded remnants, when analysed with appropriate techniques, can significantly enrich our understanding of karst palaeohydrology.

6 Conclusion

The sedimentological characterisation of sparsely preserved Merjasec unroofed cave deposits from Laze Plain (central Slovenia) provided very valuable information about past regional hydrological conditions:

1) Stratigraphy and sedimentary characteristics of the exposed cave deposits reveal five cut-and-fill sequences formed during high-energy ephemeral flood-flows and intra-channel deposition, terminated by a longer period of subaerial exposure under epiphreatic conditions.
2) Most of the bedforms indicate high-energy flows generated by the rising stages of stream floods, while low-energy bedforms indicate the flood´s waning stages.
3) The direct stacking of high-energy bedforms and low-energy bedforms indicates fast changes in the flow energy and consequently depositional dynamics. The interpreted sediment characteristics indicate that the flood flows range from conduit-wide and laterally stable flows to oscillating flows with increased localised incisions formed by thalweg migration. Sedimentary data of the Merjasec cave suggests that the regional palaeohydrology was mostly affected by the storm periods and/or allogenic discharge, leading to a sudden rise in the water table and epiphreatic zone reactivation.
4) Similar conditions are also present in a current hydrological regime of the regional system with variable recharge conditions, characterised by increased discharge of influent rivers, causing pulsating flooding of the system.

This work demonstrates that even fragmentary or degraded remnants of unroofed cave deposits, when studied in detail, can provide most valuable information about karst palaeohydrology and therefore should not be overlooked. We suggest that a similar detailed methodological approach in studying comparable palaeocave deposits in other regions.

ACKNOWLEDGEMENT: The research was financially supported by the Slovenian Research and Innovation Agency, Research Programme P1-0195: »Geoenvironment and Geomaterials«, Research Programme P6-0101: »Geography of Slovenia«, Research Project J6-50213 »Unroofed Caves of the Nullarbor Plain«, Unesco IGCP Project 661: »The Critical Zone in Karst Systems« and IGCP Project 715: »A new karst modelling approach along different tectonic contacts«.

RESEARCH DATA: For information on the availability of research data related to the study, please visit the article webpage: https://doi.org/10.3986/AGS.14446.

7 References

Adams, N. F., Candy, I., Schreve, D. C., Barendregt, R. W. 2019: Deposition and provenance of the Early Pleistocene Siliceous Member in Westbury Cave, Somerset, England. *Proceedings of the Geologists' Association* 130-2. https://doi.org/10.1016/j.pgeola.2019.02.005

Bella, P., Gradziński, M., Hercman, H., Leszczyński, S., Nemec, W. 2020: Sedimentary anatomy and hydrological record of relic fluvial deposits in a karst cave conduit. *Sedimentology* 68-1. https://doi.org/10.1111/sed.12785

Blatnik, M., Mayaud, C., Gabrovšek, F. 2019: Groundwater dynamics between Planinsko Polje and springs of the Ljubljanica river, Slovenia. *Acta Carsologica* 48-2. https://doi.org/10.3986/ac.v48i2.7263

Boggs, S. 2009: Petrology of sedimentary rocks. Cambridge University Press.

Borenović, T. 1993: Razvoj jurskih plasti v profilu zahodno od Pokojišča. *MS thesis*. Univerza v Ljubljani.
Bosák, P. 2002: Karst processes from the beginning to the end: How can they be dated? In: Evolution of Karst: From Prekarst to Cessation. *Carsologica* 1. Založba ZRC.
Bosák, P., Knez, M., Otrubová, D., Pruner, P., Slabe, T., Venhodová, D. 2000: Palaeomagnetic research of fossil cave in the highway construction at Kozina, SW Slovenia. *Acta Carsologica* 29-2. https://doi.org/10.3986/ac.v29i2.446
Bosch, R. F., White, W. B. 2007: Lithofacies and transport of clastic sediments in karstic aquifers. In: Studies of Cave Sediments. Springer. https://doi.org/10.1007/978-1-4020-5766-3_1
Buser, S. 1978: Razvoj jurskih plasti Trnovskega gozda, Hrušice in Logaške planote. *Rudarsko-metalurški zbornik* 25-4.
Caldeira, D., Uagoda, R., Nogueira, A. M., Garnier, J., Sawakuchi, A. O., Hussain, Y. 2021: Late Quaternary episodes of clastic deposition in the Tarimba Cave, Central Brazil. *Quaternary International* 580. https://doi.org/10.1016/j.quaint.2021.01.012
Campaña, I., Benito-Calvo, A., Pérez-González, A., Álvaro-Gallo, A., Miguens-Rodríguez, L., Iglesias-Cibanal, J., Bermúdez de Castro, J. M., Carbonell, E. 2022: Revision of TD1 and TD2 stratigraphic sequence of Gran Dolina cave (Sierra de Atapuerca, Spain). *Journal of Iberian Geology* 48. https://doi.org/10.1007/s41513-022-00200-8
Campaña, I., Benito-Calvo, A., Pérez-González, A., Ortega, A. I., Bermúdez de Castro, J. M., Carbonell, E. 2017: Pleistocene sedimentary facies of the Gran Dolina archaeopaleopological site (Sierra de Atapuerca, Burgos, Spain). *Quaternary International* 433-A. https://doi.org/10.1016/j.quaint.2015.04.023
Campaña, I., Benito-Calvo, A., Pérez-González, A., Ortega, A. I., Álvaro-Gallo, A., Miguens-Rodríguez, L., Iglesias-Cibanal, J., Bermúdez de Castro, J. M., Carbonell, E. 2023: Reconstructing depositional environments through cave interior facies: The case of Galería Complex (Sierra de Atapuerca, Spain). *Geomorphology* 440. https://doi.org/10.1016/j.geomorph.2023.108864
Čar, J. 2010: Geološka zgradba idrijsko - cerkljanskega hribovja: Tolmač h geološki karti idrijsko – cerkljanskega hribovja med Stopnikom in Rovtami 1 : 25 000/Geological structure of the Idrija - Cerkno hills: Explanatory book to the geological map of the Idrija - Cerkljansko hills 1: 25 000. Geološki zavod Slovenije.
Čar, J. 2018: Geostructural mapping of karstified limestones. *Geologija* 61-2. https://doi.org/10.5474/geologija.2018.010
Collinson, J. D. 1970: Bedforms of the Tana River, Norway. *Geografiska Annaler* 52-1.
De Waele, J., Gutiérrez, F. 2022: Karst hydrogeology, geomorphology and caves. John Wiley & Sons Ltd. https://doi.org/10.1002/9781119605379
Fairchild, I. J., Baker, A. 2012: Speleothem science: From process to past environments. Wiley. https://doi.org/10.1002/9781444361094
Fairchild, I. J., Frisia, S., Borsato, A., Tooth, A. F. 2007: Speleothems. In: Geochemical Sediments and Landscapes. Blackwell Publishing. https://doi.org/10.1002/9780470712917.ch7
Fairchild, I. J., Smith, C. L., Baker, A., Fuller, L., Spötl, C., Mattey, D. 2006: Modification and preservation of environmental signals in speleothems. *Earth-Science Reviews* 75-1,2,3,4. https://doi.org/10.1016/j.earscirev.2005.08.003
Fambrini, G. L., Neumann, V. H. M. L., Menezes-Filho, J. A. B., da Silva-Filho, W. F., de Oliveira, É. V. 2017: Facies architecture of the fluvial Missão Velha Formation (Late Jurassic–Early Cretaceous), Araripe Basin, Northeast Brazil: Paleogeographic and tectonic implications. *Acta Geologica Polonica* 67-4. https://doi.org/10.1515/agp-2017-0029
Ferk, M., Lipar, M., Šmuc, A., Drysdale, R. N., Zhao, J. 2019: Chronology of heterogeneous deposits in the side entrance of Postojna cave, Slovenia. *Acta geographica Slovenica* 59-1. https://doi.org/10.3986/AGS.7059
Ford, D. C., Williams, P. 2007: Karst hydrogeology and geomorphology. John Wiley & Sons Ltd. https://doi.org/10.1002/9781118684986
Gabrovšek, F., Häuselmann, P., Audra, P. 2014: 'Looping caves' versus 'water table caves': the role of base-level changes and recharge variations in cave development. *Geomorphology* 204. https://doi.org/10.1016/j.geomorph.2013.09.016

Gabrovšek, F., Mihevc, A., Mayaud, C., Blatnik, M., Kogovšek, B. 2022: Slovene classical karst: Kras Plateau and the recharge area of Ljubljanica River. *Folia Biologica et Geologica* 63-2. https://doi.org/10.3986/fbg0097

Gabrovšek, F., Turk, J. 2010: Observations of stage and temperature dynamics in the epiphreatic caves within the catchment area of the Ljubljanica river. *Geologia Croatica* 63-2. https://doi.org/10.4154/gc.2010.16

Ghinassi, M., Colonese A. C., Di Giuseppe, Z., Govoni, L., Lo Vetro, D., Malavasi, G., Martini, F. et al. 2009: The Late Pleistocene clastic deposits in the Romito Cave, Southern Italy: A proxy record of environmental changes and human presence. *Journal of Quaternary Science* 24-4. https://doi.org/10.1002/jqs.1236

Gillieson, D. 1986: Cave sedimentation in the New Guinea highlands. *Earth Surface Processes and Landforms* 11-5. https://doi.org/10.1002/esp.3290110508

Hercman, H., Gąsiorowski, M., Szczygieł, J., Bella, P., Gradziński, M., Błaszczyk, M., Matoušková, Š. et al. 2023: Delayed valley incision due to karst capture (Demänová Cave System, Western Carpathians, Slovakia). *Geomorphology* 437. https://doi.org/10.1016/j.geomorph.2023.108809

Herman, E. K., Toran, L., White, W. B. 2012: Clastic sediment transport and storage in fluviokarst aquifers: an essential component of karst hydrogeology. *Carbonates and Evaporites* 27. https://doi.org/10.1007/s13146-012-0112-7

https://doi.org/10.1017/CBO9780511626487

Jež, J., Otoničar, B. 2018: Late Cretaceous geodynamics of the northern sector of the Adriatic Carbonate Platform (W Slovenia). *Newsletters on Stratigraphy* 51-4. https://doi.org/10.1127/nos/2018/0439

Korbar, T. 2009: Orogenic evolution of the External Dinarides in the NE Adriatic region: a model constrained by tectonostratigraphy of Upper Cretaceous to Paleogene carbonates. *Earth-Science Reviews* 96-4. https://doi.org/10.1016/j.earscirev.2009.07.004

Laureano, F. V., Karmann, I., Granger, D. E., Auler, A. S., Almeida, R. P., Cruz, F. W., Strícks, N. M., Novello, V.F. 2016: Two million years of river and cave aggradation in NE Brazil: Implications for speleogenesis and landscape evolution. *Geomorphology* 273. https://doi.org/10.1016/j.geomorph.2016.08.009

Miall, A. D. 1977: A review of the braided-river depositional environment. *Earth-Science Reviews* 13-1. https://doi.org/10.1016/0012-8252(77)90055-1

Miall, A. D. 1981: Analysis of fluvial depositional systems. *AAPG Continuing Education Course Notes Series* 20. American Association of Petroleum Geologists. https://doi.org/10.1306/CE20422

Miall, A. D. 1996: The geology of fluvial deposits. Sedimentary facies, basin analysis, and petroleum geology. Springer. https://doi.org/10.1007/978-3-662-03237-4

Miall, A. D., 2014: Fluvial depositional systems. Springer. https://doi.org/10.1007/978-3-319-00666-6

Mihevc, A. 1996: Brezstropa jama pri Povirju. *Naše jame* 38.

Mihevc, A. 1999: Unroofed caves, cave sediments and karst surface geomorphology – Case study from Kras, W Slovenia. *Naš krš* 32.

Mihevc, A., Zupan Hajna, N. 1996: Clastic sediments from dolines and caves found during the construction of the motorway near Divača, on the Classical Karst. *Acta Carsologica* 25.

Nehme, C., Verheyden, S., Noble, S. R., Farrant, A. R., Sahy, D., Hellstrom, J., Delannoy, J. J., Claeys, P. 2015: Reconstruction of MIS 5 climate in the central Levant using a stalagmite from Kanaan Cave, Lebanon. *Climate of the Past* 11-12. https://doi:10.5194/cp-11-1785-2015

Opluštil, S., Martínek, K., Tasáryová, Z. 2005: Facies and architectural analysis of fluvial deposits of the Nýřany Member and the Týnec Formation (Westphalian D – Barruelian) in the Kladno-Rakovník and Pilsen basins. *Bulletin of Geosciences* 80-1.

Palmer, A. N. 2007: Cave geology. Cave Books.

Placer, L. 2008: Principles of the tectonic subdivision of Slovenia. *Geologija* 51-2. https://doi.org/10.5474/geologija.2008.021

Pleničar, M., Buser, S., Ferjančič, L., Grad, K., Kerčmar-Turnšek, D., Mencej, Z., Orehek, S., Pavlovec, R., Prestor, M., Rijavec, L., Šribar, L. 1970: Tolmač za list Postojna L 33-77: Osnovna geološka karta SFRJ 1: 100.000. Zvezni geološki zavod.

Prelovšek, M., Turk, J., Gabrovšek, F. 2008. Hydrodynamic aspect of caves. *International Journal of Speleology* 37-1. https://doi.org/10.5038/1827-806X.37.1.2

Ramos, A., Sopeña, A. 1983: Gravel bars in low-sinuosity streams (Permian and Triassic, central Spain). In: Modern and Ancient Fluvial System. Wiley. https://doi.org/10.1002/9781444303773.ch24

Reading, H. G. 2001: Clastic facies models, a personal perspective. *Bulletin of the Geological Society of Denmark* 48. https://doi.org/10.37570/bgsd-2001-48-05

Scherer, C. M. S., Goldberg, K., Bardola, T. 2015: Facies architecture and sequence stratigraphy of an early post-rift fluvial succession, Aptian Barbalha Formation, Araripe Basin, northeastern Brazil. *Sedimentary Geology* 322. https://doi.org/10.1016/j.sedgeo.2015.03.010

Sierpień, P., Pawlak, J., Hercman, H., Pruner, P., Zupan Hajna, N., Mihevc, A., Bosák, P. 2021: Flowstones from the Račiška Pečina Cave (SW Slovenia) Record 3.2-Ma-Long History. *Geochronometria* 48-1. https://doi.org/10.2478/geochr-2021-0004

Simms, M. J. 1994: Emplacement and preservation of vertebrates in caves and fissures. *Zoological Journal of the Linnean Society* 112-1,2. https://doi.org/10.1111/j.1096-3642.1994.tb00320.x

Stepišnik, U., Ferk, M. 2023: Morphogenesis and classification of corrosion plains in Slovenia. *Acta geographica Slovenica* 64-1. https://doi.org/10.3986/AGS.11774

Šebela, S. 1999: Morphological and geological characteristics of two denuded caves in SW Slovenia. *Acta Carsologica* 28-2. https://doi.org/10.3986/ac.v28i2.491

Šebela, S., Sasowsky, I. 2000: Paleomagnetic dating of sediments in caves opened during highway construction near Kozina, Slovenia. *Acta Carsologica* 29-2. https://doi.org/10.3986/ac.v29i2.468

Šušteršič, F. 1994: Classic dolines of classical site. *Acta Carsologica* 23.

Šušteršič, F. 1996: Poljes and caves of Notranjska. *Acta Carsologica* 25.

Šušteršič, F. 1998: Interaction between a cave system and the lowering karst surface; Case study: Laški Ravnik. *Acta Carsologica* 27-2. https://doi.org/10.3986/ac.v27i2.506

Šušteršič, F. 2002: Where does underground Ljubljanica flow?. *RMZ - Materials and Geoenvironment* 49-1.

Trappe, M. 2010: Actualistic approaches to the systematics and facies relations of clastic karst deposits. *Geodinamica Acta* 23-1,2,3. https://doi.org/10.3166/ga.23.41-48

Vlahović, I., Tišljar, J., Velić, I., Matičec, D. 2005: Evolution of the Adriatic carbonate platform: Palaeogeography, main events and depositional dynamics. *Palaeogeography, Palaeoclimatology, Palaeoecology* 220-3,4. https://doi.org/10.1016/j.palaeo.2005.01.011

White, W. B. 2007: Cave sediments and paleoclimate. *Journal of Cave and Karst Studies* 69-1.

Zhang, C., Song, X., Wang, X., Wang, X., Zhao, K., Shuang, Q., Li, S. 2020: Origin and depositional characteristics of supported conglomerates. *Petroleum Exploration and Development* 47-2. https://doi.org/10.1016/S1876-3804(20)60047-7

Zupan Hajna, N., Bosák, P., Pruner, P., Mihevc, A, Hercman, H., Horáček, I. 2020: Karst sediments in Slovenia: Plio–Quaternary multi–proxy records. *Quarternary International* 546. https://doi.org/10.1016/j.quaint.2019.11.010

Zupan Hajna, N., Mihevc, A., Bosák, P., Pruner, P., Hercman, H., Horáček, I., Wagner, J. et al. 2021: Pliocene to Holocene chronostratigraphy and palaeoenvironment records from cave sediments: Račiška pečina section (SW Slovenia). *Quaternary International* 605,606. https://doi.org/10.1016/j.quaint.2021.02.035

Zupan Hajna, N., Pruner, P., Bosák, P., Mihevc, A. 2024: Temporal insights into karst system evolution: A case study of the unroofed cave above Škocjanske Jame, NW Dinarides. *Geomorphology* 461. https://doi.org/10.1016/j.geomorph.2024.109282

Acta geographica Slovenica, 65-2, 2025, 47–63

SPATIAL DISTRIBUTION OF SOCIAL INNOVATION POTENTIAL IN DISADVANTAGED AREAS: THE CASE OF TWO HUNGARIAN COUNTIES

Krisztina Varga, Géza Tóth

CSONGOR HORVÁTH

Mád, a settlement in a developing district of Borsod-Abaúj-Zemplén county.

DOI: https://doi.org/10.3986/AGS.14410
UDC: 332.122(1-77):001.895(439)
314.15:001.895(439)

Krisztina Varga[1], Géza Tóth[1]

Spatial distribution of social innovation potential in disadvantaged areas: The case of two Hungarian counties

ABSTRACT: Social innovation has emerged as a strategic tool to foster development in disadvantaged areas. The study analyzes the spatial distribution and temporal changes of social innovation potential and its link to population dynamics in two disadvantaged Hungarian counties. Using indicators classified into input, output, and impact categories, a composite index was constructed for municipalities over three census years (2001, 2011, 2022). Moran I statistics and clustering tested spatial dependence of social innovation potential and the relationship between clusters and migration balance. Findings show positive spatial autocorrelation weakened over time. A strong link exists between social innovation potential and migration balance, with innovative settlements showing lower outmigration.

KEYWORDS: social innovation potential, population changes, migration balance, Moran I statistic, disadvantaged area, Hungary

Prostorska razporeditev potenciala za družbene inovacije na območjih z razvojnimi omejitvami: primer dveh madžarskih županij

POVZETEK: Družbene inovacije so se uveljavile kot strateško orodje za spodbujanje razvoja na območjih z razvojnimi omejitvami. Članek analizira prostorsko razporeditev in časovne spremembe potenciala za družbene inovacije ter njegovo povezavo z gibanjem prebivalstva v dveh madžarskih županijah z razvojnimi omejitvami. Na podlagi kazalnikov, razvrščenih v kategorije izhodišč, rezultatov in učinkov, je bil oblikovan sestavljeni indeks za občine v treh popisnih letih (2001, 2011 in 2022). Z Moranovo statistiko I in razvrščanjem v skupine je bila preverjena prostorska odvisnost potenciala za družbene inovacije ter povezava med skupinami in selitvenim saldom. Izsledki kažejo, da je pozitivna prostorska avtokorelacija v opazovanem časovnem intervalu oslabela. Obstaja močna povezava med potencialom za družbene inovacije in selitvenim saldom, saj je za inovativna naselja značilna nižja stopnja odseljevanja.

KLJUČNE BESEDE: potencial za družbene inovacije, prebivalstvene spremembe, selitveni saldo, Moranova statistika I, območje z omejitvenimi dejavniki, Madžarska

The article was submitted for publication on May 19th, 2025.
Uredništvo je prejelo prispevek 19. maja 2025.

[1] University of Miskolc, Miskolc, Hungary
krisztina.varga.t@uni-miskolc.hu (https://orcid.org/0000-0001-7112-8800), geza.toth@ksh.hu (https://orcid.org/0000-0002-9233-1899)

1 Introduction

In recent years, social innovation has become an increasingly prominent concept in regional development, especially in addressing spatial inequalities and revitalizing disadvantaged and peripheral areas. Social innovation is increasingly understood as a systemic, multi-actor, and iterative process embedded in institutional and structural contexts, analogous to technological and economic innovation (Dawson and Daniel 2010; Cajaiba-Santana 2014; Veresné Somosi and Varga 2021; Varga and Tóth 2024). Broadly, it encompasses novel and effective responses to unmet societal needs, aiming to enhance community well-being, cooperation, and local capacities (Szendi 2018; Varga and Tóth 2021). Based on the literature review, social innovation can be defined as a process that, beyond measures aimed at improving living standards, encompasses the emergence of new structures, the stimulation of societal agency, as well as both top-down policy mechanisms and bottom-up civic initiatives. Consequently, it enables a dual-perspective approach that can be assessed through input, output, and impact indicators. Within this context, social innovation potential refers to the aggregate of institutional, human, and economic capacities that enable a locality to initiate and sustain socially innovative practices (Benedek et al. 2015; Varga et al. 2023). These capacities are spatially uneven and rooted in structural and demographic legacies.

Past studies examined social innovation processes, stakeholders, and their relation to technological innovation, with a focus on measuring social innovation potential and its link to competitiveness (Varga and Tóth 2021; Nagy and Tóth 2021; Varga and Tóth 2024). We adopt the widely accepted view that social innovation addresses needs unmet by the market and can provide alternative pathways to development in lagging regions (Benedek et al. 2015; Bosworth et al. 2016; Szendi 2018; Vercher 2022). In Hungary's most disadvantaged settlements, these needs are associated with unemployment, educational inequalities, health challenges, and poor housing. These areas suffer from low population retention, underdeveloped infrastructure, low-income levels, and a negative migration balance. The local economy is weak and lacks innovation capacity. In such contexts, social innovation is critically needed (Woolcock 1998; Mumford et al. 2002; Hazel and Onaga 2003; Mulgan et al. 2007; Pol and Ville 2009; Young 2011; European Commission 2013; Castro Spila et al. 2016; Unceta et al. 2016; Kleverbeck et al. 2019; Varga et al. 2023; Varga and Tóth 2024).

Social innovation potential is not identical to social innovation itself but represents its preconditions – such as institutional infrastructure, human and social capital, and local governance – that together define a locality's innovativeness and adaptability (Cajaiba-Santana 2014; Szendi 2018; Kleverbeck et al. 2019; Varga and Tóth 2021). Settlements with high social innovation potential are more likely to mobilize local actors, foster participation, and develop cross-sectoral collaboration. These capacities support resilience, improve quality of life, and can enhance both competitiveness and population retention. In contrast, areas with low social innovation potential may reinforce social inequality and suffer continuous decline.

As Nemes Nagy (2006) argues, spatial structures are relatively stable in the short term, with significant changes occurring only over medium (10–15 years) or long-term horizons. While this issue has been explored theoretically (Schmitz et al. 2013; Castro Spila et al. 2016), empirical studies remain scarce (Benedek et al. 2015; Szendi 2018; Nagy and Tóth 2019).

Our approach draws on a narrower economic interpretation of spatial structure, focusing on the distribution of economic activity. Spatial configuration affects macroeconomic growth by concentrating benefits and externalities, both positive (e.g., economies of scale) and negative (e.g., congestion, high land prices) (Varga 2005). In line with Hungarian literature, we define territorial development using per capita income, which best reflects local conditions and is widely accessible (Nemes Nagy et al. 2001; Németh 2008; Pénzes 2014). While unemployment data once served as a complementary measure (Lőcsei 2010; Tóth and Nagy 2013), its utility has declined with the rise of public work schemes. Few empirical efforts have explored the social innovation potential and development nexus (Szendi 2018; Nagy and Tóth 2019). We also include settlement size as a variable, given its relevance to spatial structure.

Based on literature, methods for measuring social innovation primarily focus on assessing macro-level social innovation processes (Cajaiba-Santana 2014; Carvache-Franco et al. 2018; Varga et al. 2023; Cunha et al. 2024). Although macro-level initiatives dominate, methods aimed at quantifying the processes and impacts of local and regional efforts are emerging with increasing intensity. Building on the reviewed literature and our previous research (Varga et al. 2020; Varga and Tóth 2021; Veresné Somosi et al. 2023), a research gap can be identified that motivates further investigations. We revisit the municipalities of two

Hungarian counties to determine whether spatial patterns of social innovation potential show regularity or randomness, and whether they correlate with migration and development outcomes.

Our current analysis examines the measurement and spatial distribution of social innovation potential in two disadvantaged counties, using census data from 2001, 2011, and 2022. This time frame allows us to track temporal changes and compare them with earlier findings, while raising new questions. We analyze social innovation potential alongside demographic processes, particularly internal migration, to better understand why certain disadvantaged areas show greater resilience to depopulation. Our primary research question is: To what extent is there a spatially observable relationship between social innovation potential and the migration balance of municipalities in disadvantaged areas? We also explore whether social innovation potential can alter spatial structural patterns.

Based on previous findings, two of Hungary's most structurally disadvantaged counties – Borsod-Abaúj-Zemplén and Szabolcs-Szatmár-Bereg – were selected to examine the spatial distribution of social innovation potential, since social innovation can be identified as a new tool and model for fostering the convergence of disadvantaged peripheral regions.

2 Literature review

Based on prior analyses of local, regional, and national measurement approaches (Veresné Somosi and Varga 2021; Varga and Tóth 2024), various efforts have been made to evaluates social innovation processes and capacities. Despite these efforts, a universally accepted methodology remains absent (Cajaiba-Santana 2014; Szendi 2018). Initial frameworks primarily relied on economic indicators; however, the core aim of social innovation – enhancing well-being – requires a broader, more integrated approach (Hochgerner 2011). Measurement frameworks should account for rural specificities (Bosworth et al. 2016; Vercher 2022; Varga and Tóth 2024) and the systemic nature of innovation (Dawson and Daniel 2010; Carvache-Franco et al. 2018; Neumeier 2017; Cajaiba-Santana 2014; Benedek et al. 2015; Szendi 2018).

Academic discourse increasingly highlights social innovation's potential in addressing regional inequalities, especially in peripheral areas (Neumeier 2017; Veresné Somosi and Varga 2021). In line with European Union (EU) cohesion policy, social innovation is regarded as a key instrument for reducing disparities (Ewers and Brenck 1992; Benedek et al. 2015; Szendi 2018; De Palo et al. 2018; Widuto 2019).

The measurement of social innovation involves evaluating inputs, outputs, and impacts, with emphasis on societal outcomes. Current methodologies focus on assessing social innovation potential – the capacities enabling innovation (Benedek et al. 2015; Szendi 2018; Kleverbeck et al. 2019; Nagy and Tóth 2019; Varga et al. 2023) – as distinct from the contextual prerequisites required for its emergence (Szendi 2018; Varga et al. 2023).

Table 1: Methods used to measure social innovation based on a structured review of the literature (based on Veresné Somosi and Varga 2021; Varga and Tóth 2024).

LOCAL MEASUREMENT	REGIONAL MEASUREMENT	NATIONAL MEASUREMENT
Social Innovation Indicators (IndiSI project, Kleverbeck et al. 2019) *data collection without calculation*	Regional Innovation Capability (IndiSI project, Kleverbeck et al. 2019) *elaboration of indicators without calculation*	European Social Innovation Index (ESII) *pilot study without calculation*
Social innovation capacity (Schmitz et al. 2013) *data collection without calculation*	Regional Vulnerability Index (SIMPACT project, Castro Spila et al. 2016) *development of indicators without calculation*	Blueprint of Social Innovation Indicator (TEPSIE project, Schmitz et al. 2013) *pilot study without calculation*
Measurement of social innovation process according to Triple Bottom Line (Dainiené and Dagiliené 2016) *elaboration of indicators without calculation*	Regional social innovation potential (Benedek et al. 2015) *Examination of 15 micro-regions (social innovation potential)*	Measuring social impact (OECD, Eurostat 2018) *pilot study without calculation*
Complex social innovation index (Szendi 2018) *Survey of 610 localities (social innovation potential)*	Regional Social Innovation Index (RESINDEX) *282 regional organisations*	Social Innovation Index (SII) *Survey of 45 countries (ranking)*

The methodological approaches for measuring social innovation rely on the use of different indicators at various measurement levels. The individual methods may vary by country, primarily due to the differing range of available data. There are general recommendations that can primarily be applied to national-level measurements. A significant portion of the calculations attempt to adapt the indicators involved in macro-level studies for local and regional measurement. Different measurement methods are interconnected in a hierarchical system, although there are discrepancies in the indicators used. In the structured review of the literature, we examined four methods at each level, which are detailed in Table 1.

3 Methods

The methodological chapter describes the analytical process in three main steps (Figure 1). First, the indicators are defined, forming the basis for measuring social innovation potential. This is followed by an examination of the spatial distribution of the indicators, which enables the identification of regional disparities and temporal changes. Finally, the analysis addresses the relationship with migration processes, revealing the connection between social innovation and demographic dynamics.

3.1 Establishing and analysis of the indicators

Based on the literature (Kocziszky 2004; Schmitz et al. 2013; Benedek et al. 2015; OECD, Eurostat 2018; Szendi 2018; Kleverbeck et al. 2019; Nagy and Tóth 2019; Varga et al. 2020; Veresné Somosi et al. 2023), an indicator system and a social innovation potential indicator can be defined to support the measurement of social innovation concerning the municipalities of the examined counties. In this case, we applied the indicator system compiled based on literature for measuring social innovation. Its complexity requires a multidimensional measurement framework. Following research and development evaluation models (OECD, Eurostat 2018), input, output, and impact indicators are used to capture different stages of the process. Inputs reflect foundational conditions (e.g., institutions, employment, education); outputs represent immediate results (e.g., participation, service uptake); impacts cover long-term effects (e.g., income, quality of life, attitude shifts). This threefold structure is especially relevant in disadvantaged regions, where traditional economic metrics may overlook key aspects of local development and resilience (Varga et al. 2023).

In our study, each group included seven indicators. When compiling the indicator system, it was necessary to consider that the indicators do not always point in the same direction; that is, there are indicators where an increase is positive, while for others, a decrease is viewed favorably. For indicators where lower values signify a favorable situation, we calculated the inverse of the indicators. As for the averages of the input, output, and impact indicator groups, a comprehensive indicator measuring social innovation potential can be determined. We normalized the indicators within each indicator group to ensure that our data, which varies in scale, can be compared with one another. We calculated the average of the normalized data for each indicator group. No weighting was performed during the calculations.

The indicators selected as input, output and impact indicators are presented in Table 2.

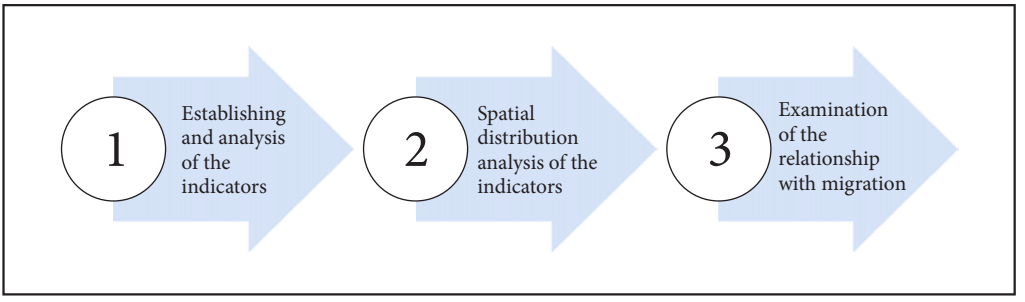

Figure 1: The structure and logic of the methodological framework.

Table 2: Indicators for the input, output and impact indicator group (based on Varga et al. 2023).

INPUT INDICATOR GROUP	INDICATORS
institutional factors	1. number of non-profit enterprises per 1000 inhabitants (2001, 2011, 2022)
locational factors	2. number of active enterprises per 1000 inhabitants (2001, 2011, 2022)
human factors	3. child population as a percentage of the resident population (2001, 2011, 2022)
	4. elderly per 100 children (2001, 2011, 2022)
	5. dependency ratio (children (0–14 years) and elderly population (>65 years) as a percentage of the population aged 15–64) (2001, 2011, 2022)
	6. proportion of the population aged 7 and over with primary education (including those who have not completed school) (2001, 2011, 2022)
activity factors	7. employment rate (2001, 2011, 2022)
OUTPUT INDICATOR GROUP	INDICATORS
economic factors	1. ratio of public employees to the population aged 15–64 (2006, 2011, 2022)
cultural factors	2. number of participants in cultural events per 1000 inhabitants (2001, 2011, 2022)
social factors	3. average amount used for child protection allowances (2006, 2011, 2022)
	4. number of individuals receiving social meals per 1000 inhabitants (2001, 2011, 2022)
	5. number of individuals receiving home assistance per 1000 inhabitants (2001, 2011, 2022)
	6. unemployment rate (2001, 2011, 2022)
health factors	7. patient flow per family doctor and pediatrician (2001, 2011, 2022)
IMPACT INDICATOR GROUP	INDICATORS
factors of social conditions	1. per capita income (1000 HUF) (2001, 2011, 2022)
	2. proportion of the population aged 7 and over with a high school education and above (2001, 2011, 2022)
family factors	3. proportion of single person households (2001, 2011, 2022)
	4. proportion of families with three or more children (2001, 2011, 2022)
perception of safety factors	5. number of registered crimes per 1000 inhabitants (2001, 2011, 2022)
factors of social infrastructure	6. number of places in long-term residential care per 1000 inhabitants (2001, 2011, 2022)
factors of environmental conditions	7. municipal green area per 1000 inhabitants (2008, 2011, 2022)

In order to examine the internal dynamics of social innovation potential over time, a pair-wise correlation analysis was conducted between the social innovation potential indicator and its three component dimensions: input, output and impact indicators. As referred to above, the complex indicator of social innovation potential was calculated as the arithmetic average of the normalised values of the input, output and impact dimensions, without applying any further weighting.

The pair-wise correlation coefficients (r^2 values) were also calculated between the same components in consecutive years (2001–2011, 2011–2022 and 2001–2022) and for the social innovation potential complex indicator itself. This approach allowed us to examine:

- how strongly each component correlates with itself over time (persistence over time),
- whether the overall social innovation potential indicator remains stable or changes structurally over the periods.

3.2 Spatial distribution analysis of the indicators

Furthermore, we aimed to examine the spatial distribution of social innovation potential and sought to determine whether any regularities, spatial patterns, or instead a random distribution could be observed. To test spatial dependency, we applied Moran's I statistic. Like all spatial autocorrelation tests, Moran's I starts with the null hypothesis that there is no spatial dependence in the sample. This is what we explored. The formula for Moran's I (Equation 1) is as follows (Moran 1948):

$$I = \frac{n}{2A} * \frac{\sum_{i=1}^{n}\sum_{j=1}^{n}\delta_{ij}(y_i-\bar{y})((y_j-\bar{y})}{\sum_{i=1}^{n}(y_i-\bar{y})^2} \quad \text{(Equation 1)},$$

where n is the number of settlements, y_i represents the social innovation potential in each settlement, $\bar{y}$ is the arithmetic mean of the social innovation potential, A denotes the number of neighborhood connections, and the coefficient δ_{ij} equals 1 if i and j are neighbors, otherwise, it is 0 (Dusek 2004; Dusek and Kotosz 2016).

For interpreting the data, it is important to consider that the calculated indicator should be understood within the following ranges and manner:
$I > -1/(N-1)$ → positive spatial autocorrelation,
$I = -1/(N-1)$ → no spatial autocorrelation,
$I < -1/(N-1)$ → negative spatial autocorrelation.

In the next step, we aimed to examine the spatial pattern in more detail. Following Anselin (1995), research on spatial autocorrelation emerged, often referred to in international literature as LISA (Local Indicators of Spatial Association).

Anselin (1995), by introducing Moran's I, developed one of the most widely used methods for quantifying and visualizing spatial autocorrelation: Local Moran's I statistic. According to the notation introduced by Getis and Ord (1996), the definition of I is given in Equation 2:

$$I_i = \frac{Z_i-\bar{Z}}{S_{\bar{Z}}^2} * \sum_{j=1}^{N}\left[W_{ij} * (Z_i - \bar{Z})\right] \quad \text{(Equation 2)},$$

where $\bar{Z}$ is the average of all units, Z_i is the value of unit i, Sz^2 is the variance of the Z variable across all examined units, and W_{ij} is the distance weight factor between units i and j, derived from the neighborhood matrix W.

For determining the neighborhood matrix, we applied the so-called queen contiguity criterion, meaning that settlements are considered neighbors if they share either an edge or a corner.

For the obtained Local Moran's I values:
- negative values indicate negative autocorrelation,
- positive values indicate positive autocorrelation.

However, the function's range extends beyond the *[–1, +1]* interval.

The Local Moran's I statistics are useful for identifying areas that are like or different from their neighbors. The higher the Local Moran's I value, the stronger the spatial similarity. Conversely, a negative value suggests that the spatial distribution of variables approaches randomness.

The scatter plot categorizes settlements into four groups based on their quadrant placement:
1. High–High (HH): areas with high values where the neighboring units also have high values.
2. High–Low (HL): areas with high values surrounded by low-value neighbors.
3. Low–Low (LL): areas with low values where the neighboring units also have low values.
4. Low–High (LH): areas with low values surrounded by high-value neighbors.

The groups labeled with odd numbers indicate positive autocorrelation, while those with even numbers indicate negative autocorrelation. Choosing Local Moran's I as a local spatial autocorrelation indicator is particularly useful when identifying spatial outliers. It reveals:
- where HH and LL values cluster in space, indicating regions with strong spatial similarity,
- where HL and LH areas appear, highlighting territorial units that significantly differ from their neighbors.

3.3 Examination of the relationship with migration

Drawing on the clusters identified by Local Moran's I statistics, the relationship between social innovation potential and migration was systematically examined. Social innovation potential – as previously noted – can be understood as a proxy for well-being. In line with earlier studies (Lockley et al. 2008; Wright 2012; Moralli 2023; Varga et al. 2023), the analysis of migration provides an empirically grounded way to

understand how people perceive well-being, which underlies their mobility decisions. Building on this rationale, our study examines whether social innovation potential clusters are quantitatively linked to internal migration patterns: is there a measurable relationship between social innovation potential (as a quasi-well-being indicator), people's perceptions of it, and resulting migration decisions. Recent research underscores why this linkage is critical (Moralli 2025). Methodologically, mixed-method approaches combining quantitative migration modeling with qualitative insights deliver deep, context-rich evidence. Moreover, advanced quantitative tools such as network analyses of migration flows and multilevel modeling illuminate how spatial clusters of social innovation potential influence movement dynamics (Salamońska 2022). Our investigation advances understanding of how social innovation capacity impacts population retention and movement – and vice versa.

4 Results and discussion

4.1 Spatial and temporal shifts in social innovation potential

Our findings indicate a substantial transformation in the social innovation potential of municipalities between 2001 and 2022, as past data do not correlate with recent data (Table 3). The most significant shifts occurred in input indicators. Declining correlation values – particularly for input indicators and the overall social innovation potential – indicate growing spatial divergence and imply that the structural determinants of social innovation have substantially changed over time.

Table 3: Pair-wise correlations between social innovation potential and its components (r^2).

Indicators	2001/2011	2011/2022	2001/2022
Input indicators	0,548	0,154	0,005
Output indicators	0,214	0,258	0,164
Impact indicators	0,457	0,390	0,234
Social innovation potential	0,575	0,395	0,222

After reviewing the indicator system – based on the composite indicator measuring social innovation potential, determined from the averages of the input, output, and impact indicator groups – the 2022 situation shows that the most favorable conditions are found in the two county seats and the settlements within their spheres of influence. In contrast, the settlements in the most disadvantaged positions are primarily peripheral villages. This pattern is consistent with several findings in the international literature on centre-periphery and migration issues (Avdić et al. 2022; Ljubenović et al. 2025) and our previous findings, as is the fact that input indicators play the most significant role in shaping the level of social innovation potential, as their values are the highest for most settlements. In this regard, our findings are entirely consistent with our previous research (Nagy and Tóth 2021; Varga and Tóth 2021). The composite indicator confirms that, although the most advantaged settlements within the two counties are relatively scattered across space, the proximity to major cities plays a clear role. The most disadvantaged settlements are primarily those near the national border, but in many cases, settlements along county borders also exhibit similarly unfavorable conditions (Figure 2 and 3).

4.2 Spatial clustering of social innovation potential

The Moran I statistic was used to test for spatial dependence. The global spatial autocorrelation of social innovation potential, covering all settlements in the two counties, in 2022 was: I = 0.230 (in 2001, I = 0.393; in 2011, I = 0.334).

Based on this, we can determine that the phenomenon exhibits positive spatial autocorrelation (I = –1/(577-1) = –0.00174), meaning that the spatial concentration of similar values is higher than what

would be expected due to natural processes. Settlements with high social innovation potential tend to have high-value neighbors, while settlements with low values tend to be surrounded by other low-value settlements.

Using Local Moran's I, we conducted calculations on social innovation potential at the settlement level for 2022. To analyze whether the high degree of similarity is driven by the concentration of high or low values of the variable, we compared the Local Moran's I results with the initial data using Moran scatter plots.

As a next step, we plotted the standardized values of the observation units on the horizontal axis of the diagram, while the vertical axis represented the corresponding standardized Local Moran's I values (i.e., the average values of neighboring units).

Based on their placement in the respective quadrants of the scatter plot, the municipalities categorized into four groups can be presented as follows:

- The HH cluster primarily includes the most advantaged settlements, with a total of 57 settlements. Most of these are part of the Miskolc agglomeration and the Nyíregyháza urban area (both are cities with county status). Beyond these two groups, Sárospatak and two neighboring settlements, as well as some villages in the Kisvárda region, also belong to this cluster. However, urban status alone does not guarantee inclusion in the HH cluster, as several cities in the two counties do not belong to any cluster at a 95% significance level.
- The LL cluster consists of 37 settlements, representing the most disadvantaged areas of the two counties. Within this cluster, two distinct groups emerge: the external peripheries along the national border (e.g., Lónya, Barabás, Hidasnémeti, Pusztaradvány), and the internal peripheries near county borders (e.g., Szabolcs) and settlements far from urban centers (e.g., Vaja, Porcsalma), which also face significant disadvantages.
- The LH cluster includes 13 settlements, primarily located near HH cluster settlements. Among the most substantial are Tunyogmatolcs and Sajópetri.
- The HL cluster consists of 17 settlements, primarily neighboring areas with low social innovation potential. The most significant among them are Csengersima and Krasznokvajda.

Building on earlier studies (Nagy and Tóth 2021; Varga and Tóth 2021), the overall spatial structure of social innovation potential remains consistent; however, the number of settlements within each cluster has particularly increased. Given the absence of methodological changes and the observed decline in global spatial autocorrelation, this trend points to the emergence of localized clusters with similar innovation dynamics. To assess cluster stability, a bivariate spatial autocorrelation analysis was conducted, comparing 2022 values with neighboring settlements' 2001 data (Figure 2, Figure 3).

Minor spatial shifts were observed in the cluster dynamics. In Sárospatak, the absence of significant similarity with its surroundings in 2001 – due to neighboring settlements' low innovation potential – suggests improvements in adjacent areas over time (Borsod-Abaúj-Zemplén county). In regions such as the Cserhát, Rakaca Basin, and Torna Hills, several settlements remained in LL or HL clusters, while others lost statistical significance, reflecting stagnation or modest improvement (Borsod-Abaúj-Zemplén county). Conversely, in the vicinity of Mátészalka (e.g., Nyírmeggyes, Kocsord), former HH cluster settlements lost statistical significance by 2022, indicating a relative decline in innovation potential, while modest improvement is observed in the neighboring settlements of Kisvárda (Szabolcs-Szatmár-Bereg county).

4.3 The impact of social innovation potential on migration

We examined how belonging to different clusters is reflected in the migration balance. It was found that there is a clear relationship between cluster membership and the magnitude of migration balance. HH cluster settlements have the lowest outmigration, while LL cluster settlements experience the highest outmigration. In this case, it can be concluded that there is a fundamentally strong and positive relationship between social innovation potential and migration balance. However, in the case of the two outlier clusters (LH, HL), this relationship is much less evident (Table 4, Figure 4).

Figure 2: Local Moran's I of the composite indicator measuring social innovation, 2022. ► p. 56
Figure 3: Bivariate Local Moran's I of the composite indicator measuring social innovation, 2022/2001. ► p. 57

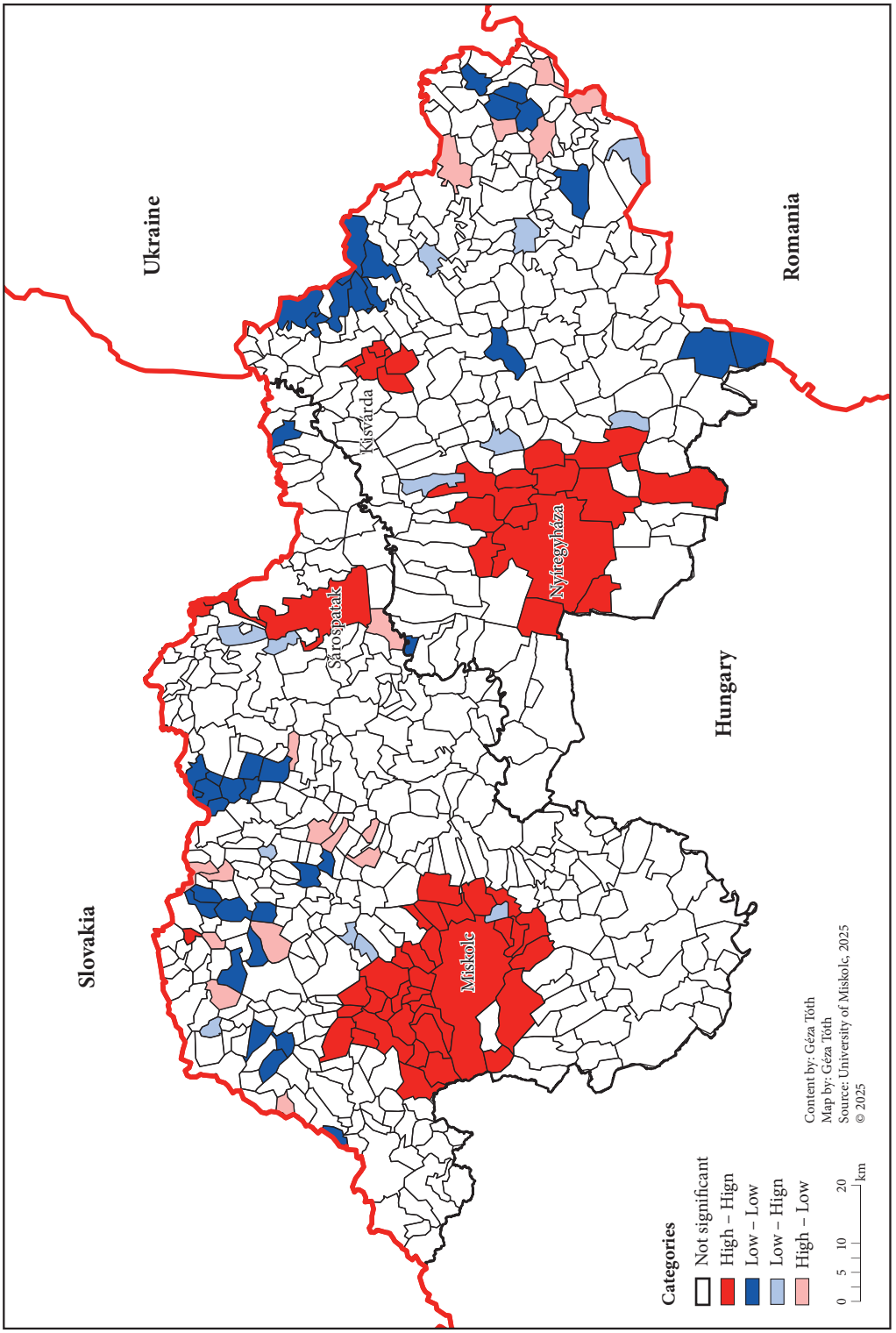
Slovakia
Ukraine
Romania
Hungary
Miskolc
Sárospatak
Kisvárda
Nyíregyháza
Categories
Not significant
High – High
Low – Low
Low – High
High – Low
0 5 10 20
km
Content by: Géza Tóth
Map by: Géza Tóth
Source: University of Miskolc, 2025
© 2025

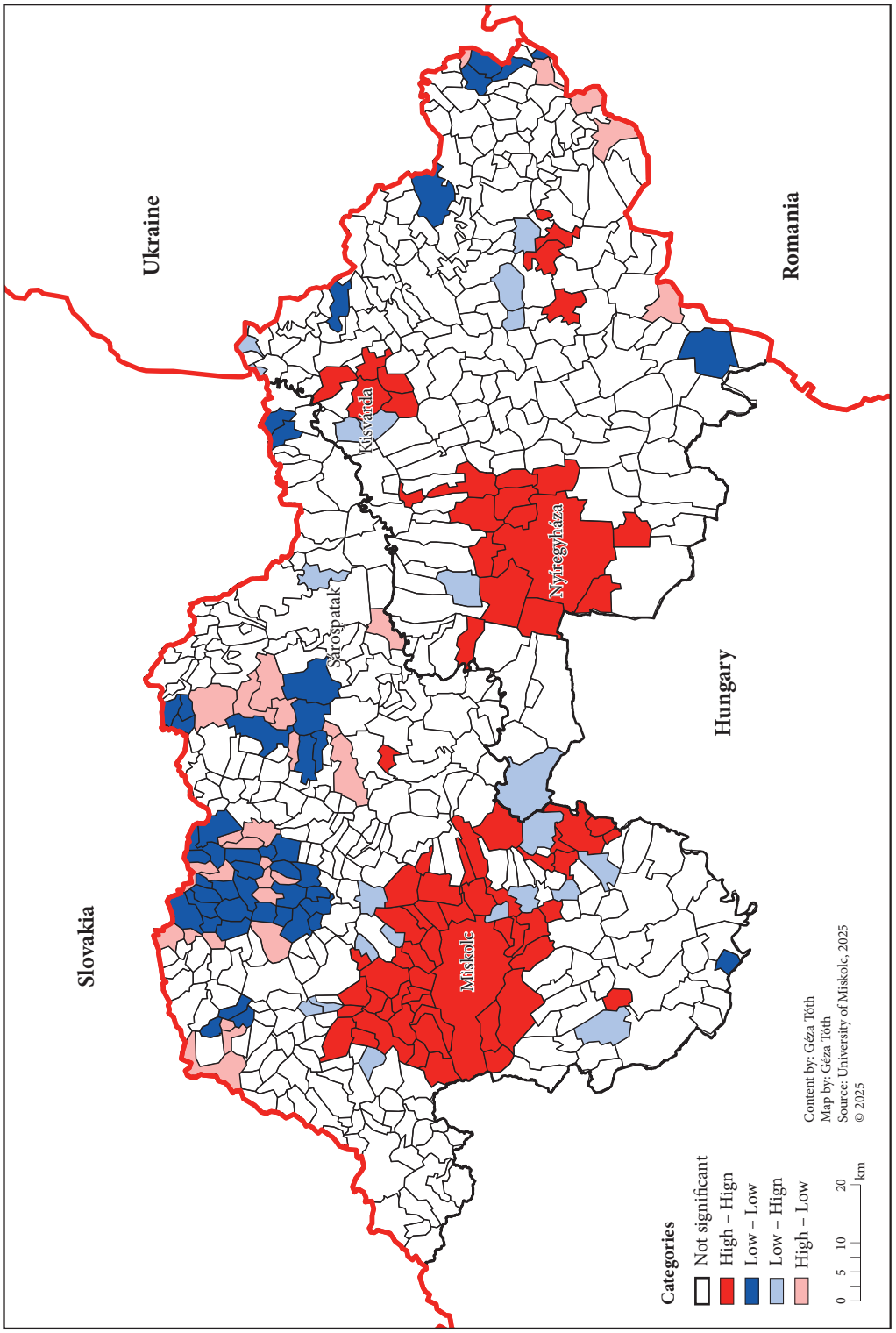
Slovakia
Ukraine
Hungary
Romania
Miskolc
Sárospatak
Kisvárda
Nyíregyháza
Categories
Not significant
High – High
Low – Low
Low – High
High – Low
0 5 10 20 km
Content by: Géza Tóth
Map by: Géza Tóth
Source: University of Miskolc, 2025
© 2025

Table 4: Migration balance per 1,000 inhabitants in the examined clusters.

Clusters	1990–1999	2000–2009	2010–2019	2020–2022	1990–2022
Not significant	–4,3	–6,2	–8,0	–7,6	–6,2
High–High	–2,7	–4,0	–3,8	–4,7	–3,6
Low–Low	–8,2	–9,6	–10,5	–14,9	–9,9
Low–High	–3,3	–5,5	–11,1	–9,5	–6,8
High–Low	–3,0	–5,6	–9,0	–7,0	–6,0
Average	–3,8	–5,5	–6,5	–6,7	–5,3

Across all clusters, negative trends are prevalent, with the LL cluster experiencing the most pronounced decline over time. Some clusters, especially LH and HL, exhibit fluctuations, indicating periods of instability or short-term improvements that were not maintained. In contrast, the High-High cluster showed greater stability, with gradual declines over the years, but without the sharp drops observed in other clusters.

The data reveals a consistent decline across all clusters, with the most significant decrease observed in the LL cluster (areas with low values where the neighboring units also have low values). While regions with high innovation potential have generally seen less drastic declines, the overall trend indicates that social innovation potential has weakened in most areas over the time periods examined. This suggests a need for targeted interventions to address the challenges faced by the most disadvantaged regions.

LL and LH clusters require targeted interventions to reverse negative trends, HL regions need policies to fully realize their innovation potential, and HH clusters benefit from measures that sustain or modestly enhance it.

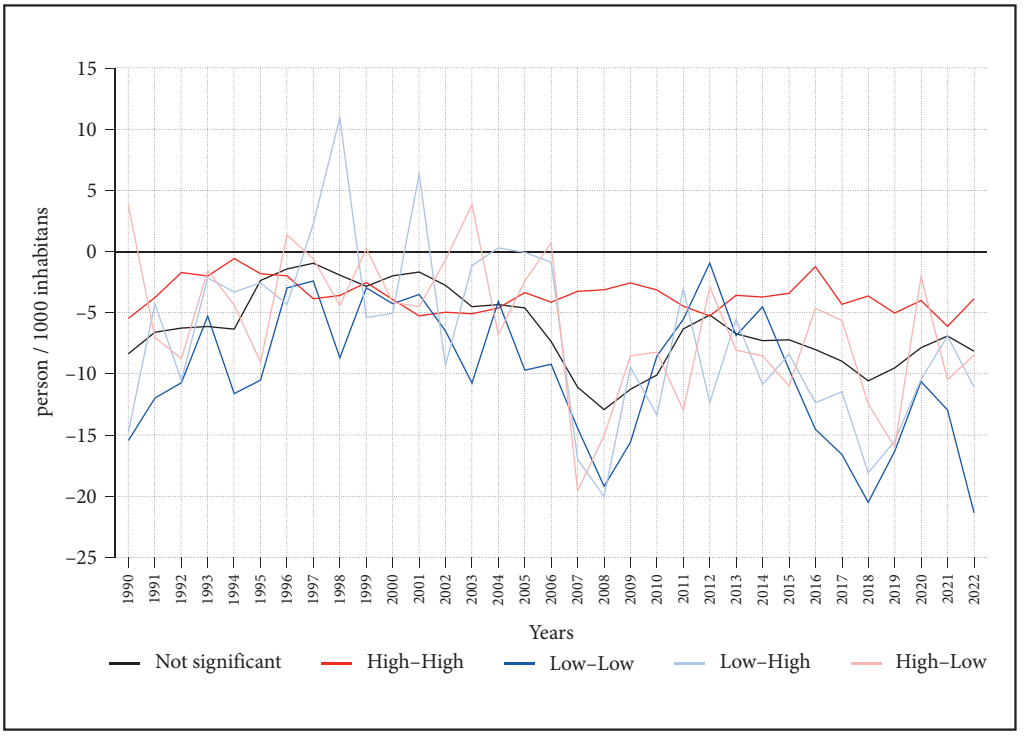

Figure 4: Migration balance per 1,000 inhabitants in the examined clusters.

4.4 Discussion

The results of the study provide important insights into the spatial dynamics of social innovation potential and its relationship with demographic trends in two disadvantaged Hungarian counties. However, beyond the general trends and clusters identified, several methodological and interpretative considerations deserve attention. The study used a carefully selected composite set of indicators, comprising 21 variables in three main categories: input, output and impact indicators. Although this three-dimensional structure reflects the systemic nature of social innovation – similar to technological or economic innovation processes – it is important to recognise the different levels of sensitivity and explanatory power between these dimensions.

Notably, the input indicators proved to be the most volatile and determinant over time, while the impact indicators showed greater stability over time. Output indicators fell in between. These differences highlight the need for greater selectivity in the use of indicators: future research and policy evaluation efforts should favour indicators that are theoretically sound and empirically sensitive to local changes. In disadvantaged regions, where data gaps are common and overly complex, composite indicators may mask rather than clarify meaningful differences.

The proposed use of the variables of social innovation potential indicator is presented in Table 5.

Table 5: Proposed use of the variables of social innovation potential indicator.

Indicator group	Example of variables	Analysis framework	Proposed use
Input	employment rate, number of nonprofits, age structure, education level	strongly reflects local dynamics	for short- and medium-term policy design and trend analysis
Output	participation in cultural activities, social services uptake	indicates activation and short-term effects	to monitor program implementation or early-stage impact
Impact	per capita income, crime rate, housing quality	captures structural outcomes	for long-term evaluation, complement with contextual analysis

Further examination of intra-county differences is crucial. Key tasks include analyzing settlements with slightly lower social innovation potential than county seats, targeting border areas lacking social foundations with locally tailored programs, identifying stakeholders, planning resources, and fostering communication and institutional support (Dusek and Szalka 2012; Schmitz et al. 2013; Veresné Somosi and Varga 2018; Kleverbeck et al. 2019; Cappellano et al. 2022; Varga et al. 2023). Additionally, linking measurement levels and methods, and assessing the long-term impact of social innovation initiatives (Varga et al. 2020; Cunha et al. 2024; Tóth and Varga 2024; Schwab Foundation … 2025), may reveal important correlations and explain outlier clusters. A clear limitation of the current study is the scope of available indicators and the lack of a deeper examination of the relative positional changes of individual settlements. Reflecting these relative positional changes in terms of migration balance remains a subject for further research. The key question is whether declining positions coincide with the settlements most affected by outmigration in the counties and to what extent an improving position translates into a more favorable migration situation over time. While spatial statistical methods identify patterns, social innovation is inherently qualitative and context-dependent, shaped by local actors, norms, and networks (Mulgan et al 2007; Veresné Somosi and Varga 2018; Schwab Foundation … 2025; Bresciani et al. 2025). Future research should integrate embedded case studies and qualitative methods within HH, LL, HL, and LH categories to explore the mechanisms behind observed spatial patterns, including institutional drivers in HH areas or latent capacities in LL areas, and to explain gaps in HL and LH municipalities.

5 Conclusion

Based on our latest study of settlements in Borsod-Abaúj-Zemplén and Szabolcs-Szatmár-Bereg counties, we conclude that the social innovation potential of settlements has changed between 2001 and 2022. Due

to the relatively slow changes in spatial processes, we aimed to analyze a longer time span. This approach allows for a comparison between our previous studies and current research while also providing a foundation for assessing the direction and extent of these changes. The most striking transformation is observed in the input indicators (institutional, locational, human, and activity factors), suggesting that the resources and conditions underlying social innovation have partially changed. The most significant shifts are primarily visible in the demographic and employment conditions of the settlements.

Our research also showed a correlation between social innovation potential and the population retention capacity of settlements in the two examined counties. In settlements with improving social innovation potential, less population decline was observed during the analyzed period, indicating that more socially innovative settlements are more attractive to residents. Our analysis revealed a correlation between social innovation potential and migration balance in the two disadvantaged counties of Hungary. Settlements with higher social innovation potential experienced lower emigration rates, reinforcing the idea that social innovation plays a crucial role in the population retention capacity of settlements. Conversely, settlements with worsening positions exhibited the highest emigration rates.

Overall, the research results confirm that social innovation is a key factor in the development and population retention of settlements. The promotion of social innovation may contribute to reducing spatial inequalities and supporting the integration of lagging settlements, reaffirming our previous research findings. According to the reviewed literature (Moulaert and Nussbaumer 2005; McNeill 2017; Lipták 2019; Castro-Arce and Vanclay 2020; Alina 2023) and our earlier studies (Varga et al. 2023; Varga and Tóth 2024), the social innovation potential of settlements aligns with their current development status. However, social innovation may generate positive transformation potential in the medium term, in line with slow-changing spatial processes. Investing in, promoting, and strengthening social innovation has a fundamental impact on competitiveness and, ultimately, on improving quality of life.

ACKNOWLEDGEMENT: Supported by the »University Research Scholarship Program of the Ministry for Culture and Innovation from the source of the National Research, Development and Innovation Fund.«

RESEARCH DATA: For information on the availability of research data related to the study, please visit the article webpage: https://doi.org/10.3986/AGS.14410.

6 References

Alina, K. 2023: Social innovation and territorial development. In: Encyclopedia of Social Innovation. Edward Elgar Publishing. https://doi.org/10.4337/9781800373358.ch49

Anselin, L. 1995: Local indicators of spatial association–LISA. *Geographical Analysis* 27-2. https://doi.org/10.1111/j.1538-4632.1995.tb00338.x

Avdić, A., Avdić, B., Zupanc, I. 2022: Socio-demographic analysis of border regions of Bosnia and Herzegovina. *Acta geographica Slovenica* 6/AGS.10859

Benedek, J., Kocziszky, G., Veresné Somosi, M., Balaton. K. 2015: Regionális társadalmi innováció generálása szakértői rendszer segítségével. *Észak-magyarországi Stratégiai Füzetek* 12-2.

Bosworth, G., Rizzo, F., Marquardt, D., Strijker, D., Haartsen, T., Aagaard Thuesen, A. 2016: Identifying social innovations in European local rural development initiatives. *Innovation: The European Journal of Social Science Research* 29-4. https://doi.org/10.1080/13511610.2016.1176555

Bresciani, S., Mondal, R., Schmidt-Thome, K., Noera, F. M. 2025: Ten social innovation case studies to address cities' challenges: Citizens engagement, energy and behavioral change. In: Social Innovation Projects for Climate Neutral Cities: Making Municipalities Sustainable with People-Based Solutions. SpringerBriefs in Applied Sciences and Technology. Springer. https://doi.org/10.1007/978-3-031-87726-1_5

Cajaiba-Santana, G. 2014: Social innovation: Moving the field forward. A conceptual framework. *Technological Forecasting and Social Change* 82. https://doi.org/10.1016/j.techfore.2013.05.008

Cappellano, F., Sohn, C., Makkonen, T., Kaisto, V. 2022: Bringing borders back into cross-border regional innovation systems: Functions and dynamics. *Environment and Planning A: Economy and Space* 54-5. https://doi.org/10.1177/0308518X221073987

Carvache-Franco, O., Candela, G. G., Barreno, E. Z. 2018: The key factors in social innovation projects. *Mediterranean Journal of Social Sciences* 9-5. https://doi.org/10.2478/mjss-2018-0142

Castro Spila, J., Luna, A., Unceta, A. 2016: Social innovation regime: An exploratory framework to measure social innovation. *Simpact Working Paper* 1.

Castro-Arce, K., Vanclay, F. 2020: Transformative social innovation for sustainable rural development: An analytical framework to assist community-based initiatives. *Journal of Rural Studies.* 74. https://doi.org/10.1016/j.jrurstud.2019.11.010

Cunha, J., Alves, J., Araujo, J. 2024: Social impact measures for social innovation: Challenges and pathways. *Revista de Administração Mackenzie* 25-3. https://doi.org/10.1590/1678-6971/eRAMR240012

Dainiené, R., Dagiliené, L. 2016: Measurement of social innovation at organisation's level: Theoretical issues. *Economics and Business* 29. https://doi.org/10.1515/eb-2016-0027

Dawson, P. M., Daniel, L. 2010: Understanding social innovation: a provisional framework. *International Journal of Technology Management* 51-1. https://doi.org/10.1504/IJTM.2010.033125

De Palo, C., Karagiannis, S., Raab, R. 2018: Innovation and inequality in the EU: for better or for worse? *Report*. Publications Office of the European Union. https://doi.org/10.2760/365700

Dusek, T. 2004: A területi elemzések alapjai. *Regionális Tudományi Tanulmányok 10*. ELTE Regionális Földrajzi Tanszék – MTA – ELTE Regionális Tudományi Kutatócsoport.

Dusek, T., Kotosz, B. 2016: Területi Statisztika. Akadémiai Kiadó. https://doi.org/10.1556/9789634540014

Dusek, T., Szalka, E. 2012: Is there a county border effect in spatial income differences in Hungary? In: 52nd Congress of the European Regional Science Association: »Regions in Motion - Breaking the Path«. European Regional Science Association (ERSA).

European Commission 2013: Guide to social innovation. Regional and Urban Policy. *Guide*.

Ewers, H. J., Brenck, A. 1992: Innovationsorientierte Regionalpolitik: Zwischenfazit eine Forschungsprogramms. In: Regionale und sektorale Strukturpolitik: Festschrift zum 60. Geburtstag von Rainer Thoss. Universität Münster.

Getis, A., Ord, J. K. 1996: Local spatial statistics: an overview. In: Spatial Analysis: Modelling in a GIS Environment. John Wiley & Sons.

Hazel, K. L., Onaga, E. 2003: Experimental social innovation and dissemination: The promise and its delivery. *American Journal of Community Psychology* 32-3,4. https://doi.org/10.1023/B:AJCP.0000004748.50885.2e

Hochgerner, J. 2011: The analysis of social innovation as social practice. In: ICICI Vienna 2011: Challenge Social Innovation – Innovating Innovation by Research – 100 Years after Schumpeter. NET4SOCIETY.

Kleverbeck, M., Krlev, G., Mildenberger, G., Strambach, S., Thurmann, J-F., Terstriep, J., Wloka, L. 2019: Indicators for measuring social innovation. In: Atlas of Social Innovation. 2nd Volume: A World of New Practices. Oekom Verlag GmbH.

Kocziszky, G. 2004: Az Észak-magyarországi régió innovációs potenciáljának vizsgálata. *Észak-magyarországi Stratégiai Füzetek* 1-01.

Lipták, K. 2019: The importance of social innovations in rural areas. *DETUROPE - The Central European Journal of Regional Development and Tourism* 11-3. https://doi.org/10.32725/det.2019.031

Ljubenović, M., Bogdanović Protić, I., Dinić Branković, M., Đekić, J., Igić, M. 2025: Identifying characteristics and typology of small shrinking towns in Serbia: The case of the Region of Southern and Eastern Serbia. *Acta geographica Slovenica* ://doi.org/10.3986/AGS.13717

Lockley, R., Altamirano, T., Copestake, J. 2008: Wellbeing and migration. In: Wellbeing and Development in Peru. *Studies of the Americas*. Palgrave Macmillan. https://doi.org/10.1057/9780230616998_5

Lőcsei, H. 2010: Területi növekedési pályák Magyarországon, 1990–2008. *Ph.D*. thesis. Eötvös Loránd Tudományegyetem.

McNeill, J. 2017: Enabling social innovation assemblages: Strengthening public sector involvement. *Ph.D. thesis*. Western Sydney University.

Moralli, M. 2023: Opening the black box of social innovation in migration governance. *Innovation: The European Journal of Social Science Research* 36-4. https://doi.org/10.1080/13511610.2023.2246663

Moralli, M. 2025: Social innovation and migration. In: Elgar Encyclopedia of Global Migration. Edward Elgar Publishing. https://doi.org/10.4337/9781035300389.ch169

Moran, P. A. P. 1948: The interpretation of statistical maps. *Journal of the Royal Statistical Society: Series B (Methodological)* 10-2. https://doi.org/10.1111/j.2517-6161.1948.tb00012.x

Moulaert, F., Nussbaumer, J. 2005: The social region: Beyond the territorial dynamics of the learning economy. *European Urban and Regional Studies* 12-1. https://doi.org/10.1177/0969776405048500

Mulgan, G., Tucker, S., Ali, R., Sanders, B. 2007: Social innovation: What it is, why it matters and how it can be accelerated. *Working paper*. University of Oxford.

Mumford, M. D., Scott, G. M., Gaddis, B. H., Strange, J. M. 2002: Leading creative people: Orchestrating expertise and relationships. *The Leadership Quarterly* 13-6. https://doi.org/10.1016/S1048-9843(02)00158-3

Nagy, Z., Tóth, G. 2019: A társadalmi innovációs potenciál mérési lehetőségei Borsod-Abaúj-Zemplén példáján. *Észak-magyarországi Stratégiai Füzetek* 16-2.

Nagy, Z., Tóth, G. 2021: A társadalmi innováció mérési lehetőségei Borsod-Abaúj-Zemplén megye települései példáján. In: Társadalmi innováció – társadalmi jólét. Ludovika Egyetemi Kiadó.

Nemes Nagy, J. 2006: A területi versenyképesség elemzési módszerei. In: Régiók és települések versenyképessége. MTA Regionális Kutatások Központja.

Nemes Nagy, J., Jakobi, Á., Németh, N. 2001: A jövedelemegyenlőtlenségek térségi és településszerkezeti összetevői. *Statisztikai Szemle* 79-10,11.

Németh, N. 2008: Fejlődési tengelyek az új hazai térszerkezetben. Az autópálya-hálózat szerepe a regionális tagoltságban. *Ph.D. Thesis*. Eötvös Loránd Tudományegyetem.

Neumeier, S. 2017: Social innovation in rural development: identifying the key factors of success. *The Geographical Journal* 183-1. https://doi.org/10.1111/geoj.12180

OECD, Eurostat 2018: Oslo Manual 2018: Guidelines for collecting, reporting and using data on innovation, 4th edition. The measurement of scientific, technological and innovation activities. *Report*. https://doi.org/10.1787/9789264304604-en

Pénzes, J. 2014: Periférikus térségek lehatárolása – dilemmák és lehetőségek. Didakt Kiadó.

Pol, E., Ville, S. 2009: Social innovation: Buzz word or enduring term? *The Journal of Socio-Economics* 38-6. https://doi.org/10.1016/j.socec.2009.02.011

Salamońska, J. 2022: Quantitative methods in migration research. In: Introduction to Migration Studies. *IMISCOE Research Series*. Springer. https://doi.org/10.1007/978-3-030-92377-8_26

Schmitz, B., Krlev, G., Mildenberger, G., Bund, E., Hubrich, D. 2013: Paving the way to measurement – A blueprint for social innovation metrics: A short guide to the research for policy makers. *Project deliverable*. TEPSIE.

Schwab Foundation for Social Entrepreneurship 2025: The future is collective: Advancing collective social innovation to address society's biggest challenges. *Report*.

Szendi, D. 2018: A társadalmi innovációs potenciál mérésének lokális szintű lehetőségei. *Erdélyi Társadalom* 16-1. https://doi.org/10.17177/77171.207

Tóth, G., Nagy, Z. 2013: Eltérő vagy azonos fejlődési pályák? A hazai nagyvárosok és térségek összehasonlító vizsgálata. *Területi Statisztika* 53-6.

Tóth, G., Varga, K. 2024: Social innovation potential and quality of Life: The example of Hungarian settlements. *DETUROPE – The Central European Journal of Regional Development and Tourism* 16-2. https://doi.org/10.32725/det.2024.008

Unceta, A., Castro Spila, J., Garcia Fronti, J. 2016: Social innovation indicators. *Innovation: The European Journal of Social Science Research* 29-2. https://doi.org/10.1080/13511610.2015.1127137

Varga, A. 2005: Agglomeráció, technológiai haladás és gazdasági növekedés. A K+F térszerkezet makrogazdasági hatásainak vizsgálata. *Ph.D. Thesis*. Pécsi Tudományegyetem.

Varga, K. Tóth, G. 2024: A társadalmi innováció mérési módszertana – mit és hogyan mérjünk?. In: »Mérleg és Kihívások« XIII. Nemzetközi Tudományos Konferencia Collection of studies. Miskolci Egyetem Gazdaságtudományi Kar.

Varga, K., Tóth, G. 2021: Szabolcs-Szatmár-Bereg megye települései társadalmi innovációs potenciáljának térstatisztikai elemzése. In: Társadalmi innováció – társadalmi jólét. Ludovika Egyetemi Kiadó.

Varga, K., Tóth, G. 2024: Social innovation initiatives of NGOs in a Hungarian disadvantaged area. *Észak-magyarországi Stratégiai Füzetek* 21-01. https://doi.org/10.32976/stratfuz.2024.9

Varga, K., Tóth, G., Nagy, Z. 2020: Examination of social innovation potential characteristics in the example of Borsod-Abaúj-Zemplén county. *Theory, Methodology, Practice - Review of Business and Management* 16-1. https://doi.org/10.18096/TMP.2020.01.07

Varga, K., Veresné Somosi, M., Tóth, G. 2023: Cluster analysis of competitive advantage in Hungarian settlements based on their social innovation potential. *Pakistan Journal of Life and Social Sciences* 21-1. https://doi.org/10.57239/PJLSS-2023-21.1.0027

Vercher, N. 2022: The role of actors in social innovation in rural areas. *Land* 11-5. https://doi.org/10.3390/land11050710

Veresné Somosi M., Tóth, G., Varga, K. 2023: A társadalmi innovációs potenciál és az életminőség területi vizsgálata Magyarországon. *Statisztikai Szemle* 101-10. https://doi.org/10.20311/stat2023.10.hu0865

Veresné Somosi M., Varga K. 2018: How does social innovation contribute to solving social problems? A process-oriented framework for measuring social innovation. *European Journal of Social Science Education and Research* 12-1. https://doi.org/10.2478/ejser-2018-0007

Veresné Somosi, M., Varga, K. 2021: Conceptualisation as a tool in understanding social innovation – methods, case studies, practices. University of Miskolc, Faculty of Economics.

Widuto, A. 2019: Regional inequalities in the EU. EPRS | European Parliamentary Research Service.

Woolcock, M. 1998: Social capital and economic development: Toward a theoretical synthesis and policy framework. *Theory and Society* 27-2. https://doi.org/10.1023/A:1006884930135

Wright, K. 2012: International migration, development and human wellbeing. Palgrave Macmillan. https://doi.org/10.1057/9781137284853

Young, H. P. 2011: The dynamics of social innovation. *Proceedings of the National Academy of Sciences of the United States of America* 108-4. https://doi.org/10.1073/pnas.1100973108

Acta geographica Slovenica, 65-2, 2025, 65–89

SPATIOTEMPORAL ANALYSIS OF LIGHT POLLUTION IN SAMSUN (TURKEY) USING SPATIAL STATISTICS AND ALGEBRA FROM SNPP/VIIRS SATELLITE IMAGERY

Sarp Doruk Ozturk, Derya Ozturk

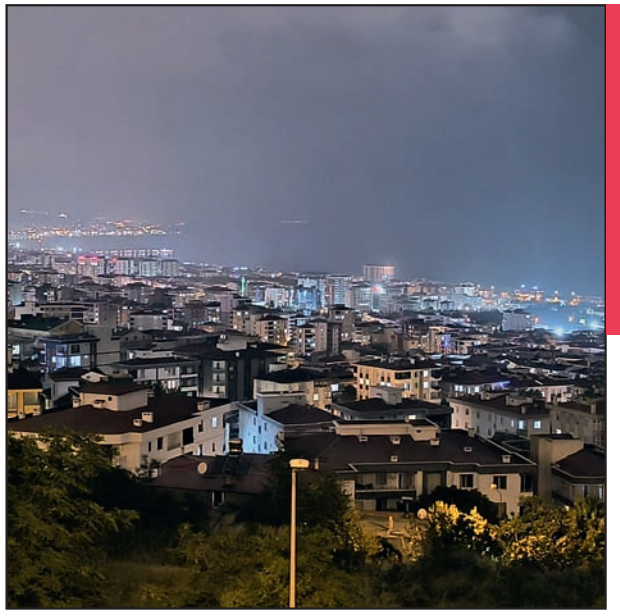

SARP DORUK OZTURK

Nighttime urban glow illustrating the extent of light pollution in Samsun, Turkey.

DOI: https://doi.org/10.3986/AGS.14506
UDC: 504.6:628.971.7(560Samsun)"2012/2024"
528.8(560Samsun)"2012/2024"

Sarp Doruk Ozturk[1], Derya Ozturk[2]

Spatiotemporal analysis of light pollution in Samsun (Turkey) using spatial statistics and algebra from SNPP/VIIRS satellite imagery

ABSTRACT: This study analyzes the spatiotemporal changes in light pollution in Samsun (Turkey) from 2012 to 2024 using remote sensing and geographic information systems. SNPP/VIIRS satellite data from five years were examined using spatial statistics and algebraic methods to measure nighttime light variations. Results show a sharp decline in dark sky areas and expansion of high light zones from 85.9 km² to 139.5 km², and medium zones from 87.6 km² to 145.5 km², driven by urbanization and industrial growth. Rapid changes occurred in Atakum, Ilkadim, Canik, and Tekkekoy, affecting sensitive ecological and astronomical sites. The strong correlation between light emissions and socio-economic indicators highlights the need for sustainable lighting policies to mitigate adverse environmental impacts.

KEYWORDS: light pollution, remote sensing, geographic information systems, spatiotemporal analysis, SNPP/VIIRS, urbanization, environmental sustainability

Prostorsko-časovna analiza svetlobnega onesnaženja v Samsunu (Turčija) z uporabo prostorske statistike in algebre na podlagi satelitskih posnetkov SNPP/VIIRS

POVZETEK: Članek na podlagi daljinskega zaznavanja in geografskih informacijskih sistemov analizira prostorsko-časovne spremembe svetlobnega onesnaženja v turškem mestu Samsun med letoma 2012 in 2024. Za merjenje sprememb nočne svetlobe so bili na podlagi prostorske statistike in algebrskih metod preučeni satelitski podatki SNPP/VIIRS za pet let. Rezultati kažejo izrazito krčenje območij temnega neba ter širitev površine močno osvetljenih območij s 85,9 km² na 139,5 km² in srednje osvetljenih območij z 87,6 km² na 145,5 km², kar je posledica urbanizacije in industrijske rasti. Najhitrejše spremembe so bile zabeležene v četrtih Atakum, Ilkadim, Canik in Tekkekoy, kar vpliva na občutljiva ekološka in astronomska območja. Zaradi močne povezave med svetlobnimi emisijami in družbenogospodarskimi kazalniki je poudarjena potreba po trajnostnih politikah na področju razsvetljave, s katerimi bi se zmanjšali negativni vplivi na okolje.

KLJUČNE BESEDE: svetlobno onesnaženje, daljinsko zaznavanje, geografski informacijski sistemi, prostorsko-časovna analiza, SNPP/VIIRS, urbanizacija, okoljska trajnost

The article was submitted for publication on June 11th, 2025.
Uredništvo je prejelo prispevek 11. junija 2025.

[1] Samsun Bahcesehir College Atakum Science and Technology High School, Samsun, Turkey
sarpdorukozturk2026@yahoo.com (https://orcid.org/0009-0006-6159-4852)

[2] Ondokuz Mayis University, Department of Geomatics Engineering, Samsun, Turkey
dzozturk@gmail.com (https://orcid.org/0000-0002-0684-3127)

1 Introduction

Light pollution refers to the harmful effects of excessive or misdirected artificial lighting, including skyglow, glare, light trespass, and over-illumination. These effects disrupt ecosystems, human health, astronomy, and energy efficiency (Chepesiuk 2009; Pan and Du 2021). Since the invention of electric lighting in the 19th century, global light emissions have steadily increased, particularly in urban areas, due to expanding residential, industrial, and commercial activity (Nurbandi et al. 2016; Levin and Zhang 2017; Cox et al. 2022). This increase has been further accelerated by uncontrolled urbanization (Hu et al. 2018; Gaston et al. 2023).

Excessive artificial nighttime lighting disrupts circadian rhythms, causes sleep disorders, and alters wildlife behavior, including feeding and migration patterns (Butt 2012; Hu et al. 2018; Brayley et al. 2022). It also impairs the visibility of celestial objects and reduces the effectiveness of astronomical instruments (Faid et al. 2024). Moreover, inefficient outdoor lighting wastes energy, leading to economic losses (Tong et al. 2022). Light pollution has thus become a growing concern across disciplines, including astronomy, environmental science, ecology, and public health (Chepesiuk 2009; Wu and Wang 2019; Green et al. 2022).

Light pollution is measured through both in situ methods and remote sensing (RS) (Mander et al. 2023). While tools like Sky Quality Meters (SQM) provide local precision, they lack large-scale coverage (Ji et al. 2024). RS enables wide-area monitoring of nocturnal lighting using satellite-based nighttime light (NTL) imagery, especially from the Defense Meteorological Satellite Program's Operational Linescan System (DMSP/OLS) and Suomi National Polar-orbiting Partnership's Visible Infrared Imaging Radiometer Suite (SNPP/VIIRS) satellites (Hu et al. 2018; Wu and Wang 2019). Compared to DMSP/OLS, SNPP/VIIRS provides higher spatial and radiometric resolution and filters out non-artificial light sources for greater accuracy (Levin and Zhang 2017; Ma et al. 2020).

However, several challenges remain in interpreting SNPP/VIIRS-derived trends. First, the satellite does not capture blue wavelengths characteristic of modern white Light Emitting Diode (LED) lighting. Second, the dataset is relatively limited, as SNPP/VIIRS only began recording nighttime radiance in late 2011, with data available for download from April 2012 onward (Carias et al. 2021; Levin 2025). Despite these constraints, SNPP/VIIRS remains a crucial dataset and is widely used to detect long-term urban brightness patterns and transient events such as wildfires or maritime activity (Cheon and Kim 2020; Yerli et al. 2021).

With the deployment of high spatial resolution NTL data from the Glimmer Imager for Urbanization (GIU) sensor aboard the Sustainable Development Goals Satellite 1 (SDGSAT-1) by the Chinese Academy of Sciences (CAS), new opportunities have emerged to address some of the current gaps in light pollution research (Xie et al. 2024). The GIU sensor provides multispectral NTL imagery with a 40-m resolution and panchromatic imagery at 10-m resolution. Importantly, these data are globally accessible since September 2022 (Yin et al. 2024), offering the highest quality NTL observations currently available and enabling the differentiation of light sources, including the effects of LED transitions, which are not always accurately captured by SNPP/VIIRS (Liu et al. 2024; Wang et al. 2024). Nevertheless, SNPP/VIIRS NTL data remain indispensable for long-term change detection compared to SDGSAT-1 (Xie et al. 2024). Importantly, recent studies indicate that NTL radiance values are highly variable, and that the effects of seasonal fluctuations and cultural events on NTL intensity must be carefully considered (Martinez et al. 2023; Dong et al. 2025). In change-detection studies, these effects can be minimized by using comparable time periods. Moreover, RS-derived NTL data are often validated using ground-based measurements (e.g., SQM) or high-resolution airborne imagery to improve accuracy and reliability (Guk and Levin 2020; Levin 2023).

Many studies have employed RS and geographic information systems (GIS) to analyze the spatial distribution and temporal dynamics of NTL intensity (Nurbandi et al. 2016; Levin and Zhang 2017; Yerli et al. 2021; Cox et al. 2022). However, most studies rely on conventional GIS techniques and focus on national or regional scales, with limited application of spatial statistical or algebraic methods. Consequently, localized patterns and urban-scale variations often remain underexplored.

Samsun, the most populous and economically developed city in Turkey's Black Sea region (Samsun Chamber of… 2022), encompasses ecologically critical zones such as the Kizilirmak Delta (a Ramsar site), the Yesilirmak Delta, and Lake Ladik (Eken et al. 2006), as well as one of Turkey's fifteen astronomical observatories, located in Atakum as listed by the Scientific and Technological Research Council of Turkey. Rapid urbanization, industrial expansion, and infrastructure development have led to significant losses in dark sky areas, affecting both urban and rural zones. Despite these challenges, academic research on light pollution

in Samsun remains scarce. Existing studies are limited to either a single district (Türk and Yavuz 2023) or national-scale data that ends in 2020 (Yerli et al. 2021), lacking detailed spatial analyses.

This study addresses these gaps by applying SNPP/VIIRS imagery to conduct a fine-grained, district-level analysis of Samsun from 2012 to 2024. By integrating RS and GIS with advanced spatial statistical and algebraic techniques, the study moves beyond descriptive mapping and establishes a quantitative framework to detect spatial heterogeneity and temporal trends in artificial lighting, which represents an approach that has rarely been applied in previous NTL studies.

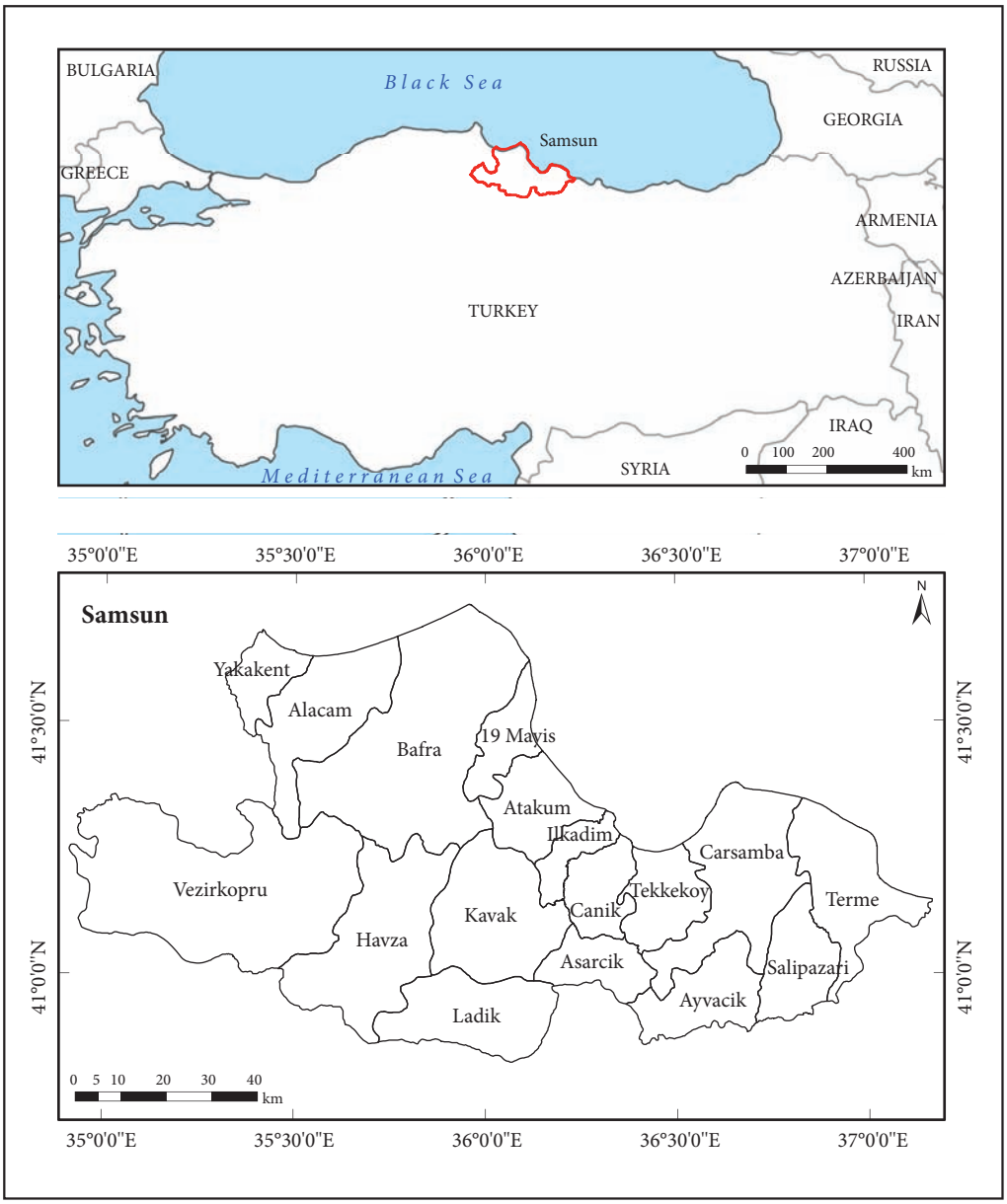

Figure 1: Study area: Samsun.

The study makes three primary contributions: (i) it demonstrates the effectiveness of RS and GIS integration in identifying light pollution patterns at the sub-city scale; (ii) it advances the underutilized application of spatial statistics and algebra in NTL research; and (iii) it provides a replicable methodology applicable to other rapidly urbanizing contexts. These methodological contributions are complemented by the study's regional focus, which provides a rare, spatially detailed assessment of a city with significant ecological and astronomical value. The findings provide practical insights for urban planning, sustainable environmental management, and dark sky conservation.

2 Study area

Samsun (Figure 1) is located in northern Turkey (40°50′–41°51′ N, 34°25′–37°08′ E), and by the data from General Directorate of Mapping, it covers approximately 9,730 km². According to data from Statistical Institute, Samsun had a population of around 1.4 million in 2024, making it the Black Sea region's most populous province (Öztürk and Gündüz 2019). Comprising 17 districts and a 210 km coastline, it serves as a metropolitan and industrial hub attracting internal migration (Samsun Chamber of … 2022).

Samsun is undergoing rapid urbanization, especially in coastal areas such as Atakum, Ilkadim, Canik, and Tekkekoy, which show the highest population growth (Ozturk 2017). According to the Socio-Economic Development Index (SEDI) by General Directorate of Development Agencies, Atakum ranks in the top tier and hosts both an astronomical observatory and a major tourism sector, while the other three districts fall into the second-highest tier.

While some districts experience intense urban growth, others contain ecologically sensitive zones vulnerable to light pollution. The Kizilirmak Delta (31,327 ha), located in 19 Mayis, Bafra, and Alacam, is one of Turkey's most biodiverse wetlands, home to 362 bird species and various habitats. It holds Ramsar, Natural Site, and Wildlife Development Area designations (General Directorate of … 2019). Similarly, the Yesilirmak Delta (20,658 ha) spans Carsamba, Tekkekoy, and Terme, supporting over 323 bird species and serving as a key habitat for waterfowl. Ladik Lake, a nationally important wetland, also hosts rich fish and bird biodiversity (Eken et al. 2006; General Directorate of … 2024).

3 Methodology

This study employs RS and GIS to assess district-level changes in light pollution in Samsun between 2012 and 2024. The primary data source is SNPP/VIIRS Day/Night Band (DNB) monthly cloud-free composite NTL imagery from 2012, 2015, 2018, 2021, and 2024. The values in SNPP/VIIRS DNB are expressed in nanowatts per square centimeter per steradian (nW/cm²/sr). Data processing was conducted in ArcGIS 10.3 (ESRI, Redlands, CA), using spatial statistics and algebra. With the Zonal Statistics tool, key metrics (minimum, maximum, mean, and standard deviation) were extracted for each district and Samsun overall. To visualize spatial variation, change maps (2012–2015, 2015–2018, 2018–2021, 2021–2024, and 2012–2024) were generated using Algebraic Change Mapping, and a range map (2012–2024) was produced with the Cell Statistics tool. Light emission values were classified into five categories to generate light pollution maps for each study year, and the area of each class was calculated to evaluate temporal trends. Finally, Pearson correlation analysis was performed using Multivariate Statistics tools to examine the relationship between mean light emission and variables such as population, population density, and SEDI scores. An overview of the methodological workflow is presented in Figure 2.

3.1 Data

This study utilizes SNPP/VIIRS DNB monthly cloud-free composite Version 1 imagery (Earth Observation Group, Colorado School of Mines 2025) to assess nighttime light emissions. SNPP/VIIRS DNB is a satellite-based dataset widely used in Earth system science for measuring visible and near-infrared nocturnal light (Wu and Wang 2019; Earth Data, NASA 2025). The cloud-free composite provides globally calibrated mosaics of monthly average observations, excluding stray light-affected data (Levin and Zhang 2017). The composites are produced by the Suomi National Polar Partnership, a NOAA (National Oceanic and

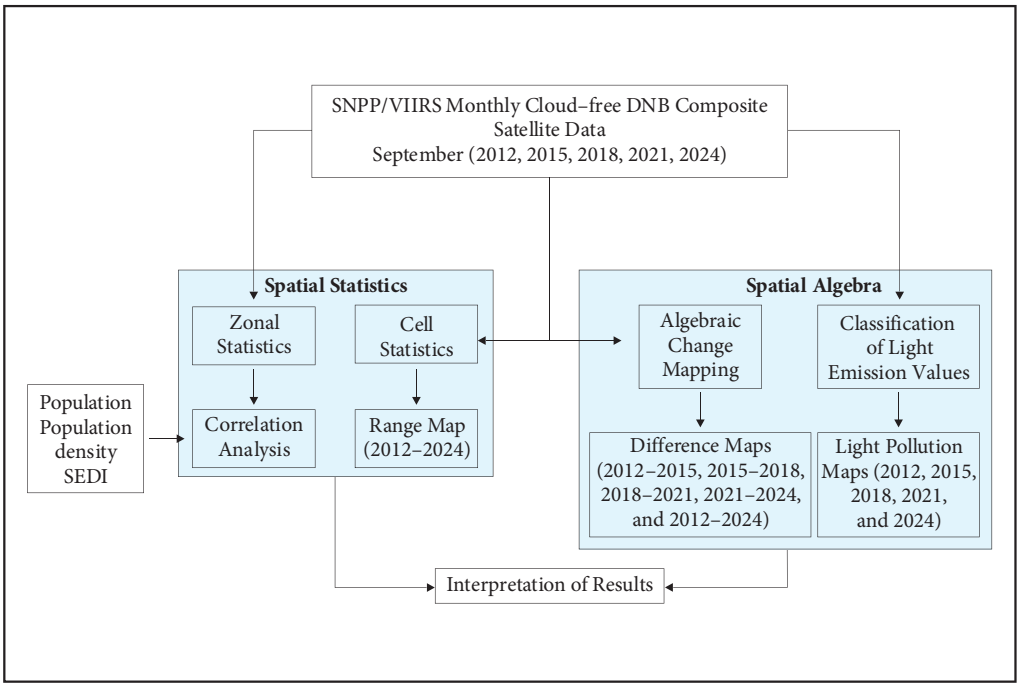

Figure 2: Workflow of the study.

Atmospheric Administration) and NASA (National Aeronautics and Space Administration) collaboration (Miller et al. 2013; Nurbandi et al. 2016). They are radiometrically calibrated and geometrically corrected, which ensures their suitability for direct scientific analysis (Levin 2017). This study used tile 2 (75N/060W) for the years 2012, 2015, 2018, 2021, and 2024, focusing on September due to its typically low cloud cover over Samsun. Data specifications of SNPP/VIIRS DNB are summarized in Table 1 according to the technical information published by NASA, Earth Data.

Additional data on population, population density, and SEDI were used to examine the relationship between light pollution and urban characteristics (Table 2). District-level population figures were sourced from the Statistical Institute, and density was calculated using population and district area data, with boundaries provided by the General Directorate of Mapping. SEDI scores and rankings, derived from 56 variables across six domains, were obtained from the data by General Directorate of Development Agencies. Central districts (Atakum, Ilkadim, Canik, Tekkekoy) show higher population, population density, and SEDI scores, whereas rural districts such as Ayvacik, Asarcik, Salipazari, Yakakent, and Vezirkopru have lower values, reflecting urban–rural contrasts.

Table 1: SNPP/VIIRS DNB data specifications.

Specification	Description
Image Resolution	15 arc seconds (~742 m at nadir)
Unit	nW/cm^2/sr
Coordinate Reference System	EPSG:4326 (Geographic Lat/Long)
Equatorial Crossing Time	1:30 PM (ascending)
Data Coverage	2012-01-02 to Present

Table 2: Area, population, population density, SEDI rank, and SEDI score of districts in Samsun (2012–2024).

District	Area (km^2)	SEDI rank	SEDI score	Population (Population density)				
				2012	2015	2018	2021	2024
19 Mayis	233.1	3	-0.137	24288 (104.2)	24627 (105.7)	26337 (113.0)	26366 (113.1)	28318 (121.5)
Alacam	598.2	4	-0.417	28315 (47.3)	26301 (44.0)	25854 (43.2)	24860 (41.6)	24686 (41.3)
Asarcik	254.5	5	-0.745	18215 (71.6)	17238 (67.7)	17628 (69.3)	16278 (64.0)	16128 (63.4)
Atakum	351.4	1	1.734	139730 (397.6)	169809 (483.2)	202618 (576.6)	238702 (679.3)	253437 (721.2)
Ayvacik	383.9	5	-0.784	22623 (58.9)	20619 (53.7)	21847 (56.9)	19436 (50.6)	19556 (50.9)
Bafra	1502.5	3	0.256	143366 (95.4)	141401 (94.1)	142210 (94.7)	142341 (94.7)	143600 (95.6)
Canik	262.2	2	0.553	92201 (351.6)	96541 (368.2)	97564 (372.1)	99369 (379.0)	100591 (383.6)
Carsamba	773.3	3	-0.015	136802 (176.9)	136775 (176.9)	138840 (179.5)	140439 (181.6)	141850 (183.4)
Havza	864.9	3	-0.124	43520 (50.3)	41146 (47.6)	40194 (46.5)	38872 (44.9)	38493 (44.5)
Ilkadim	154.8	2	1.343	312332 (2017.7)	321714 (2078.3)	332230 (2146.2)	340421 (2199.1)	325775 (2104.5)
Kavak	696.8	4	-0.331	20312 (29.2)	20130 (28.9)	21692 (31.1)	21260 (30.5)	25469 (36.6)
Ladik	543.2	4	-0.260	17274 (31.8)	16474 (30.3)	16734 (30.8)	16320 (30.0)	16309 (30.0)
Salipazari	349.0	5	-0.730	19379 (55.5)	18869 (54.1)	22923 (65.7)	19305 (55.3)	20046 (57.4)
Tekkekoy	326.5	2	0.650	48997 (150.1)	49843 (152.7)	52258 (160.1)	55369 (169.6)	58889 (180.4)
Terme	557.5	4	-0.202	73094 (131.1)	71910 (129.0)	72354 (129.8)	71366 (128.0)	71720 (128.6)
Vezirkopru	1672.2	5	-0.537	102212 (61.1)	97815 (58.5)	95569 (57.2)	91978 (55.0)	88564 (53.0)
Yakakent	204.5	5	-0.538	9062 (44.3)	8672 (42.4)	8864 (43.3)	8592 (42.0)	8945 (43.7)
Total (SAMSUN)	**9729.0**			**1227434 (126.2)**	**1255257 (129.0)**	**1309379 (134.6)**	**1344908 (138.2)**	**1354058 (139.2)**

3.2 Spatial statistical analysis

Spatial statistics involves applying statistical methods to geographically referenced data, where location is essential to analysis (Unwin 2009). These methods treat spatial attributes as variables, enabling detection of patterns and relationships (Forster 2000). This study employed three techniques: Zonal Statistics, Cell Statistics, and Multivariate Statistics.

Zonal statistics summarize raster data within defined zones such as administrative boundaries (Winsemius and Braaten 2023), helping to characterize regional patterns (Song et al. 2016). In this study, the Zonal Statistics as Table tool in ArcGIS was used to calculate the minimum, maximum, mean, and standard deviation of light emission values for each district. This enabled both temporal comparison and spatial trend analysis (Levin and Zhang 2017; Winsemius and Braaten 2023).

Cell statistics are local functions that generate new rasters by applying statistical operations (e.g., maximum, minimum, range) across multiple input rasters on a cell-by-cell basis (Ozturk and Kilic 2016). In this study, the Cell Statistics tool in ArcGIS was employed to determine the range of light emission values for each cell. This identified areas with the greatest temporal variation in light emissions (Li et al. 2008).

Multivariate statistics examine relationships among multiple variables or data layers. **Correlation analysis** is a commonly used multivariate statistical method that quantifies the strength and direction of linear relationships between variables (Ozturk and Kilic 2016). In this study, Pearson correlation analysis (Profillidis and Botzoris 2018; Xu 2020) was used to assess the linear relationship between mean light emission values and three urban variables: population, population density, and SEDI scores.

3.3 Spatial algebra

Spatial algebra is a mathematical framework comprising various algebraic, logical, and topological operations used to analyze spatial data (Kankanhalli et al. 1995; Li et al. 2002; Nobre et al. 2009). In this study, algebraic change mapping and the classification of light emission values were applied to analyze changes in light pollution.

Algebraic change detection uses image algebra to highlight temporal changes by calculating pixel-wise differences, producing a single-band image (Close et al. 2021). It is valued for simplicity, speed, and sensitivity to radiometric differences (Afify 2011; Goswami et al. 2022). This study used image differencing, subtracting values in an earlier image (Image 1) from a later one (Image 2), as shown in Equation 1 (Alphan 2011; Tenneson et al. 2023):

$$\text{Change} = \text{Image 2} - \text{Image 1} \quad \text{(Equation 1)},$$

To evaluate light pollution levels, SNPP/VIIRS **light emission values are categorized** based on ecological and astronomical thresholds. The International Astronomical Union recommends a maximum artificial sky brightness of no more than 10% above natural levels (~0.25 mcd/m²) for observatory locations (Lowenthal et al. 2022). In ecological contexts, artificial light exceeding certain thresholds can disrupt wildlife and ecosystems (Widmer et al. 2022).

Building on the classification by Hügli (2021), which refines earlier schemes by Hale et al. (2018) and Hale and Arlettaz (2019), light emission values are divided into five categories (Table 3). In this classification, a threshold of 2 nW/cm²/sr represents the typical radiance level associated with small villages or sparsely populated residential areas. Radiance values around 10 nW/cm²/sr are characteristic of larger towns with relatively high population densities. In extensive urban settlements, where various lighting systems are employed, measured values commonly reach approximately 20 nW/cm²/sr (Widmer et al. 2022). Light emissions exceeding 2 nW/cm²/sr are expected to have at least a minor impact on ecosystems and wildlife (Hale et al. 2018; Widmer et al. 2022). In this study, light emission values were classified according to the Table 3.

Table 3: Classification of light emission values.

Radiance (nW/cm²/sr)	Category
< 0.5	Lowest light emission
0.5–2	Very low light emission
2–10	Low light emission
10–20	Medium light emission
>=20	High light emission

4 Results

This section presents the findings from the analysis of SNPP/VIIRS data across Samsun's districts from 2012 to 2024. The results reveal spatial and temporal variations in light intensity, reflecting trends in urbanization, industrial activity, and infrastructure development. The analysis is organized into four components:

(i) zonal statistics summarizing district-level light emissions; (ii) difference and range mapping highlighting temporal variation; (iii) light pollution classification showing the spatial distribution of artificial lighting; and (iv) correlation analysis exploring links between light intensity and socio-economic variables.

4.1 Zonal statistics

Zonal statistics were computed using SNPP/VIIRS data for 2012, 2015, 2018, 2021, and 2024. Key metrics per district are summarized in Table 4, and temporal trends in mean light intensity are shown in Figure 3.

Table 4: Summary statistics of SNPP/VIIRS light intensity (nW/cm^2/sr) by district (2012–2024).

	2012		2015		2018		2021		2024	
District	min **mean**	max **std dev**	min **mean**	max **std dev**	min **mean**	max **std dev**	min **mean**	max **std dev**	min **mean**	max **std dev**
19 Mayis	0.15 **1.61**	27.32 **2.99**	0.09 **1.71**	23.77 **2.82**	0.24 **2.34**	33.74 **3.62**	0.32 **2.92**	34.51 **3.88**	0.47 **3.32**	42.55 **3.93**
Alacam	0.08 **0.50**	19.80 **1.14**	0.00 **0.69**	51.25 **2.49**	0.11 **1.03**	46.95 **2.67**	0.20 **1.34**	57.11 **3.07**	0.27 **1.38**	46.84 **2.72**
Asarcik	0.14 **0.40**	12.36 **0.61**	0.03 **0.44**	12.45 **0.81**	0.14 **0.69**	17.63 **1.11**	0.28 **0.96**	22.11 **1.31**	0.40 **1.18**	18.93 **1.30**
Atakum	0.15 **4.29**	88.36 **11.37**	0.10 **4.90**	70.07 **10.85**	0.21 **5.62**	79.30 **12.32**	0.34 **5.73**	75.19 **12.24**	0.44 **6.01**	67.93 **11.71**
Ayvacik	0.12 **0.43**	9.08 **0.63**	0.00 **0.39**	10.94 **0.76**	0.09 **0.58**	13.23 **0.80**	0.22 **0.99**	18.38 **1.12**	0.33 **1.29**	14.32 **1.07**
Bafra	0.07 **0.65**	51.43 **2.28**	0.00 **0.72**	57.49 **2.91**	0.11 **1.08**	72.36 **3.64**	0.16 **1.51**	83.91 **4.07**	0.26 **1.71**	67.22 **3.69**
Canik	0.17 **1.77**	65.28 **6.07**	0.06 **2.32**	77.17 **7.88**	0.25 **2.79**	69.99 **8.54**	0.42 **2.86**	80.91 **7.92**	0.55 **3.07**	60.84 **6.68**
Carsamba	0.14 **1.25**	45.15 **2.83**	0.00 **1.53**	42.16 **3.50**	0.10 **1.90**	47.18 **3.91**	0.29 **2.76**	65.60 **4.87**	0.38 **3.27**	60.16 **4.43**
Havza	0.09 **0.60**	57.33 **2.25**	0.00 **0.64**	71.98 **2.80**	0.10 **0.99**	61.37 **3.05**	**0.25** **1.18**	54.52 **2.79**	0.34 **1.38**	53.61 **2.94**
Ilkadim	0.23 **9.43**	121.14 **18.79**	0.26 **10.14**	88.66 **17.08**	0.46 **12.09**	89.48 **19.58**	0.59 **11.51**	85.76 **17.94**	0.89 **10.64**	73.66 **15.09**
Kavak	0.13 **0.64**	33.68 **1.95**	0.02 **0.95**	43.63 **2.85**	0.16 **1.09**	40.88 **2.81**	0.25 **1.21**	39.71 **2.71**	0.36 **1.42**	48.09 **2.70**
Ladik	0.10 **0.49**	40.94 **1.62**	0.00 **0.52**	45.22 **1.97**	0.14 **0.80**	51.94 **2.33**	0.25 **0.97**	0.25 **2.19**	0.30 **1.19**	47.14 **2.37**
Salipazari	0.14 **0.50**	17.10 **0.75**	0.03 **0.47**	13.84 **0.70**	0.18 **0.79**	26.09 **1.30**	0.29 **1.11**	18.69 **1.24**	0.48 **1.45**	17.52 **1.25**
Tekkekoy	0.17 **2.35**	42.84 **5.49**	0.00 **3.20**	171.04 **9.61**	0.21 **3.95**	75.96 **9.32**	0.38 **4.38**	146.97 **9.70**	0.53 **4.41**	48.79 **7.18**
Terme	0.15 **1.15**	50.92 **2.58**	0.04 **1.40**	48.43 **1.40**	0.22 **1.94**	59.86 **3.70**	0.32 **2.58**	49.14 **3.66**	0.47 **2.95**	53.98 **3.57**
Vezirkopru	0.09 **0.41**	39.83 **1.66**	0.00 **0.35**	51.16 **1.90**	0.10 **0.62**	71.63 **2.63**	0.15 **0.86**	73.40 **2.94**	0.28 **1.02**	70.15 **2.84**
Yakakent	0.10 **0.35**	9.54 **0.73**	0.00 **0.33**	10.86 **0.86**	0.10 **0.92**	29.78 **2.91**	0.25 **1.05**	32.89 **2.75**	0.31 **1.06**	23.64 **2.16**
SAMSUN	0.07 **1.02**	121.14 **4.22**	0.00 **1.18**	171.04 **4.66**	0.09 **1.57**	89.48 **5.26**	0.15 **1.90**	146.97 **5.28**	0.26 **2.10**	73.66 **4.76**

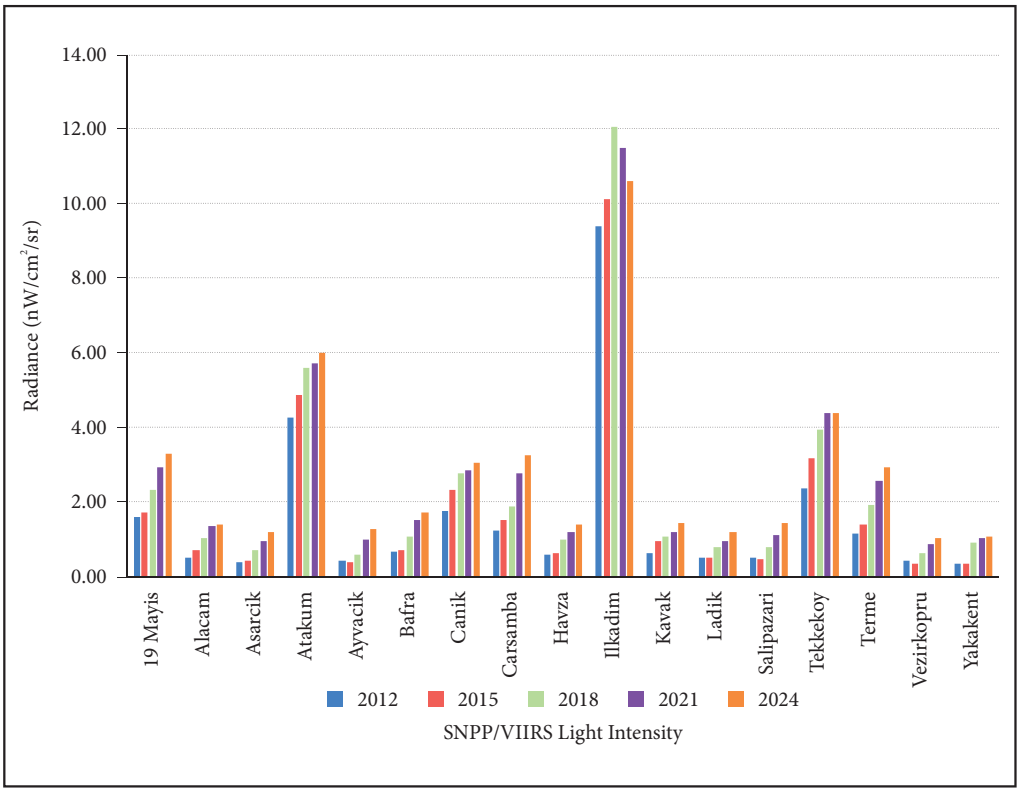

Figure 3: Change in mean SNPP/VIIRS light intensity.

The results show a general upward trend in light intensity across most districts between 2012 and 2024. Among all districts, Atakum and Ilkadim consistently recorded the highest mean light levels throughout the study period. While a sharp increase occurred from 2012 to 2018, the growth rate slowed in 2021 and 2024. Notably, Ilkadim reached a peak mean intensity of 12.09 nW/cm²/sr in 2018, representing the highest value across all districts and years. Following 2018, radiance levels in Ilkadim experienced a decline, which is directly attributable to the implementation of municipal energy conservation and lighting policies under the framework of Samsun Metropolitan Municipality's sustainable energy strategies (Samsun Metropolitan … 2019).

Canik and Tekkekoy showed a steady increase, peaking in 2024. Similarly, districts with prominent industrial and commercial zones, such as Bafra, Carsamba, Terme, Havza, and Kavak, experienced a consistent increase in light intensity over the years. Conversely, more rural and low-population districts (e.g., 19 Mayis, Alacam, Asarcik, Yakakent, Vezirkopru, Salipazari, and Ladik) exhibited consistently low values, with a gradual increase over time. Overall, the upward trends observed in most districts up to 2018 appear to have partially decelerated in the period following 2018.

4.2 Difference and range maps

Difference and range maps were generated using SNPP/VIIRS data (2012–2024) to analyze spatial and temporal variations in light emissions (Figure 4). Image differencing was applied to consecutive intervals and the full study period, with positive values indicating increases and negative values representing decreases. The range map, calculated as the per-pixel difference between maximum and minimum values across

all years, highlights maximum variation at each location. In Figure 4, colors are scaled to each period's min–max values, highlighting relative differences between districts.

Temporal trends in light emissions indicate distinct phases of urban expansion. Between 2012 and 2015, significant light emission increases were observed in the coastal districts of Atakum, Ilkadim, Canik, and Tekkekoy, particularly along Atakum's coastal strip and the Canik-Tekkekoy corridor. These increases align with rapid urban development and expanding infrastructure. From 2015 to 2018, light pollution continued to grow in these central districts but also began to spread inland, suggesting the emergence of new residential and commercial zones. In 2018–2021, the spatial spread of light pollution accelerated, extending from core urban areas to peripheral and interior districts, indicating a broader geographical expansion of artificial lighting. By 2021–2024, nearly all districts experienced increased emissions, highlighting intensified urban sprawl and the proliferation of artificial light even in rural areas. The observed decline in certain areas after 2018 is attributable to energy efficiency measures and urban lighting policies implemented under the framework of Samsun Metropolitan Municipality's sustainable energy strategies (Samsun Metropolitan … 2019). Upgrading streetlights to LED technology, implementing dimming, and optimizing lighting schedules directly led to reduced light emissions, reflecting the municipality's efforts to balance illumination needs with environmental considerations. Furthermore, this slowdown was reinforced by reduced economic activity following the COVID-19 pandemic.

The long-term difference map (2012–2024) confirms a net increase in light emissions across Samsun, with hotspots in urban coastal corridors and industrial transport zones, while the range map (2012–2024) reveals the highest variability in central and coastal districts, while rural areas display minimal change, reflecting relatively stable light conditions over time. Comparing the difference (2012–2024) and range (2012–2024) maps reveals similar spatial patterns, indicating that light emission trends have generally followed a stable, unidirectional trajectory with minimal fluctuations. Central and coastal areas have undergone the most dramatic changes, driven by concentrated urbanization, while rural districts remain less affected by artificial lighting expansion.

4.3 Light pollution classification

Figure 5 displays classified light pollution maps for 2012, 2015, 2018, 2021, and 2024 based on SNPP/VIIRS satellite data and categorized using the thresholds defined in Table 3. These maps visualize the spatial distribution of light emissions and their progression over time, revealing a clear and steady increase in artificial lighting, particularly in urban and peri-urban areas.

Table 5: Area (km^2) and percentage distribution of light emission classes in Samsun (2012–2024).

Year	Lowest	Very low	Low	Medium	High	Total area
2012	6791.8 (69.8%)	2412.0 (24.8%)	351.4 (3.6%)	87.6 (0.9%)	85.9 (0.9%)	9729
2015	6368.8 (65.5%)	2644.8 (27.2%)	493.9 (5.1%)	110.9 (1.1%)	110.3 (1.1%)	9729
2018	4935.1 (50.7%)	3804.6 (39.1%)	724.9 (7.5%)	129.1 (1.3%)	135.0 (1.4%)	9729
2021	3309.3 (34.0%)	4776.7 (49.1%)	1362.5 (14.0%)	136.7 (1.4%)	143.6 (1.5%)	9729
2024	1853.5 (19.1%)	5584.6 (57.4%)	2005.6 (20.6%)	145.5 (1.5%)	139.5 (1.4%)	9729

Figure 4: Difference and range maps of light emissions (2012–2024). ► p. 76–77
Figure 5: Classified light pollution maps (2012, 2015, 2018, 2021, and 2024). ► p. 78–79

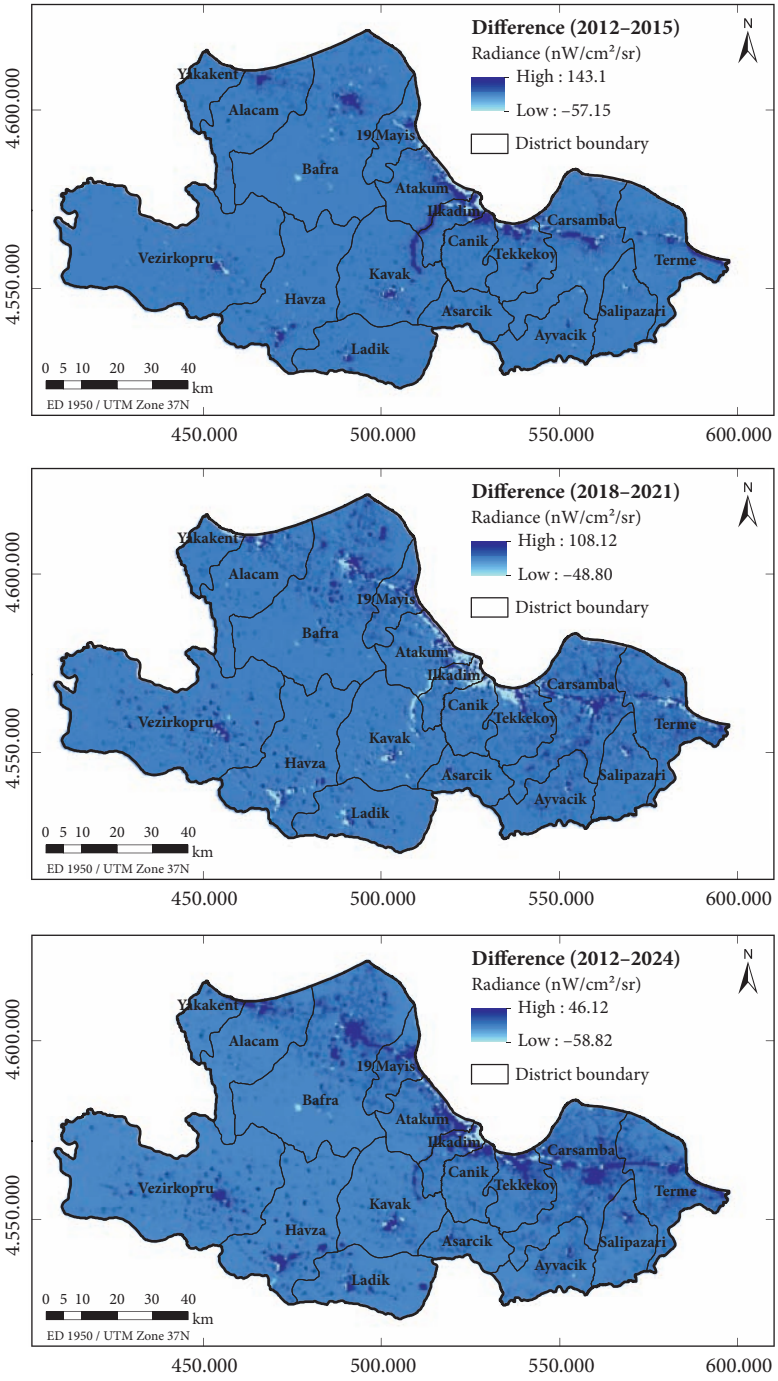
Difference (2012–2015)
Radiance (nW/cm²/sr)
High : 143.1
Low : –57.15
District boundary
N
Yakakent
Alacam
19 Mayis
Bafra
Atakum
Ilkadim
Carsamba
Canik
Tekkekoy
Terme
Vezirkopru
Kavak
Havza
Asarcik
Salipazari
Ayvacik
Ladik
0 5 10 20 30 40
km
ED 1950 / UTM Zone 37N
4.600.000
4.550.000
450.000
500.000
550.000
600.000
Difference (2018–2021)
Radiance (nW/cm²/sr)
High : 108.12
Low : –48.80
District boundary
N
Yakakent
Alacam
19 Mayis
Bafra
Atakum
Ilkadim
Carsamba
Canik
Tekkekoy
Terme
Vezirkopru
Kavak
Havza
Asarcik
Salipazari
Ayvacik
Ladik
0 5 10 20 30 40
km
ED 1950 / UTM Zone 37N
4.600.000
4.550.000
450.000
500.000
550.000
600.000
Difference (2012–2024)
Radiance (nW/cm²/sr)
High : 46.12
Low : –58.82
District boundary
N
Yakakent
Alacam
19 Mayis
Bafra
Atakum
Ilkadim
Carsamba
Canik
Tekkekoy
Terme
Vezirkopru
Kavak
Havza
Asarcik
Salipazari
Ayvacik
Ladik
0 5 10 20 30 40
km
ED 1950 / UTM Zone 37N
4.600.000
4.550.000
450.000
500.000
550.000
600.000

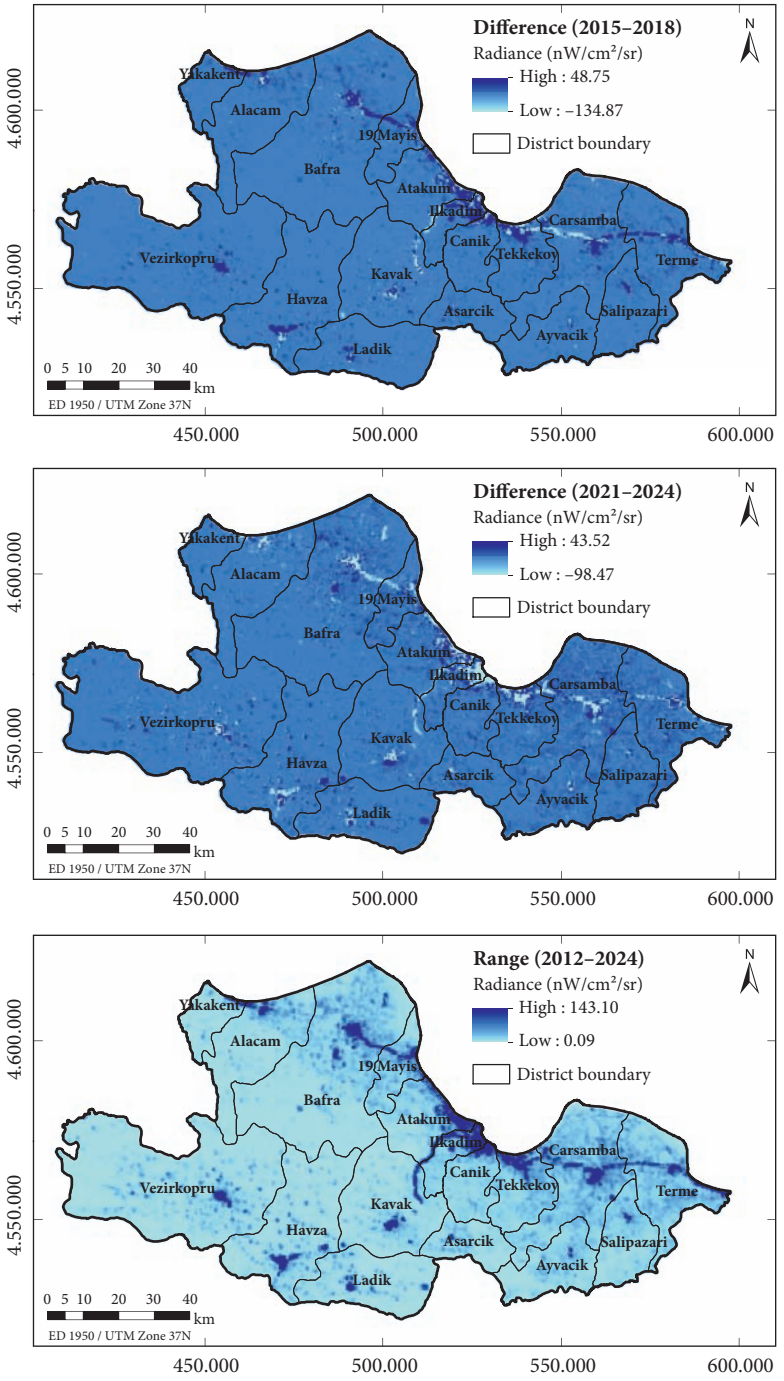

Content by: Sarp Doruk Ozturk
Map by: Sarp Doruk Ozturk, Derya Ozturk
Source: SNPP/VIIRS, Earth Observation Group

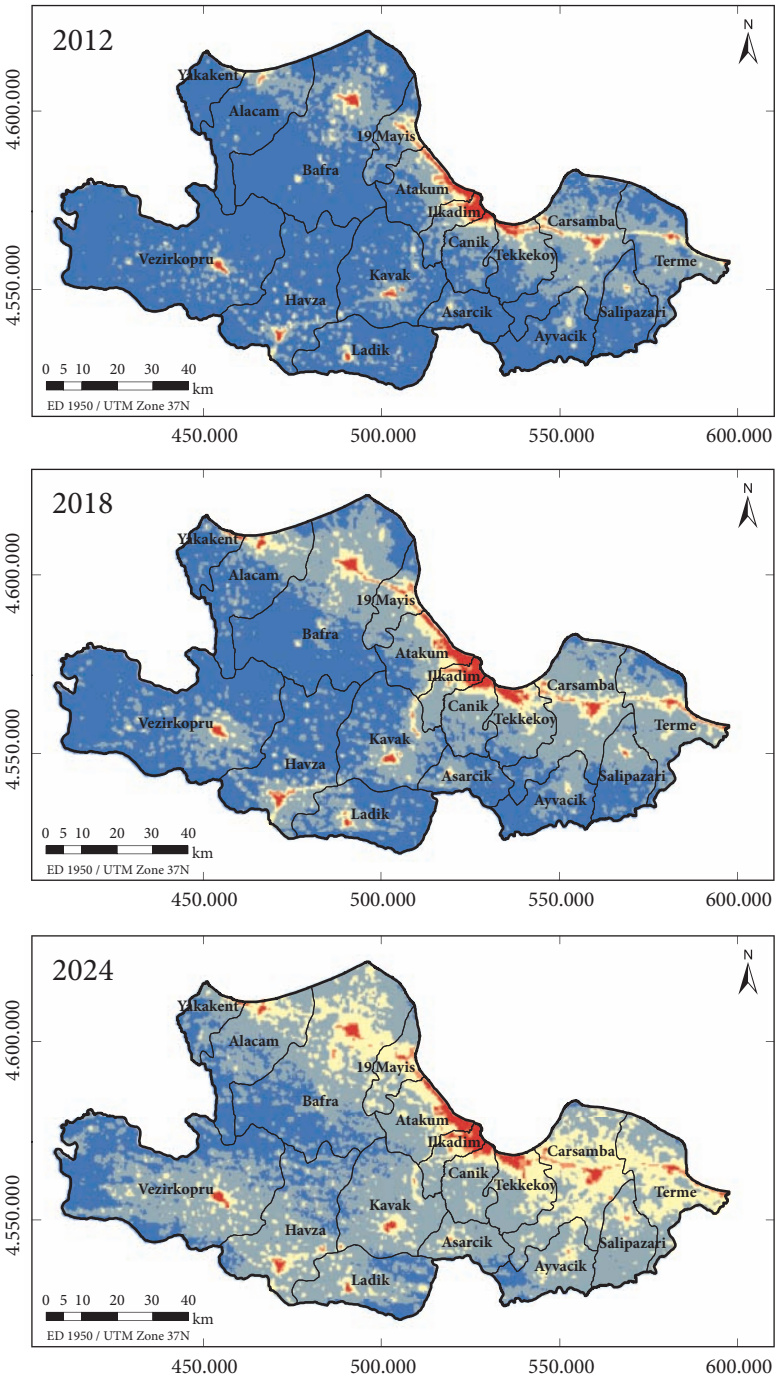
2012
2018
2024
N
Yakakent
Alacam
19 Mayis
Bafra
Atakum
Ilkadim
Carsamba
Canik
Tekkekoy
Terme
Vezirkopru
Kavak
Havza
Asarcik
Salipazari
Ayvacik
Ladik
0 5 10 20 30 40
km
ED 1950 / UTM Zone 37N
4.600.000
4.550.000
450.000
500.000
550.000
600.000

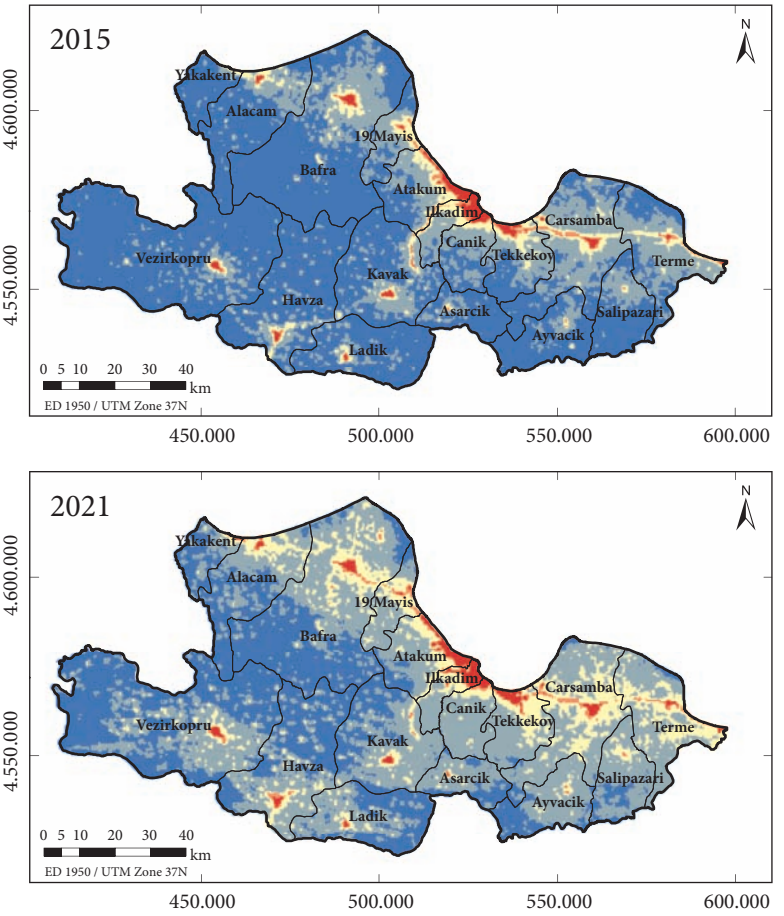

Radiance (nW/cm²/sr)	**Classification**
< 0.5	Lowest light emission
0.5–2	Very low light emission
2–10	Low light emission
10–20	Medium light emission
> 20	High light emission
District boundary	

Conte nt by: Sarp Doruk Ozturk
Map by: Sarp Doruk Ozturk, Derya Ozturk
Source : SNPP/VIIRS, Earth Observation Group

In 2012, the highest light intensities were concentrated in the central districts of Atakum, Ilkadim, Canik, and Tekkekoy, forming a bright corridor along the Middle Black Sea coastal road. In contrast, rural and inland regions showed predominantly low emission levels. By 2015, emissions intensified in central districts and along key transportation routes, indicating early signs of urban expansion and infrastructure growth. The year 2018 marked a notable shift, with increased emissions spreading inland from the coast. Significant growth was observed in new residential zones, commercial centers, and industrial areas, especially in Atakum, Ilkadim, and eastern Tekkekoy. Between 2018 and 2021, light pollution expanded further into peripheral districts, reflecting continued urbanization and rising infrastructure development. By 2024,

Table 6: Area (km^2) and percentage distribution of light emission classes by district (2012 and 2024).

District	Year	Lowest	Very low	Low	Medium	High	Total
19 Mayis	2012	89.2 (38.3%)	107.6 (46.1%)	27.0 (11.6%)	8.7 (3.7%)	0.6 (0.3%)	233.1
19 Mayis	2024	2.6 (1.1%)	112.7 (48.3%)	102.2 (43.9%)	13.7 (5.9%)	1.9 (0.8%)	233.1
Alacam	2012	464.0 (77.6%)	118.8 (19.9%)	13.0 (2.2%)	2.4 (0.4%)	0.0 (0.0%)	598.2
Alacam	2024	160.9 (26.9%)	347.4 (58.1%)	81.3 (13.6%)	5.6 (0.9%)	2.9 (0.5%)	598.2
Asarcik	2012	217.5 (85.5%)	33.8 (13.3%)	3.1 (1.2%)	0.2 (0.1%)	0.0 (0.0%)	254.5
Asarcik	2024	20.7 (8.1%)	205.3 (80.7%)	27.2 (10.7%)	1.3 (0.5%)	0.0 (0.0%)	254.5
Atakum	2012	137.0 (39.0%)	137.6 (39.2%)	37.6 (10.7%)	17.7 (5.0%)	21.5 (6.1%)	351.4
Atakum	2024	8.0 (2.3%)	191.5 (54.5%)	101.9 (29.0%)	15.8 (4.5%)	34.2 (9.7%)	351.4
Ayvacik	2012	313.3 (81.6%)	63.8 (16.6%)	6.8 (1.8%)	0.0 (0.0%)	0.0 (0.0%)	383.9
Ayvacik	2024	54.2 (14.1%)	269.8 (70.3%)	58.8 (15.3%)	1.1 (0.3%)	0.0 (0.0%)	383.9
Bafra	2012	1141.9 (76.0%)	308.0 (20.5%)	41.3 (2.7%)	4.5 (0.3%)	6.8 (0.4%)	1502.5
Bafra	2024	426.5 (28.4%)	738.7 (49.2%)	316.1 (21.0%)	11.6 (0.8%)	9.6 (0.6%)	1502.5
Canik	2012	121.5 (46.4%)	115.8 (44.1%)	14.5 (5.5%)	4.3 (1.7%)	6.1 (2.3%)	262.2
Canik	2024	0.0 (0.0%)	192.6 (73.5%)	54.8 (20.9%)	5.9 (2.3%)	8.8 (3.4%)	262.2
Carsamba	2012	288.1 (37.3%)	417.8 (54.0%)	51.9 (6.7%)	11.7 (1.5%)	3.7 (0.5%)	773.3
Carsamba	2024	9.8 (1.3%)	324.8 (42.0%)	404.5 (52.3%)	23.8 (3.1%)	10.4 (1.4%)	773.3
Havza	2012	709.5 (82.0%)	125.7 (14.5%)	24.3 (2.8%)	2.6 (0.3%)	2.9 (0.3%)	864.9
Havza	2024	181.7 (21.0%)	566.4 (65.5%)	104.7 (12.1%)	8.0 (0.9%)	4.2 (0.5%)	864.9
Ilkadim	2012	36.7 (23.7%)	61.6 (39.8%)	22.3 (14.4%)	10.3 (6.6%)	24.0 (15.5%)	154.8
Ilkadim	2024	0.0 (0.0%)	65.0 (42.0%)	45.8 (29.6%)	13.7 (8.8%)	30.4 (19.6%)	154.8
Kavak	2012	536.6 (77.0%)	140.4 (20.1%)	13.2 (1.9%)	3.9 (0.6%)	2.7 (0.4%)	696.8
Kavak	2024	73.1 (10.5%)	534.9 (76.8%)	79.7 (11.4%)	4.8 (0.7%)	4.2 (0.6%)	696.8
Ladik	2012	460.9 (84.8%)	70.1 (12.9%)	10.0 (1.8%)	0.8 (0.1%)	1.4 (0.3%)	543.2
Ladik	2024	136.5 (25.1%)	349.0 (64.2%)	54.0 (9.9%)	1.9 (0.4%)	1.8 (0.3%)	543.2
Salipazari	2012	257.7 (73.8%)	86.8 (24.9%)	3.9 (1.1%)	0.6 (0.2%)	0.0 (0.0%)	349.0
Salipazari	2024	0.8 (0.2%)	293.7 (84.2%)	52.7 (15.1%)	1.8 (0.5%)	0.0 (0.0%)	349.0
Tekkekoy	2012	125.7 (38.5%)	151.0 (46.2%)	27.8 (8.5%)	11.4 (3.5%)	10.6 (3.2%)	326.5
Tekkekoy	2024	0.0 (0.0%)	165.8 (50.8%)	128.5 (39.3%)	14.8 (4.5%)	17.5 (5.4%)	326.5
Terme	2012	190.3 (34.1%)	323.5 (58.0%)	37.3 (6.7%)	4.3 (0.8%)	2.1 (0.4%)	557.5
Terme	2024	2.3 (0.4%)	249.7 (44.8%)	284.9 (51.1%)	15.9 (2.9%)	4.8 (0.9%)	557.5
Vezirkopru	2012	1512.7 (90.5%)	138.7 (8.3%)	13.2 (0.8%)	4.2 (0.2%)	3.4 (0.2%)	1672.2
Vezirkopru	2024	702.2 (42.0%)	860.6 (51.5%)	97.6 (5.8%)	4.2 (0.2%)	7.6 (0.5%)	1672.2
Yakakent	2012	189.1 (92.5%)	11.1 (5.4%)	4.3 (2.1%)	0.0 (0.0%)	0.0 (0.0%)	204.5
Yakakent	2024	74.1 (36.2%)	116.9 (57.2%)	10.8 (5.3%)	1.6 (0.8%)	1.1 (0.6%)	204.5

artificial lighting had reached its highest levels across all years, with a noticeable spread of medium and high-emission areas in core districts and an expanding footprint of low-emission lighting in previously unlit rural zones.

Table 5 quantifies the area and percentage distribution of each light emission class across Samsun from 2012 to 2024. The most significant change is the sharp decline in »Lowest« light emission areas, from 69.8% (6791.8 km²) in 2012 to just 19.1% (1853.5 km²) in 2024, representing a reduction of over 50 percentage points. This decline is mirrored by an increase in »Very low« and »Low« categories, indicating that previously dark areas are now exposed to artificial light. Although the »Medium« and »High« categories have not expanded as dramatically, their steady growth reflects an increased concentration of artificial lighting, particularly in commercial and industrial zones.

Table 6 presents the spatial breakdown of light emission classes by district for 2012 and 2024. The »Lowest« emission class declined significantly across all districts and was entirely eliminated in Canik, Ilkadim, and Tekkekoy, underscoring intensified urbanization and infrastructure development. The expansion of »Very low« and »Low« classes across most districts reflects widespread electrification, rural development, and urban sprawl. While increases in »Medium« and »High« categories were more modest in terms of area, their concentration in urban cores and industrial zones points to localized intensification of artificial lighting. Notably, even traditionally rural districts such as Bafra, Carsamba, Terme, and 19 Mayis began transitioning into higher light emission classes, likely due to increased coastal development and transportation activity.

To further illustrate the transformation of previously dark areas and the potential ecological impact of artificial lighting, Figure 6 shows a map of regions with radiance lower than 2 nW/cm²/sr as well as areas where light emissions exceed this threshold for the years 2012, 2015, 2018, 2021, and 2024. This map illustrates the progressive reduction of »dark areas« over time, while regions where light emissions exceed 2 nW/cm²/sr, a level associated with measurable impacts on ecosystems and wildlife (Hale et al. 2018; Widmer et al. 2022), have expanded, reflecting the increasing spread of ecologically critical artificial lighting.

4.4 Correlation analysis

To explore the drivers of light emissions, a correlation analysis was conducted between mean SNPP/VIIRS light emission values and three variables: population, population density, and SEDI score. Across all years, correlations with population remained consistently strong ($r \geq 0.85$), while correlations with population density were higher ($r \geq 0.94$), highlighting the predominant influence of population concentration on light intensity and, by extension, urbanization. Correlations with SEDI were also substantial ($r \geq 0.80$), indicating that areas with greater artificial lighting correspond to more socio-economically developed regions characterized by denser infrastructure, services, and economic activity. Yearly correlation coefficients for all variables are summarized in Table 7.

Table 7: Correlation coefficients of mean light emission with population, population density, and SEDI score.

Relationship	2012	2015	2018	2021	2024
r (Mean light emission-Population)	0.85	0.86	0.86	0.87	0.87
r (Mean light emission-Population density)	0.96	0.95	0.96	0.95	0.94
r (Mean light emission-SEDI score)	0.80	0.82	0.81	0.82	0.84

Note: All correlation coefficients are statistically significant at $p < 0.001$.

Figure 6: Spatial distribution of areas exceeding the ecological threshold of 2 nW/cm²/sr in Samsun for 2012, 2015, 2018, 2021, and 2024. ➤ p. 82–83

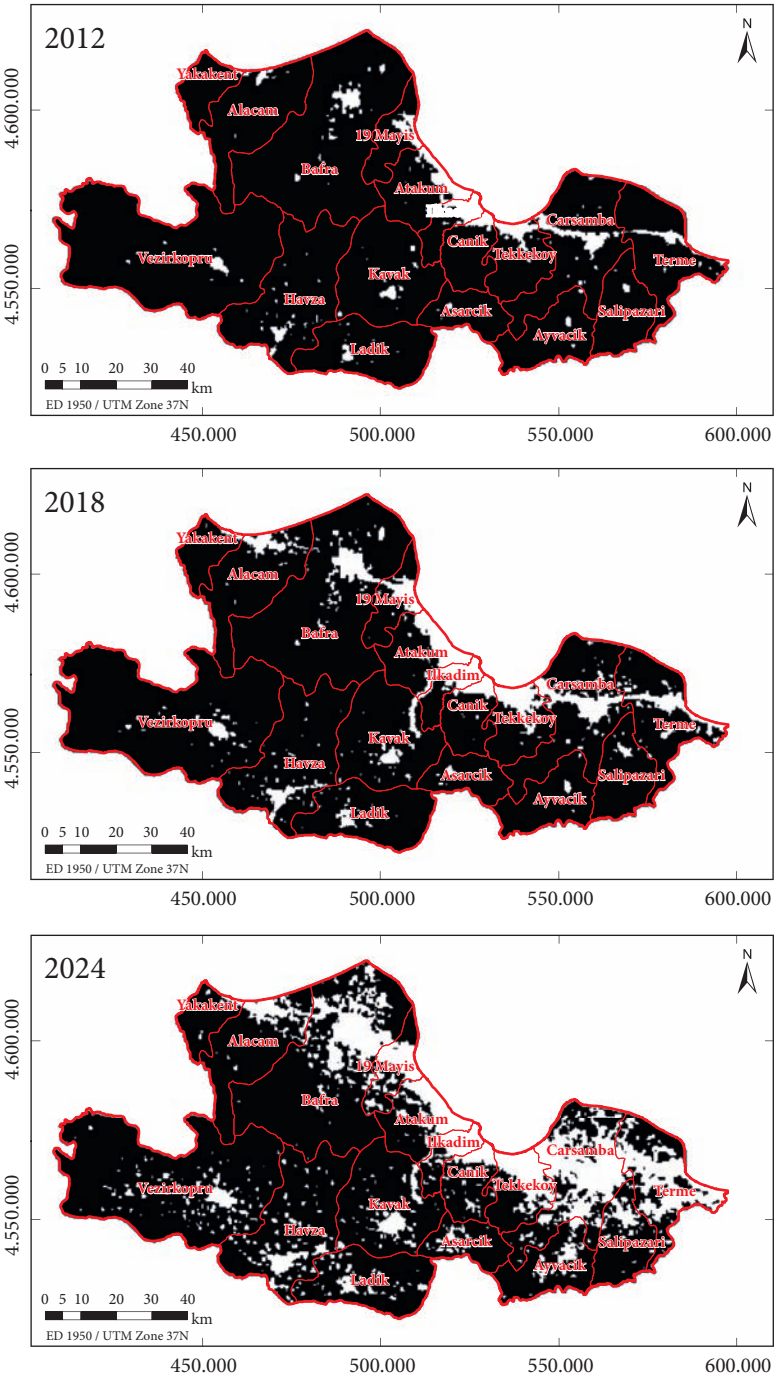
2012
2018
2024
N
Yakakent
Alacam
19 Mayis
Bafra
Atakum
Ilkadim
Carsamba
Canik
Tekkekoy
Terme
Vezirkopru
Kavak
Havza
Asarcik
Salipazari
Ayvacik
Ladik
0 5 10 20 30 40
km
ED 1950 / UTM Zone 37N
4.600.000
4.550.000
450.000
500.000
550.000
600.000

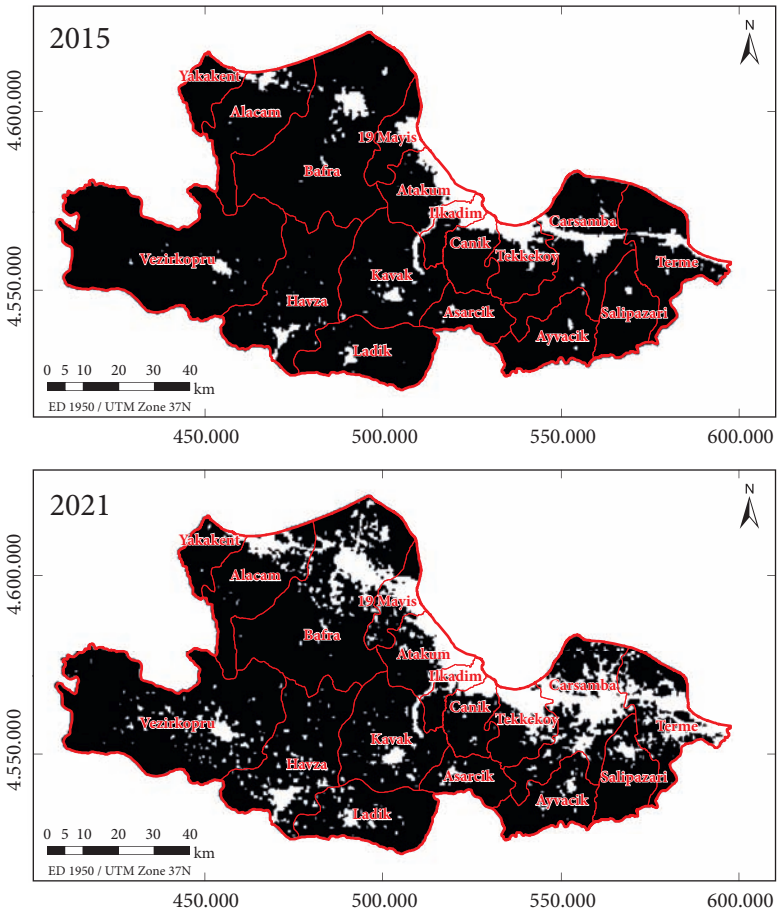

Areas Exceeding Critical Light Emission Thresh old (> 2 nW/cm²/sr)

Radiance (nW/cm²/sr)

≤ 2

> 2

District boundary

Content by: Sarp Doruk Ozturk
Map by: Sarp Doruk Ozturk, Derya Ozturk
Source: SNPP/VIIRS, Earth Observation Group

5 Discussion

RS and GIS are essential for tracking spatial and temporal patterns of light emissions (Butt 2012). Using SNPP/VIIRS DNB satellite data from 2012 to 2024 and spatial analysis methods, this study evaluated light emission trends in Samsun. The results reflect urbanization, economic growth, and infrastructure expansion, supporting previous research on the value of satellite-derived NTL data for socio-economic monitoring (Levin and Zhang 2017; Hu et al. 2018).

In 2012, most districts had low or very low emissions, indicating early urban development. By 2024, the central and coastal districts of Atakum, Ilkadim, Canik, and Tekkekoy showed substantial increases during the period from 2012 to 2018. Atakum, characterized by high population density, exhibited a stable and significant increase in light emissions, primarily due to rapid population growth driven by coastal attractiveness, expansion of residential areas, increased commercial activity, industrial growth, and infrastructure development. Similar trends were reported by Yerli et al. (2021), indicating a general increase in light emissions across Samsun. Higher emissions were primarily concentrated in coastal areas, aligning with findings from SQM measurements on light pollution in Atakum by Türk and Yavuz (2023). Although direct validation with ground-based SQM measurements or high-resolution airborne imagery was not conducted in this study due to data availability and logistical limitations, the correspondence of observed trends with these independent measurements suggests that the RS-derived NTL data reasonably reflect actual light emissions. The observed increase in light intensity also reflects urban sprawl, as noted by Ozturk (2017), highlighting a shift toward human-centered land use at the expense of natural areas. Ilkadim's port and economic base contributed to high values, while Tekkekoy and Canik grew due to industrialization and urban sprawl. These findings are consistent with studies by Cheon and Kim (2020) in Seoul, South Korea, which linked major increases in light emissions to urbanization, commercial growth, and industrialization. Growth slowed post-2018 in major districts, likely due to COVID-19 impacts and energy-saving policies. Similarly, Bustamante-Calabria et al. (2021) demonstrated that post-pandemic economic downturns in Granada, Spain, directly impacted light emissions. Meanwhile, moderate increases in light emissions were seen in Bafra, Carsamba, Terme, and 19 Mayis between 2012 and 2024, tied to trade and local industry. Rural districts (e.g., Asarcik, Ayvacik, and Yakakent) remained largely stable, consistent with the findings of Massetti (2020).

Atakum, hosting an observatory, saw »Lowest« emission areas fall from 39.0% to 2.3%, while »Medium« and »High« zones rose from 6.1% to 9.7%, threatening night sky visibility, as shown in Figure 7. Studies by Butt (2012) and Green et al. (2022) stress the importance of monitoring such zones to preserve sky quality. Figure 7 also highlights ecological areas, including the Kizilirmak Delta, Yesilirmak Delta, and Lake Ladik, which experienced shifts from »Lowest« to »Very low« categories. While still relatively dark, increasing emissions in adjacent areas indicate rising pressure from nearby development. Research by Jägerbrand and Bouroussis (2021) and Mayer-Pinto et al. (2022) emphasize the ecological risks of light pollution in sensitive habitats.

A strong correlation exists between light emissions, population metrics, and SEDI, suggesting NTL data are useful proxies for human activity (Levin and Zhang 2017). While correlation does not imply causation (Hu et al. 2018), the relationship underscores the need for integrating light pollution management into urban planning.

This study highlights the utility of RS and spatial techniques in light pollution monitoring. SNPP/VIIRS provides consistent, wide-scale data with improved radiometric quality. However, spatial resolution remains a limitation (Levin and Zhang 2017), and the lack of information on the structure of outdoor lighting (e.g., unobscured, semi-obscured, fully obscured), shielding, power, and spectral characteristics further constrains the analysis. The widespread introduction of white LED technology in urban areas has substantially altered the spectral composition of emissions and their spatial distribution. Due to their higher proportion of blue light, these LEDs intensify atmospheric scattering and amplify light pollution effects, particularly skyglow. Since SNPP/VIIRS sensors are insensitive to the extreme blue range, this spectral shift cannot be fully captured, which may partially explain discrepancies in observed radiance trends (Carias et al. 2021; Levin 2025). Future research incorporating higher-resolution imagery such as the Sustainable Development

Figure 7: Ecologically sensitive areas (Kizilirmak Delta, Yesilirmak Delta, and Ladik Lake) and the astronomical observatory. ► p. 85

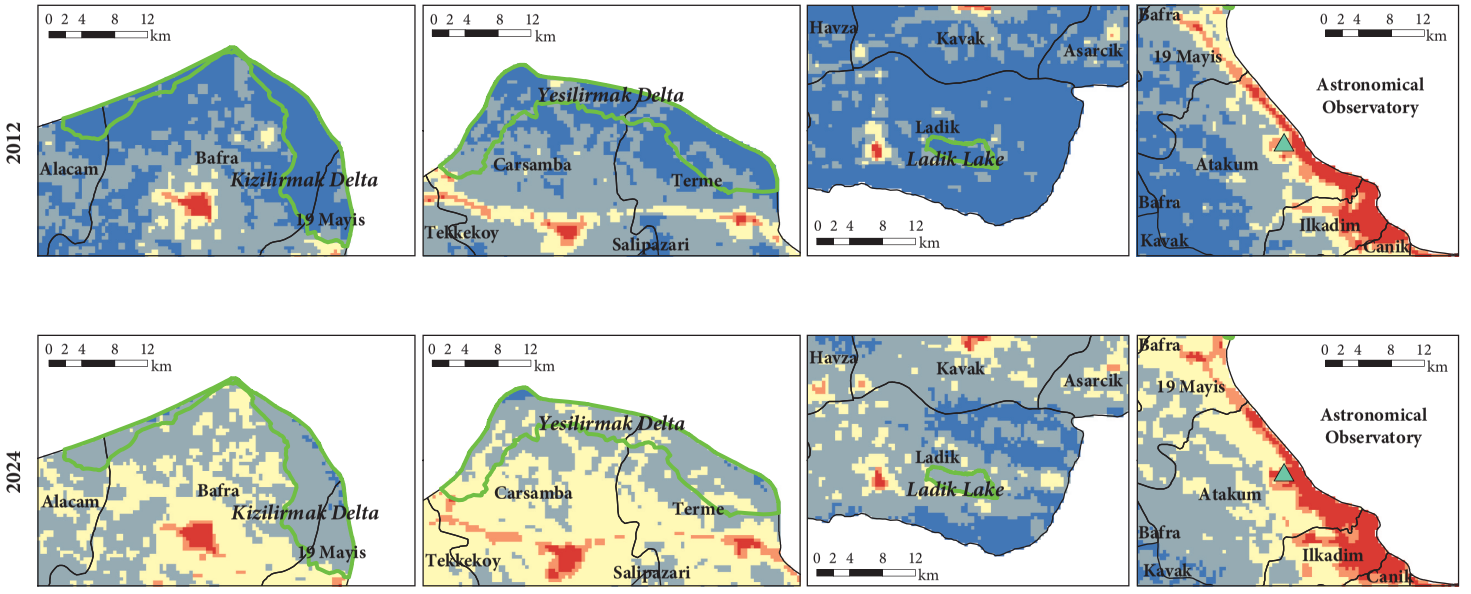

Content by: Sarp Doruk Ozturk
Map by: Sarp Doruk Ozturk, Derya Ozturk
Source: SNPP/VIIRS, Earth Observation Group

Science Satellite 1 – SDGSAT-1/GIU (Xie et al. 2024), ground-based inventories, and spectral measurements would help overcome these limitations, thereby enhancing the precision and robustness of urban light pollution assessments and enabling finer-scale planning and conservation efforts.

6 Conclusion

This study underscores the effectiveness of integrating RS and GIS techniques by advancing the application of spatial statistical and algebraic methods to identify light pollution patterns at sub-city scales. Utilizing SNPP/VIIRS DNB data spanning 2012 to 2024, the study assessed district-level changes in light pollution in Samsun. Results show a steady rise in artificial lighting, especially in coastal and central districts. Industrial zones, transport corridors, and urban sprawl contributed significantly to this increase. Areas with »Lowest« emissions declined, while »Low« and »Very low« zones expanded, reflecting a widespread diffusion of artificial light.

Light intensity correlated strongly with population, population density, and SEDI. Districts with high urban and economic activity, such as Atakum, Ilkadim, Canik, and Tekkekoy, showed the most significant increases in light pollution. Rural and agricultural districts remained less affected.

The loss of dark zones raises critical concerns regarding environmental sustainability. Atakum's observatory and natural areas like the Kizilirmak and Yesilirmak Deltas, and Lake Ladik face increasing pressure from nearby development. Immediate action is needed to protect these zones through dark sky preservation, lighting restrictions, and urban planning reforms.

The findings of this study demonstrate the significant potential of SNPP/VIIRS nighttime light data for analyzing artificial light pollution. However, future studies should incorporate higher-resolution imagery and complementary RS methodologies to assess long-term impacts and guide sustainable urban planning. The findings provide critical input for policymakers in addressing light pollution and balancing urban growth with environmental protection.

RESEARCH DATA: For information on the availability of research data related to the study, please visit the article webpage: https://doi.org/10.3986/AGS.14506.

7 References

Afify, H. A. 2011: Evaluation of change detection techniques for monitoring land-cover changes: A case study in new Burg El-Arab area. *Alexandria Engineering Journal* 50-2. https://doi.org/10.1016/j.aej.2011.06.001

Alphan, H. 2011: Comparing the utility of image algebra operations for characterizing landscape changes: The case of the Mediterranean coast. *Journal of Environmental Management* 92-11. https://doi.org/10.1016/j.jenvman.2011.07.009

Brayley, O., How, M., Wakefield, A. 2022: The biological effects of light pollution on terrestrial and marine organisms. *International Journal of Sustainable Lighting* 24-1. https://doi.org/10.26607/ijsl.v24i1.121

Bustamante-Calabria, M., Sánchez de Miguel, A., Martín-Ruiz, S., Ortiz, J. L., Vílchez, J. M., Pelegrina, A., Garcia, A. et al. 2021: Effects of the COVID-19 lockdown on urban light emissions: Ground and satellite comparison. *Remote Sensing* 13-2. https://doi.org/10.3390/rs13020258

Butt, M. J. 2012: Estimation of light pollution using satellite remote sensing and geographic information system techniques. *GIScience & Remote Sensing* 49-4. https://doi.org/10.2747/1548-1603.49.4.609

Carias, M., Fujioka, S., Phaneuf, J., Potter, M., Vaiciunas, I., Wilder, L., Wood, C., Yu, J. 2021: Preserving the night sky: Monitoring light pollution affecting the Central Idaho Dark Sky Reserve. *Technical report*. University of California.

Cheon, S., Kim, J. A. 2020: Quantifying the influence of urban sources on night light emissions. *Landscape and Urban Planning* 204. https://doi.org/10.1016/j.landurbplan.2020.103936

Chepesiuk, R. 2009: Missing the dark: Health effects of light pollution. *Environmental Health Perspectives* 117-1. https://doi.org/10.1289/ehp.117-a20

Close, O., Petit, S., Beaumont, B., Hallot, E. 2021: Evaluating the potentiality of Sentinel-2 for change detection analysis associated with LULUCF in Wallonia, Belgium. *Land* 10-1. https://doi.org/10.3390/land10010055

Cox, D. T. C., de Miguel, A. S., Bennie, J., Dzurjak, S. A., Gaston, K. J. 2022: Majority of artificially lit Earth surface associated with the non-urban population. *Science of the Total Environment* 841. https://doi.org/10.1016/j.scitotenv.2022.156782

Dong, B., Zhang, R., Li, S., Ye, Y., Huang, C. 2025: A meta-analysis for the nighttime light remote sensing data applied in urban research: Key topics, hotspot study areas and new trends. *Science of Remote Sensing* 11. https://doi.org/10.1016/j.srs.2024.100186

Earth Data, NASA 2025: VNP46A2 - VIIRS/NPP gap-filled lunar BRDF-adjusted nighttime lights daily L3 global 500m linear lat lon grid. *Dataset*. https://doi.org/10.5067/VIIRS/VNP46A2.002

Earth Observation Group, Colorado School of Mines 2025: Monthly cloud-free DNB composite. *Dataset*.

Eken, G., Bozdoğan, M., İsfendiyaroğlu, S., Kılıç, D. T., Lise, Y. (eds.) 2006: Türkiye'nin önemli doğa alanları. Doğa Derneği.

Faid, M. S., Shariff, N. N. M., Hamidi, Z. S., Wahab, R. A., Ahmad, N., Mohd Nawawi, M. S. A., Nahwandi, M. S. 2024: Alteration of twilight sky brightness profile by light pollution. *Scientific Reports* 14. https://doi.org/10.1038/s41598-024-76550-3

Forster, M. 2000: Review of the use of Geographical Information Systems in the marketing and planning of logistics services. *Christian Salvesen Logistics Research Paper* 3.

Gaston, K. J., Gardner, A. S., Cox, D. T. 2023: Anthropogenic changes to the nighttime environment. *Bioscience* 73-4. https://doi.org/10.1093/biosci/biad017

General Directorate of Protection of Natural Assets 2019: Samsun Kızılırmak Deltası doğal sit alanları sulak alan ve kuş cenneti: 2019–2023 yönetim planı. *Technical report*.

General Directorate of Water Management 2024: Yeşilırmak Havzası taşkın yönetim planı revizyon projesi. *Technical report*.

Goswami, A., Sharma, D., Mathuku, H., Gangadharan, S. M. P., Yadav, C. S., Sahu, S. K., Pradhan, M. K. et al. 2022: Change detection in remote sensing image data comparing algebraic and machine learning methods. *Electronics* 11- 3. https://doi.org/10.3390/electronics11030431

Green, R. F., Luginbuhl, C. B., Wainscoat, R. J., Duriscoe, D. 2022: The growing threat of light pollution to ground-based observatories. *The Astronomy and Astrophysics Review* 30. https://doi.org/10.1007/s00159-021-00138-3

Guk, E., Levin, N. 2020: Analyzing spatial variability in night-time lights using a high spatial resolution color Jilin-1 image–Jerusalem as a case study. *ISPRS Journal of Photogrammetry and Remote sensing* 163. https://doi.org/10.1016/j.isprsjprs.2020.02.016

Hale, J., Arlettaz, R. 2019: Artificial lighting and biodiversity in Switzerland. *Technical report*. University of Bern.

Hale, J., Blumenstein, C., Carannante, D., Arlettaz, R. 2018: Ecological light pollution in the Naturpark Gantrisch. *Technical report*. University of Bern.

Hu, Z., Hu, H., Huang, Y. 2018: Association between nighttime artificial light pollution and sea turtle nest density along Florida coast: A geospatial study using VIIRS remote sensing data. *Environmental Pollution* 239. https://doi.org/10.1016/j.envpol.2018.04.021

Hügli, F. 2021: Light pollution in European protected areas – Spatial variation of light pollution in Natura 2000 sites of the Member States of the European Union. *Master's thesis*. Eidgenössische Technische Hochschule Zürich.

Jägerbrand, A. K., Bouroussis, C. A. 2021: Ecological impact of artificial light at night: Effective strategies and measures to deal with protected species and habitats. *Sustainability* 13-11. https://doi.org/10.3390/su13115991

Ji, M., Xu, Y., Yan, Y., Zhu, S. 2024: Evaluation of the light pollution in the nature reserves of China based on NPP/VIIRS nighttime light data. *International Journal of Digital Earth* 17-1. https://doi.org/10.1080/17538947.2024.2347442

Kankanhalli, M. S., Jiang, X., Wu, J. K. 1995: A spatial algebra for content-based retrieval. In: Proceedings of the 2nd Asian Conference on Computer Vision (ACCV 1995). Nanyang Technological University.

Levin, N. 2017: The impact of seasonal changes on observed nighttime brightness from 2014 to 2015 monthly VIIRS DNB composites. *Remote Sensing of Environment* 193. https://doi.org/10.1016/j.rse.2017.03.003

Levin, N. 2023: Quantifying the variability of ground light sources and their relationships with spaceborne observations of night lights using multidirectional and multispectral measurements. *Sensors* 23-19. https://doi.org/10.3390/s23198237

Levin, N. 2025: Challenges in remote sensing of night lights – a research agenda for the next decade. *Remote Sensing of Environment* 328. https://doi.org/10.1016/j.rse.2025.114869

Levin, N., Zhang, Q. 2017: A global analysis of factors controlling VIIRS nighttime light levels from densely populated areas. *Remote Sensing of Environment* 190. https://doi.org/10.1016/j.rse.2017.01.006

Li, Y., Onasch, C. M., Guo, Y. 2008: GIS-based detection of grain boundaries. *Journal of Structural Geology* 30-4. https://doi.org/10.1016/j.jsg.2007.12.007

Li, Z., Zhao, R. L., Chen, J. 2002: A Voronoi-based spatial algebra for spatial relations. *Progress in Natural Science* 12-7.

Liu, S., Zhou, Y., Wang, F., Wang, S., Wang, Z., Wang, Y., Qin, G. et al. 2024: Lighting characteristics of public space in urban functional areas based on SDGSAT-1 glimmer imagery: A case study in Beijing, China. *Remote Sensing of Environmen*t 306. https://doi.org/10.1016/j.rse.2024.114137

Lowenthal, J., Walker, C., Benvenuti, P. 2022: Dark and quiet skies II working group reports. *Technical report*. Smith College.

Ma, J., Guo, J., Ahmad, S., Li, Z., Hong, J. 2020: Constructing a new inter-calibration method for DMSP-OLS and NPP-VIIRS nighttime light. *Remote Sensing* 12-6. https://doi.org/10.3390/rs12060937

Mander, S., Alam, F., Lovreglio, R., Ooi, M. 2023: How to measure light pollution – A systematic review of methods and applications. *Sustainable Cities and Society* 92. https://doi.org/10.1016/j.scs.2023.104465

Martinez, J. F., MacManus, K., Stokes, E. C., Wang, Z., de Sherbinin, A. 2023: Suitability of NASA's black marble daily nighttime lights for population studies at varying spatial and temporal scales. *Remote Sensing* 15-10. https://doi.org/10.3390/rs15102611

Massetti, L. 2020: Drivers of artificial light at night variability in urban, rural and remote areas. *Journal of Quantitative Spectroscopy and Radiative Transfer* 255. https://doi.org/10.1016/j.jqsrt.2020.107250

Mayer-Pinto, M., Jones, T. M., Swearer, S. E., Robert, K. A., Bolton, D., Aulsebrook, A. E., Dafforn, K. A. et al. 2022: Light pollution: A landscape-scale issue requiring cross-realm consideration. *UCL Open Environment* 4. https://doi.org/10.14324/111.444/ucloe.000036

Miller, S. D., Straka III, W., Mills, S. P., Elvidge, C. D., Lee, T. F., Solbrig, J., Walther, A. et al. 2013: Illuminating the capabilities of the Suomi National Polar-Orbiting Partnership (NPP) Visible Infrared Imaging Radiometer Suite (VIIRS) day/night band. *Remote Sensing* 5-12. https://doi.org/10.3390/rs5126717

Nobre, A., Pacheco, M., Jorge, R., Lopes, M. F. P., Gato, L. M. C. 2009: Geo-spatial multi-criteria analysis for wave energy conversion system deployment. *Renewable Energy* 34-1. https://doi.org/10.1016/j.renene.2008.03.002

Nurbandi, W., Yusuf, F. R., Prasetya, R., Afrizal, M. D. 2016: Using Visible Infrared Imaging Radiometer Suite (VIIRS) imagery to identify and analyze light pollution. *IOP Conference Series: Earth and Environmental Science* 47. https://doi.org/10.1088/1755-1315/47/1/012040

Ozturk, D. 2017: Assessment of urban sprawl using Shannon's entropy and fractal analysis: A case study of Atakum, Ilkadim and Canik (Samsun, Turkey). *Journal of Environmental Engineering and Landscape Management* 25-3. https://doi.org/10.3846/16486897.2016.1233881

Öztürk, D., Gündüz, U. 2019: Samsun ili arazi kullanımı/örtüsünün mekansal-zamansal değişimlerinin fraktal analiz kullanılarak belirlenmesi. *Uludağ Üniversitesi Mühendislik Fakültesi Dergisi* 24-2. https://doi.org/10.17482/uumfd.553486

Ozturk, D., Kilic, F. 2016: Geostatistical approach for spatial interpolation of meteorological data. *Anais da Academia Brasileira de Ciências* 88-4. https://doi.org/10.1590/0001-3765201620150103

Pan, W., Du, J. 2021: Impacts of urban morphological characteristics on nocturnal outdoor lighting environment in cities: An empirical investigation in Shenzhen. *Building and Environment* 192. https://doi.org/10.1016/j.buildenv.2021.107587

Profillidis, V. A., Botzoris, G. N. 2018: Statistical methods for transport demand modeling. In: Modeling of Transport Demand: Analyzing, Calculating, and Forecasting Transport Demand. Elsevier. https://doi.org/10.1016/B978-0-12-811513-8.00005-4

Samsun Chamber of Commerce and Industry 2022: Samsun iktisadi rapor 2022. *Technical report*.

Samsun Metropolitan Municipality 2019: Samsun ili sürdürülebilir enerji eylem planı. *Technical report*.

Song, M., Li, W., Zhou, B., Lei, T. 2016: Spatiotemporal data representation and its effect on the performance of spatial analysis in a cyberinfrastructure environment – A case study with raster zonal analysis. *Computers & Geosciences* 87. https://doi.org/10.1016/j.cageo.2015.11.005

Tenneson, K., Dilger, J., Wespestad, C., Zutta, B., Nicolau, A. P., Dyson, K., Paz, P. 2023: Change detection. In: Cloud-based Remote Sensing with Google Earth Engine: Fundamentals and Applications. Springer. https://doi.org/10.1007/978-3-031-26588-4_16

Tong, J. C., Lau, E. S., Hui, M. C., Kwong, E., White, M. E., Lau, A. P. 2022: Light pollution spatial impact assessment in Hong Kong: Measurement and numerical modelling on commercial lights at street level. *Science of The Total Environment* 837. https://doi.org/10.1016/j.scitotenv.2022.155681

Türk, Ö., Yavuz, M. 2023: Atakum ilçesinde insansız hava aracı ile ışık kirliliği ölçümleri ve değerlendirilmesi. *Süleyman Demirel University Faculty of Arts and Science Journal of Science* 18-2. https://doi.org/10.29233/sdufeffd.1221514

Unwin, D. J. 2009: Statistics, spatial. In: International Encyclopedia of Human Geography. Elsevier. https://doi.org/10.1016/B978-008044910-4.00539-3

Wang, Y., Huang, H., Wu, B. 2024: Evaluating the Potential of SDGSAT-1 Glimmer Imagery for urban road detection. *IEEE Journal of Selected Topics in Applied Earth Observations and Remote Sensin*g 18. https://doi.org/10.1109/JSTARS.2024.3502218

Widmer, K., Beloconi, A., Marnane, I., Vounatsou, P. 2022: Review and assessment of available information on light pollution in Europe. *Report*. European Environment Agency, European Topic Centre Human health and the environment.

Winsemius, S., Braaten, J. 2023: Zonal statistics. In: Cloud-based remote sensing with Google Earth Engine: Fundamentals and applications. Springer.

Wu, K., Wang, X. 2019: Aligning pixel values of DMSP and VIIRS nighttime light images to evaluate urban dynamics. *Remote Sensing* 11-12. https://doi.org/10.3390/rs11121463

Xie, Q., Cai, C., Jiang, Y., Zhang, H., Wu, Z., Xu, J. 2024: Investigating the performance of SDGSAT-1/GIU and NPP/VIIRS nighttime light data in representing nighttime vitality and its relationship with the built environment: A comparative study in Shanghai, China. *Ecological Indicators* 160. https://doi.org/10.1016/j.ecolind.2024.111945

Xu, J. 2020: Developments in management science in engineering 2018: Perspectives from scientific journals. Cambridge Scholars Publishing.

Yerli, S. K., Aksaker, N., Bayazit, M., Kurt, Z., Aktay, A., Erdoğan, M. A. 2021: The temporal analysis of light pollution in Turkey using VIIRS data. *Astrophysics and Space Science* 366-4. https://doi.org/10.1007/s10509-021-03942-6

Yin, Z., Chen, F., Dou, C., Wu, M., Niu, Z., Wang, L., Xu, S. 2024: Identification of illumination source types using nighttime light images from SDGSAT-1. *International Journal of Digital Earth* 17-1. https://doi.org/10.1080/17538947.2023.2297013

Guidelines for contributing authors in Acta geographica Slovenica

EDITORIAL POLICIES

1 Focus and scope

The *Acta geographica Slovenica* journal is issued by the ZRC SAZU Anton Melik Geographical Institute, published by the ZRC SAZU Založba ZRC, and co-published by the Slovenian Academy of Sciences and Arts.

Acta geographica Slovenica publishes original research articles from all fields of geography and related disciplines and provides a forum for discussing new aspects of theory, methods, issues, and research findings, especially in Central, Eastern, and Southeastern Europe.

Articles presenting new developments and innovative methods in geography are welcome. Submissions should address current research gaps and explore state-of-the-art issues. Research based on case studies should have the added value of transnational comparison and should be integrated into established or new theoretical and conceptual frameworks.

The target readership is researchers, policymakers, students, and others who are studying or applying geography.

The journal is indexed in the following bibliographic databases: Clarivate Web of Science (SCIE – Science Citation Index Expanded; JCR – Journal Citation Report/Science Edition), Scopus, ERIH PLUS, Directory of Open Access Journals (DOAJ), GEOBASE Journals, Current Geographical Publications, EBSCOhost, Georef, FRANCIS, SJR (SCImago Journal & Country Rank), OCLC WorldCat, Google Scholar, and CrossRef.

2 Types of articles

Unsolicited or invited original research articles and review articles are accepted. Articles and materials or sections of them should not have been previously published or be under consideration for publication elsewhere. The articles should cover subjects of current interest within the journal's scope.

3 Special issues

The journal also publishes special issues (thematic supplements). Special issues usually consist of invited articles and present a special topic, with an introduction by the (guest) editors. The introduction briefly presents the topic, summarizes the articles, and provides important implications.

4 Peer-review process

All articles are examined by the editor-in-chief. This includes fact-checking the content, spelling and grammar, writing style, and figures. Articles that appear to be plagiarized, are badly or ghost-written, have been published elsewhere, are outside the scope of the journal, or are of little interest to the readers of *Acta geographica Slovenica* may be rejected. If the article exceeds the maximum length, the author(s) must shorten it before the article is reviewed. The article is then sent to responsible editors, who check the relevance, significance, originality, clarity, and quality of the article. If accepted for consideration, the articles are sent to two or more peer reviewer(s) for double-blind review. Articles are rejected or accepted based on the peer reviews and the editorial board's decision.

5 Publication frequency

Acta geographica Slovenica is published three times a year.

6 Open-access policy

This journal provides immediate open access to the full-text of articles at no cost on the principle of open science, which makes research freely available to the public. There is no article processing fee (Article Processing Charge) charged to authors.

Digital copies of the journal are stored by the repository of ZRC SAZU and the digital department of the Slovenian national library NUK, dLib.

The journal's publication ethics and publication malpractice statement is available online, as well as information on subscriptions and prices for print copies.

AUTHOR GUIDELINES

Before submitting an article, please read the details on the journal's focus and scope, publication frequency, privacy statement, history, peer-review process, open-access policy, duties of participants, and publication ethics. See also the latest version of the author guidelines online. All the materials are available at https://ags.zrc-sazu.si.

1 Article structure

Research articles must be prepared using the journal's template (available at https://ags.zrc-sazu.si) and contain the following elements:

- **Title:** this should be clear, short, and simple.
- **Information about author(s):** submit names (without academic titles), affiliations, ORCiDs, and e-mail addresses through the online submission system (available at https://ags.zrc-sazu.si).
- **Highlights**: authors must provide 3–5 highlights in the form of bullets. This section must not exceed 400 characters, including spaces.
- **Abstract:** introduce the topic clearly so that readers can relate it to other work by presenting the background, why the topic was selected, how it was studied, and what was discovered. It should contain one or two sentences about each section (introduction, methods, results, discussion, and conclusions). The maximum length is 800 characters including spaces.
- **Keywords:** include up to seven informative keywords. Start with the research field and end with the place and country.
- **Main text:** the main text must not exceed 30,000 characters, including spaces (without the title, affiliation, abstract, keywords, highlights, reference list, and tables). Do not use footnotes or endnotes. Divide the article into sections with short, clear titles marked with numbers without final dots: **1 Section title**. Use only one level of subsections: **1.1 Subsection title**.

Research articles should have the following structure:

- **Introduction:** present the background of the research problem (trends and new perspectives), state of the art (current international discussion in the field), research gap, motivation, aim, and research questions.
- **Methods:** describe the study area, equipment, tools, models, programs, data collection, and analysis, define the variables, and justify the methods.
- **Results:** follow the research questions as presented in the introduction and briefly present the results.
- **Discussion:** interpret the results, generalize from them, and present related broader principles and relationships between the study and previous research. Critically assess the methods and their limitations, and discuss important implications of the results. Clarify unexpected results or lacking correlations.
- **Conclusion:** present the main implications of the findings, your interpretations, and unresolved questions, offering a short take-home message.

Review articles (narratives, best-practice examples, systematic approaches, etc.) should have the following structure:

- **Introduction:** include 1) the background; 2) the problem: trends, new perspectives, gaps, and conflicts; and 3) the motivation/justification.

- **Material and methods:** provide information, such as data sources (e.g., bibliographic databases), search terms and search strategies, selection criteria (inclusion/exclusion of studies), the number of studies screened and included, and the statistical methods of meta-analysis.
- **Literature review:** use subheadings to indicate the content of the various subsections. Possible structure: methodological approaches, models or theories, the extent of support for a given thesis, studies that agree with one another versus studies that disagree, chronological order, and geographical location.
- **Conclusions:** provide the implications of the findings and your interpretations (separate from facts), identify unresolved questions, summarize, and draw conclusions.

– **Acknowledgments:** use when relevant. In this section, authors can specify the contribution of each author.
– **Reference list:** see the guidelines below.

The journal also features in-depth articles known as ***Geoscapes***. These are a specialized type of research contribution that explore selected topics in greater detail. *Geoscapes* articles are published by invitation only and must be pre-approved by the editorial board.

2 Article submission

2.1 Open journal system

Author(s) must submit their contributions through the *Acta geographica Slovenica* Open Journal System (OJS; available at https://ags.zrc.sazu.si) using the Word document template (available at https://ags.zrc.sazu.si).

Enter all necessary information into the OJS. Any later addition, deletion, or rearrangement of names and affiliations of the author(s) in the authorship list should be made and confirmed by all co-authors before the manuscript has been accepted, and is only possible if approved by the journal editor.

To make anonymous peer review possible, the article text and figures should not include names of the author(s).

Do not use contractions or excessive abbreviations. Use plain text, with sparing use of **bold** and *italics* (e.g., for non-English words). Do not use auto-formatting, such as section or list numbering and bullets.

If a text is unsatisfactory, the editorial board may return it to the author(s) for proofreading or reject the article. See the section on the peer-review process (available at https//ags.zrc-sazu.si) for details. Author(s) may suggest reviewers when submitting an article.

2.2 Language

Articles are published in English. All articles have English and Slovenian abstracts.

Articles can be submitted in English or Slovenian.

Authors must take care to produce a high-quality English text. In the case of poor language, the article must be proofread/translated. In such a case, the translation or copyediting costs are borne by the author(s) and must be paid before layout editing. If authors are not Slovene native speakers, Slovenian abstracts are prepared by the editorial board.

2.3 Graphic file submission

Graphic files (figures) need to be submitted to the OJS packed in a single zip file not exceeding 50 MB. Multiple zip files can be uploaded if needed. See chapter 6 for details on how to prepare figures.

3 In-text citation

In-text citations should include the last name of the author(s) or the name of the publisher and the year of publication. Arrange citations by year of publication; for example: (Melik 1955; Melik et al. 1963; Gams 1982a; Gams 1982b; United Nations 1987; Royal Australian … 1988; Ford and Williams 2007). For references with more than two authors, cite only the first, followed by et al.: (Melik et al. 1956). Give page numbers only for direct quotations, for example: Perko (2016, p. 25) states: »Hotspots are …« For indirect citations, use this format: (Gunn 2002, cited in Matei et al. 2014).

When presenting publicly archived data, such as statistical and spatial data, describe the name of the dataset, the time frame, and the data provider in the main text, for example: »The 2000–2020 population data used in the analysis were provided by Eurostat« If the statistical data were published as a report, cite the document, for example: (European Commission … 2023).

When citing legal sources such as legislative acts, white papers, etc., provide the short formal title and the year, for example: »The European Commission's White paper on transport published in 2011 sets out ten strategic goals for a competitive and resource-efficient transport system.«

4 References

All references in the reference list must be cited in the text. Arrange references alphabetically and then chronologically if necessary. Identify more than one reference by the same author(s) in the same year with the letters a, b, c, etc., added to the year of publication: (1999a, 1999b). In case there are more than seven authors, list the first seven followed by et al.

Examples of references are given below. The use of »gray literature« is strongly discouraged.

Authors can use the Zotero and Endnote AGS Style templates, which are available in the Article submission section on the https://ags.zrc-sazu.si.

4.1 Articles

Last Name1, A. B., Last Name2, C. D. Year: Title. *Journal Name* Volume-Issue. https://doi.org/…

- Breg Valjavec, M., Janža, M., Smrekar, A. 2018: Environmental risk resulting from historical land degradation in alluvial plains considered for dam planning. *Land Degradation & Development* 29-11. https://doi.org/10.1002/ldr.3168
- Kladnik, D., Kruse, A., Komac, B. 2017a: Terraced landscapes: An increasingly prominent cultural landscape type. *Acta geographica Slovenica* 57-2. https://doi.org/10.3986/AGS.4770
- Kladnik, D., Šmid Hribar, M., Geršič, M. 2017b: Terraced landscapes as protected cultural heritage sites. *Acta geographica Slovenica* 57-2. https://doi.org/10.3986/AGS.4628
- Ni, J., Jin, J., Wang, Y., Li, B., Wu, Q., Chen, Y., Du, S. et al. 2024: Surface ozone in global cities: A synthesis of basic features, exposure risk, and leading meteorological driving factors. *Geography and Sustainability* 5-1. https://doi.org/10.1016/j.geosus.2023.09.008
- Unangst, M. 2023: (De)Colonial historical geography and historical GIS. *Journal of Historical Geography* 79. https://doi.org/10.1016/j.jhg.2022.12.003
- Van de Kerk, G., Manuel, A. R. 2008: A comprehensive index for a sustainable society: The SSI – The Sustainable Society Index. *Ecological Economics* 66-2,3. https://doi.org/10.1016/j.ecolecon.2008.01.029
- Yang, D.-H., Goerge, R., Mullner, R. 2006: Comparing GIS-based methods of measuring spatial accessibility to health services. *Journal of Medical Systems* 30-1. https://doi.org/10.1007/s10916-006-7400-5

4.2 Books

Last Name1, A. B., Last Name2, C. D. Year: Book title. *Book Series Title* with Number. Publisher. https://doi.org/…

If the book is edited by editors, add '(eds.)' before the year of publication.

- Achino, K. F., Velušček, A. 2022: The lake-dwelling phenomenon. *E-Monographiae Instituti Archaeologici Sloveniae* 13. Založba ZRC. https://doi.org/10.3986/9789610506560
- Gams, I. 2004: Kras v Sloveniji v prostoru in času. Založba ZRC.
- Hall, T., Barrett, H. 2018: Urban geography. Routledge. https://doi.org/10.4324/9781315652597
- Knox, P., Marston, S. 2015: Human geography: Places and regions in global context. Pearson.
- Luc, M., Somorowska, U., Szmańda, J. B. (eds.) 2015: Landscape analysis and planning. *Springer Geography*. Springer. https://doi.org/10.1007/978-3-319-13527-4
- Marshall, T. 2016: Prisoners of geography: Ten maps that explain everything about the World. *Politics of Place*. Scribner.
- Mihelič Pulsipher, L., Pulsipher, A., Johansson, O. 2019: World regional geography: Global patterns, local lives. W. H. Freeman.

4.3 Chapters of books or proceedings

Last Name1, A. B., Last Name2, C. D. Year: Chapter title. In: Book Title. *Book Series Title* with Number. Publisher. https://doi.org/…

- Griffin, A. L. 2018: Cartography, visual perception and cognitive psychology. In: The Routledge Handbook of Mapping and Cartography. Routledge. https://doi.org/10.4324/9781315736822
- Solem, M., Boehm, R. 2015: A research coordination network for geography education. In: EUGEO Budapest 2015: Congress Programme and Abstracts. Hungarian Geographical Society.
- Stethem, C. 2013: Avalanches. In: Encyclopedia of Natural Hazards. Springer. https://doi.org/10.1007/978-1-4020-4399-4_7
- Zorn, M., Ferk, M., Lipar, M., Komac, B., Tičar, J., Hrvatin, M. 2020: Landforms of Slovenia. In: The Geography of Slovenia: Small But Diverse. *World Regional Geography Book Series*. Springer. https://doi.org/10.1007/978-3-030-14066-3_3

4.4 Reports, theses, dissertations, and other materials with authors

Last Name1, A. B., Last Name2, C. D. Year: Title. *Type of document*. Publisher. https://doi.org/…

- Davies, G. 2017: The place of data papers: Producing data for geography and the geography of data production. *Blog post*. Geo: Geography and Environment.
- Easterbrook, D. J. 1976: Geologic map of western Whatcom County, Washington (1-854-B). *1:62,500 map*. United States Geological Survey.
- Fležar, U., Hočevar, L., Sindičić, M., Gomerčić, T., Konec, M., Slijepčević, V., Bartol, M. et al. 2022: Surveillance of the reinforcement process of the Dinaric - SE Alpine lynx population in the lynx-monitoring year 2020–2021. *Technical report*. LIFE Lynx.
- Hawking, S. 1966: Properties of expanding universes. *Ph.D. thesis*. University of Cambridge. https://doi.org/10.17863/CAM.11283
- Hrvatin, M. 2016: Morfometrične značilnosti površja na različnih kamninah v Sloveniji. *Ph.D. thesis*. Univerza na Primorskem.
- Šifrer, M. 1997: Površje v Sloveniji. *Technical report*. Geografski inštitut Antona Melika ZRC SAZU.

4.5 Sources without authors

Use in-text citations (see Chapter 3). If sources need to be listed in the references use the following style: Publisher/Institution Year: Title. *Type of document*. https://doi.org/…

- Geodetska uprava Republike Slovenije 1998: Državna topografska karta Republike Slovenije 1 : 25.000 (Brežice). *1:25,000 map*.
- Royal Australian Survey Corps 1988: Australia 1:50 000 topographic survey (Tamborine, Queensland). *1:50,000 map*.
- United Nations 1987: Report of the World Commission on Environment and Development: Our common future. *Report*.
- European Space Agency 2022: Copernicus Sentinel-2 MSI Level-1C TOA Reflectance. *Dataset*. https://doi.org/10.5270/S2_-742ikth

5 Tables

Number all tables in the article uniformly and provide their own titles. The number and the title text are separated by a colon, and the title ends with a period. A table title is located above the corresponding table. Examples:

- Table 1: Number of inhabitants of Ljubljana.
- Table 2: Changes in average air temperature in Ljubljana (Velkavrh 2009).

Tables must be indicated in the main text in parentheses, for example: (Table 1), or as a part of the sentence, for example »… as can be seen in Table 1.« Tables should contain no formatting and must be inserted in the article file.

6 Figures

Figures encompass different graphic presentations used in the article: photography, graphs, illustrations, maps, etc.

Number all figures in the article uniformly and provide their own titles. The number and the title text are separated by a colon, and the title ends with a period. A figure title is located below the corresponding figure. Example:

- Figure 1: Location of measurement points along the glacier.

Figures must be indicated in the main text in parentheses, for example: (Figure 1), or as a part of the sentence, for example »… as can be seen in Figure 1.«

Figures should be exactly 134 mm wide (one page) or 64 mm wide (half page, one column), and up to 200 mm high.

Titles should appear in a caption only. Save colors in CMYK. Use Times New Roman font with a minimum size of 6.

Figures must be submitted as separate files. Multiple graphic files should be uploaded in one zip file. Figures should also be inserted in the main text file in order to ease the review process.

Regardless of the graphic/cartographic software used, save or export figures to the following formats:

- jpg or tiff file for regular photos (use a minimum of 300 dpi),
- xlsx file for graphs made with MS Office Excel,
- pdf or similar common files for maps and illustrations with vector drawings and/or text (embed the font if possible). See chapter 6.3 for details.

If the graphic files cannot be uploaded according to the guidelines, consult the editorial board (ags@zrc-sazu.si) in advance.

To make anonymous peer review possible, the authorship of figures can be added by authors at a later (copyediting) stage, after the review has been completed.

6.1 Photos

Photos must be in raster format with a resolution of at least 300 dpi, preferably in jpg or tiff format.

Figures containing a screenshot should be prepared at the highest possible screen resolution. A figure can be made using Print Screen, and the captured screen is pasted to the selected graphic program (e.g., Paint) and saved as a tiff or jpg file. The size of the image or its resolution must not be changed.

6.2 Graphs

Graphs should be made using MS Excel on separate sheets and accompanied by data.

6.3 Maps and illustrations

Maps should be informative and prepared according to the journal size limitations (see general guidelines defined in chapter 6). Use Times New Roman for the legend (size 8) and colophon (size 6). List scale, source, and copyright in the colophon. List the authors of the content and authors of the maps if needed. Write the colophon in English. Use a graphic scale if possible.

Example of the colophon structure:
Content by: Name Surname
Map by: Name Surname
Source: Institution Year
© Year, Copyright holder

Maps should be submitted in an editable form if possible so that minor errors can be corrected even in the final stages of article production. **The preferred submission file is pdf**. As an exception, maps can be produced in digital raster form with at least 300 dpi resolution, preferably in jpg or tiff format.

Please, pay attention when exporting maps from these software packages:

- if using QGIS, ESRI ArcGIS Pro or similar, maps should be exported as a pdf file,
- if using Gimp, Inkscape, CorelDraw, Adobe Illustrator or similar, two separate files should be prepared: the original software file (e.g. cdr if using CorelDraw) and a pdf file,
- if using ESRI ArcGIS Desktop (ArcMap) with raster layers and vector layers (e.g., a geotiff file for shaded relief and a shp file for roads), three files should be exported and submitted: a pdf or an ai file with all the vector content without transparency (polygons, lines, points, legend, colophon, labels, etc.), a tiff file with a raster background, and a jpg file with all of the content (vector and raster elements) together showing the final version of the map; see an example of the correct file structure (available at https://ojs.zrc-sazu.si/ags/libraryFiles/downloadPublic/14) for submitting a map created with ESRI ArcGIS Desktop.

Illustrations should be prepared according to the journal size limitations (see general guidelines defined in chapter 8). Use Times New Roman font size 8. **The preferred submission file is pdf**. As an exception, illustrations can be produced in digital raster form with at least 300 dpi resolution, preferably in jpg or tiff format.

7 Research data

Authors have to make the research data used in the article published in *Acta geographica Slovenica* publicly available in a recognized online repository and provide the editorial board with a link.

The publication of the data in the repository must indicate that the data are part of the published article. The article must be properly cited when using the data.

See detailed information on our research data management web page.

SUBMISSION PREPARATION CHECKLIST

As part of the submission process, authors are required to check off their submission's compliance with all of the following items, and submissions may be returned to authors who do not adhere to these guidelines.

- I, the corresponding author, declare that this manuscript is original and is therefore based on original research, done exclusively by the authors. All information and data used in the manuscript were prepared by the authors or the authors have properly acknowledged other sources of ideas, materials, methods, and results. The authors followed the ZRC SAZU guidelines for responsible use of AI.
- Authors confirm that they are the authors of the submitting article, which is under consideration to be published (print and online) in the journal *Acta geographica Slovenica* by Založba ZRC, ZRC SAZU.
- All authors have seen and approved the article being submitted.
- The submission has not been previously published, nor it is under consideration in another journal (or an explanation has been provided in Comments to the Editor). Authors have disclosed any prior posting, publication or distribution of all or part of the manuscript to the Editor.
- Upon publishing an article in the journal, the authors agree to license non-exclusive copyrights to ZRC SAZU (Založba ZRC): they retain the copyright in the scope that enables them to continue to use their work, even by publishing it in one of the personal or institutional repositories before the publication of the article in the journal.
- Authors consent to the publication of their works under Creative Commons Attribution-ShareAlike 4.0 International (CC BY-SA 4.0).
- Permission has been obtained for the use (in printed and electronic format) of copyrighted material from other sources, including online sources. Restrictions on the transfer of copyright on this material have been clearly indicated.
- All the necessary permits to work with people have been obtained in the research related to the article (in accordance with the applicable laws and institutional guidelines and approved by the relevant institutions).
- The journal policies and guidelines have been reviewed and followed.
- The metadata (title, abstract, keywords, authors, affiliation, ORCiD, etc.) are provided in English (Slovenian authors must also provide the metadata in Slovenian).
- The list of authors is complete. Failure to do so may result in co-authors not being listed on the article at publication.
- The submission is in Microsoft Word format and the document template was used (single-spaced text, 12-point font, no formatting except italics and bold).
- The article has been checked for spelling and grammar.
- Figures are provided as separate graphic files: editable vector format (e.g., cdr, ai, pdf) for maps and illustrations; jpg or tiff for photographs; xlsx for graphs.
- Tables are placed in the Word file with text in the appropriate place.
- The reference list was prepared following the guidelines.
- All references in the reference list are cited in the text.
- Where available, URLs and DOI numbers for references are provided.
- Graphic files are in one zip file.
- Authors agree that any costs of English proofreading are borne by the author(s). No additional costs are associated with the submission.
- The instructions for ensuring a double-blind review have been followed.
- If the article is accepted, the authors will provide unique information (e.g., a DOI) about the online repository where the research data underlying the article is located. This information must be provided before the article is published. Metadata of the data in the repository must indicate that the data are part of the published article in the journal Acta geographica Slovenica. The article must be properly cited when using the data.

ACTA GEOGRAPHICA SLOVENICA EDITORIAL REVIEW FORM

This is the review form for editorial review (version 15) of an article submitted to the AGS journal.

This is an original scientific article.
(The article is original and the first presentation of research results with the focus on methods, theoretical aspects or a case study.)

- Yes
- No

The article follows the standard IMRAD/ILRAD scheme.

- Yes
- No

The article's content is suitable for reviewing in the AGS journal.
(The article is from the field of geography or related fields of interest, the presented topic is interesting for the readers of *Acta geographica Slovenica* and well presented. In case of a negative answer, add comments below.)

- Yes
- No

Editorial notes regarding the article's content.

The reference list is suitable (the author cites previously published articles with similar topics from other relevant geographic scientific journals).

- Yes, the author cited previously published articles on a similar topic.
- No, the author did not cite previously published articles on a similar topic.

Notes to the editor-in-chief regarding previously published scientific work.

Is the language of the article appropriate and understandable?

RECOMMENDATION OF THE EDITOR

- The article is accepted and can be sent to the review process.
- Reconsider after a major revision (see notes).
- The article is rejected.

ACTA GEOGRAPHICA SLOVENICA REVIEW FORM

This is the *Acta geographica Slovenica* review form (version 8).

1 RELEVANCE

Are the findings original and is the article therefore a significant one?

- yes
- no
- partly

Is the article suitable for the subject focus of the AGS journal?

- yes
- no

2 SIGNIFICANCE

Does the article discuss an important problem in geography or related fields?

- yes
- no
- partly

Does it bring relevant results for contemporary geography?

- yes
- no
- partly

What is the level of the novelty of the research presented in the article?

- high
- middle
- low

3 ORIGINALITY

Has the article already been published or is it too similar to already published work?

- yes
- no

Does the article discuss a new issue?

- yes
- no

Are the presented methods sound and adequate?

- yes
- no
- partly

Do the presented data support the conclusions?

- yes
- no
- partly

4 CLARITY

Is the article clear, logical, and understandable?

- yes
- no

If necessary, add comments and recommendations to improve the clarity of the title, abstract, keywords, introduction, methods or conclusion:

5 QUALITY

Is the article technically sound? (If not, the author should discuss with the Editorial Board [ags@zrc-sazu.si] for assistance.)

- yes
- no

Does the article take into account relevant current and past research on the topic?

- yes
- no

Propose amendments if no is selected:

Is the references list at the end of the article adequate?

- yes
- no

Propose amendments if no is selected:

Is the quoting in the text appropriate?

- yes
- no
- partly

Propose amendments if no is selected:
Which tables are not necessary?
Which figures are not necessary?

COMMENTS OF THE REVIEWER

Comments of the reviewer on the contents of the article:
Comments of the reviewer on the methods used in the article:

RECOMMENDATION OF THE REVIEWER TO THE EDITOR-IN-CHIEF

Please rate the article from 1 [low] to 100 [high] (this will NOT be presented to the author):
Personal notes of the reviewer to the editor-in-chief (this will NOT be presented to the authors):

Would you like to review the article again after corrections (in case the article needs them and is not declined)? The second review is expected to be done in 14 days.

- yes
- no

COPYRIGHT NOTICE

PRIVACY STATEMENT

By submitting their articles or other contributions the authors and reviewers consent to the collection and processing of their personal data (e.g., name, surname and email address) for the purposes of effective communication, editing, and publication of articles or other contributions.

The names and e-mail addresses provided to this journal site will be used exclusively for the stated purposes of this journal and will not be made available for any other purpose or to any other party.

PUBLISHER

Anton Melik Geographical Institute
Research Centre of the Slovenian Academy of Sciences and Arts
PO Box 306
SI–1001 Ljubljana
Slovenia

SOURCES OF SUPPORT

The journal is subsidized by the Slovenian Research and Innovation Agency (B6-7614) and is issued in the framework of the Geography of Slovenia long-term core research programme (P6-0101). The journal is also supported by the Slovenian Academy of Sciences and Arts.

JOURNAL HISTORY

Acta geographica Slovenica (print version: ISSN: 1581-6613, digital version: ISSN: 1581-8314) was founded in 1952. It was originally named *Geografski zbornik / Acta geographica* (print ISSN 0373-4498, digital ISSN: 1408-8711). Altogether, 42 volumes were published. In 2002 *Geographica Slovenica* (ISSN 0351-1731, founded in 1971, 35 volumes) was merged with the journal.

Since 2003 (from Volume 43 onward), the name of the joint journal has been *Acta geographica Slovenica*. The journal continues the numbering system of the journal *Geografski zbornik / Acta geographica*.

Until 1976, the journal was published periodically, then once a year, twice a year from 2003, and three times a year since 2019.

The online version of the journal has been available since 1995. In 2013, all volumes of the magazine were digitized from the beginning of its publication to including 1994.

All articles of the journal are available free of charge in digital form on the journal website http://ags.zrc-sazu.si**.**

Those interested in the history of the journal are invited to read the article »The History of *Acta geographica Slovenica*« in volume 50-1.

ISSN: 1581-6613
UDC – UDK: 91
ACTA GEOGRAPHICA SLOVENICA
GEOGRAFSKI ZBORNIK

65-2
2025

2025, ZRC SAZU, Geografski inštitut Antona Melika
Print/tisk: Birografika Bori

Ljubljana 2025

ACTA GEOGRAPHICA SLOVENICA
GEOGRAFSKI ZBORNIK
65-2 • 2025

Contents

ISSN 1581-6613